

1 **Rebuttal report**

2

3 We thank the reviewers for the careful thought and suggestions. We hope that we have
4 been able to address all these points below and in the text. All grammar corrections
5 were addressed as suggested except for cases where the text was removed completed,
6 all text changes are shown in the attached track changes document. The manuscript was
7 also further refined in grammar and syntax as suggested.

8

9 **Reviewer #1**

10

11 **Reviewer:**

12 Table 1 – only 7 of the 10 models are described. Please add GFDL-ESM2M, HadGEM2-ES
13 and MRI-ESM

14

15 **Response:**

16 We apologise for the missing models, it was a technical error on the submitted
17 manuscript, all models are now added.

18

19 All technical and editorial suggestions were addressed.

20

21 **Reviewer #2**

22

23 **Reviewer:**

24 I think the authors have done a good job of responding to the specific comments made in
25 the previous reviews. However, I still find the logic of the method difficult to follow in
26 places, and the general tone of the paper is more pessimistic about the models'
27 performance than I think the data warrant. I would like these authors to find a way to
28 see the cup as half full rather than half empty; I don't think their results are as damning
29 of the models' performance as their text implies (see e.g. point 2 below).

30

31 **Response:**

32 We thank the reviewer making these points. The methods section has been further
33 clarified, particularly explaining more explicitly the basis for comparing the equivalent
34 DIC $(dDIC/dt)_{SST}$ and total DIC $(FDIC/dt)_{Tot}$ changes. It should be emphasized that
35 equivalent DIC $(dDIC/dt)_{SST}$ is a "synthetic" variable in the sense that it does not

36 contribute to the "real" DIC budget $(\text{FDIC}/\text{dt})_{\text{Tot}}$. It's purpose is to scale the temperature
37 impact on solubility of CO2 in DIC-equivalent units. Below we also clarify why lumping
38 together the biological and entrainment terms when comparing the total DIC changes
39 with the temperature equivalent DIC is valid as well as why this methodology should
40 hold even for cases when the biological and entrainment terms are opposing each other
41 equally.

42

43 We tried to be as objective as possible in interpreting of our findings, avoiding a
44 negative perspective view of CMIP5 models. We do agree that CMIP5 models show a
45 strong improvement from previous generations and, in pointing out current limitations
46 and biases, we were not aiming at showing how bad models are, but highlighting
47 considerations that pointed towards potential model improvements.

48

49

50 **Reviewer:**

51 1) I still find the logic underlying equation (5) opaque. If we have

52

53 $X_{\text{TOT}} = X_{\text{T}} + X_{\text{B}} + X_{\text{E}}$

54

55 where T, B, and E indicate temperature, biology and entrainment, it isn't obvious to me
56 why

57

58 $|X_{\text{T}}| - |X_{\text{TOT}}| < 0 \text{ or } > 0$

59

60 is a useful index of whether or not T, B, or E are the dominant term. And what happens if
61 it is identically zero? For example, if $X_{\text{B}} = -1$, and $X_{\text{E}} = +1$, then $X_{\text{TOT}} = X_{\text{T}}$. If e.g.,
62 $X_{\text{T}} = 3 * X_{\text{E}}$, then in this case X_{T} is clearly the dominant term. But this index does not
63 consider it so, and if X_{T} were only slightly larger or smaller, it would flip the index into
64 one realm or the other. As I see it, X_{B} will normally be negative and X_{E} positive, while
65 X_{T} can be either. This index appears to depend rather strongly on the sign of X_{T} , which
66 has nothing to do with the relative magnitudes of the terms. Why not just make an index
67 that directly addresses the relative magnitudes, like $|X_{\text{T}}| / |X_{\text{B}} + X_{\text{E}}|$? This at least has
68 the desirable property of increasing symmetrically with either positive or negative X_{T} .

69

70 **Response:**

71 We thank the reviewer for raising this point; it shows that a further clarification of our
72 methodology was necessary.

73

74 The reviewer raises an interesting alternative to present our results, however, we hope
75 that we can, by further clarifying our thinking, show that this suggestion has its own
76 complexities.

77 Firstly, the temperature-linked equivalent DIC term $(dDIC/dt)_{SST}$ is not a contributing
78 term to the total DIC changes Eq. 1, but a construct of the temperature driven pCO_2
79 changes (solubility) converted to equivalent DIC units. Since temperature does not
80 influence DIC directly, but pCO_2 , it was necessary to convert solubility-linked pCO_2
81 changes into comparable units of DIC, and hence the DIC equivalence. It is an abstract
82 term but of great value because it scales the temperature impact on pCO_2 to DIC units -
83 essentially it reflects the amount by which DIC would have to change to have the same
84 impact on pCO_2 as the temperature change but does not contribute to the DIC budget in
85 a direct sense. This is different to the real impact of temperature on pCO_2 which then
86 results in changes to air-sea fluxes that impact on DIC_{Total} . This is incorporated into the
87 DIC_{Total} term. .

88

89 Consequently, our approach (Eq. 5) is independent of the sign and magnitude of the
90 contributing terms in Eq. 1 (entrainment and biological terms with a much smaller /
91 slower contribution from air-sea fluxes). We are quantifying the relative magnitudes of
92 the temperature and total DIC changes as drivers of pCO_2 variability. This enables us to
93 reflect on the relative dominance of the drivers. This is important because it highlights a
94 tipping point between SST and DIC control, which has implications for the climate
95 sensitivity of the models.

96

97 **Reviewer:**

98 When I look at Supplemental Figure 8, it makes me think that the models are actually
99 doing a fairly good job. The periods where X_T dominates are short and confined to the
100 spring and fall transitions. The general seasonal pattern is reproduced by almost all of
101 the models for almost all of the regions. Certainly there are models where the DIC-
102 driven seasonal variation of X_{TOT} seems too large. But generally the models reproduce
103 the observed pattern fairly well (although I admit I don't understand why X_{TOT} is
104 represented as a single line with a sign for each month, and X_T as a cloud symmetrical
105 around zero).

106

107 **Response:**

108 Indeed when comparing absolute magnitudes of X_T and X_{TOT} , the models reflect the
109 phasing of the variability reasonably well. . However, there are two issues that need to
110 be considered. Firstly, that SST or DIC control is not a gradual scale but a tipping point
111 problem. It's one or the other so even a relatively close magnitude may lead to a bias in
112 respect of how the model reflects the climate sensitivity of the carbon cycle. Secondly,
113 is that the spring/fall temperature dominance in CMIP5 models is critical to diagnosing
114 the pCO_2 and FCO_2 , biases against observational product. This is exactly the point we are
115 making with this figure. Though Landschützer et al (2014) and CMIP5 models only differ
116 during this two seasons, the separations are significant in the seasonal cycle of pCO_2
117 because of the marginal differences in SST and DIC control; it results in the out-gassing
118 CO_2 biases in late-summer (due to warming) and ingassing due to rapid early autumn
119 cooling. This, we think, causes the main bias against Landschützer et al (2014_) data
120 product.

121

122 The reason for shaded symmetry of X_T in Fig. S8 is because this figure aims to give two
123 pieces of information, (i.) to show where periods $X_{TOT} > (or <) X_T$ and elucidate on a
124 possible driver of the instantaneous X_{TOT} changes. Because X_T is only driven by
125 temperature changes, X_T is binary so it can symmetric. However X_{TOT} can be driven
126 by biology (- primary production and + respiration) and entrainment, and thus the sign
127 of total the DIC changes provide useful information in diagnosing driver of the
128 instantaneous DIC changes.

129

130 **Reviewer:**

131 What would happen if you added a fourth line to Fig. 3 representing an ensemble of ALL
132 of the models? I suspect that it would agree with the observations much better than
133 either of these two somewhat arbitrary groups alone (see e.g., Lambert and Boer (2001)
134 Climate Dynamics 17:83).

135

136 **Response:**

137 The reviewer is correct, an additional fourth line representing the ensemble of all modes
138 show a seasonal cycle that agrees more with Landschützer et al (2014). However though
139 we did this test in our analysis, it was excluded in the manuscript mainly because our
140 aim here is to explain the mechanisms responsible for model-observations biases and
141 the ensemble of all models is not useful for this regard. Notwithstanding these, other
142 than the fact that it is known that an ensemble of all models is more comparable to

143 available observations estimates (e.g. Anav et al., 2013; Boer and Lambert, 2001),
144 mechanisms of this ensemble are hard to explain. It is also not clear whether the long-
145 term simulation of FCO₂ based this ensemble (all models) is reliable. In particular it is
146 not clear whether long-term biases of individual models will significantly distort the
147 trend from the “true future trend” or alternatively continue to average out towards the
148 observed trend. Thus a good comparison with observations might be misleading. his
149 might be intuitively useful in some cases but because we are not making a point about
150 how CMIP5 models ensembles converge to observations, but evaluating the mechanistic
151 basis for the biases, we thought this fourth line was not necessary.

152

153 **Reviewer:**

154 The assumption that temperature-driven changes in pCO₂ can be converted to an
155 "equivalent DIC" change implies equilibration with the atmosphere by gas exchange. I
156 don't think this a bad assumption to make in context of this kind of analysis, but I still
157 don't think that it is stated explicitly enough (e.g., 199-206). The change in pCO₂ with
158 SST is purely a result of temperature driven changes in solubility (and to small degree,
159 speciation): DIC does not change as a result of these processes.

160

161 **Response:**

162 As communicated above, the DIC equivalent temperature we are referring to here is
163 purely a scaling of the solubility CO₂ changes to DIC units, which does not contribute to
164 the DIC budgets in a direct sense. So, in fact the opposite holds to the equilibration
165 assumption that is proposed. When DIC_T is > DIC_{Tot} and pCO₂ is controlled by
166 temperature the net effect is a strengthening disequilibrium at the air-sea interface
167 which results in a divergence between observed and modelled pCO₂. As mentioned
168 earlier, the air-sea flux adjustments are in the DIC_{Tot} term and the reason why
169 temperature driven disequilibrium persists is because the rate at which temperature
170 adjusts pCO₂ >> rate of air-sea flux equilibrium restoration.

171

172 **Reviewer:**

173 The assumption that the horizontal terms are negligible is probably OK as a first
174 approximation, but I would recommend that the authors qualify this assumption by
175 noting that, at least in the subantarctic zone, (a) there is a latitudinal gradient in DIC
176 concentration, (b) there is a wind-driven equatorward flow (Ekman transport), and (c)
177 in some regions there is a strong seasonal cycle in the wind stress. a+b+c implies that
178 there is a seasonal cycle in the divergence of the horizontal transport.

179

180 **Response:**

181 Thank you for the point, in the revised manuscript with clarified as suggested in the
182 revised manuscript.

183

184 **Terminology**

185 All terminology corrections were addressed as suggested.

186

187 **Reviewer 3**

188

189 **Reviewer:**

190 The authors added a valuable synthesis chapter. There they have strengthened a second
191 item, which focuses on the simulated homogeneity of the fluxes in the different basins
192 differing from observations. It is common practice to answer every question of remark
193 of the reviewer. On the other hand the text still does not give information about model
194 characteristics which may be responsible for exaggerated SST or DIC sensitivities on
195 FCO₂ in the different models. This has not been done. In some cases the item has been
196 ignored, in some cases it has been accounted for. Please discuss with the reviewer and,
197 in case if text change, give a note there and how the test has been improved. The
198 manuscript is still written very sloppily

199

200 **Response:**

201 We apologize that not all remarks were addressed in the submitted manuscript. The
202 manuscript has been improved in presentation for grammar and flow of structure.

203

204 We have added a new paragraph at the end of the discussion section that explicitly
205 addresses the question on what model characteristics may be responsible for
206 exaggerated seasonal cycles for the rates of change of SST .

207

208 “ The cause of differences in the seasonal rates of SST change in group-SST models
209 remains a subject of ongoing research. The Southern Ocean is a part of the global ocean
210 (upwelling) where earth systems models show a persistent warming SST bias (Hirahara
211 et al., 2014). Several studies point to highlight potential explanations but the main
212 reasons remain uncertain. For example, CMIP5 models differences in the magnitude
213 and meridional location of the peak of wind speeds in the Southern Ocean (Bracegirdle
214 et al., 2013) and MLD (Meijers, 2014; Sallée et al., 2013) may be such that the net effect

215 on surface turbulence and mixing leads to these amplified surface temperature rates.
216 Other known CMIP5 model' biases that may contribute include; heat fluxes and storage
217 (Frölicher et al., 2015) as well as sea-ice dynamics (Turner et al., 2013).
218 Notwithstanding these, investigation of the reasons for sources of these dSST/dt biases
219 is out of the scope of this study. Our aim here is to show that understanding biases in the
220 drivers of pCO₂ (DIC and SST) at the seasonal scale is necessary to understand
221 differences in the seasonal cycle of FCO₂ between models and observational products.
222 However we recommend that the mechanistic basis for the differences the seasonal
223 rates of warming and cooling be a matter of urgent investigated further”

224

225 **Reviewer:**

226 Fig. 10 shows new patterns compared with the old manuscript, why?

227 Fig. 10 legend: still wrong units

228

229 **Response:**

230 Figure 10 was corrected from the previous version hence the some differences in the
231 patterns,, there was an error on the equation we used to calculate the fluxes. This was
232 pointed out by reviewer two, and thus we made a correction and instead calculate the
233 rates of change of DIC at the base of the MLD (Eq. 6), this we now we use to infer
234 entrainment.

235 The units in Fig. 10 are however correct based on Eq. 6 - 8.

236 Fig. 10a-f shows the estimated entrainment of rate given in umol/kg month and Fig.

237 10d-l shows the vertical DIC gradients given in umol/kg m

238

239

240 **Terminology**

241 All terminology and reference corrections were addressed as suggested.

The Seasonal Cycle of pCO₂ and CO₂ fluxes in the Southern Ocean: Diagnosing Anomalies in CMIP5 Earth System Models

Precious N. Mongwe^{1,2}, Marcello Vichi^{2,3} & Pedro M.S. Monteiro^{1,2}

¹Southern Ocean Carbon-Climate Observatory (SOCCO), CSIR, Cape Town, South Africa

²Department of Oceanography, University of Cape Town, Cape Town, South Africa

³Marine Research Institute, University of Cape Town, Cape Town, South Africa

pmongwe@csir.co.za

Abstract

The Southern Ocean forms an important component of the earth system, as a major sink of CO₂ and heat. Recent studies based on the Coupled Model Intercomparison Project version 5 (CMIP5) Earth System Models (ESMs) show that CMIP5 models disagree on the phasing of the seasonal cycle of the CO₂ flux (FCO₂) and compare poorly with available observation products for the Southern Ocean. Because the seasonal cycle is the dominant mode of CO₂ variability in the Southern Ocean, its simulation is a rigorous test for models and their long-term projections. Here we examine the competing roles of temperature and dissolved inorganic carbon (DIC) as drivers of the seasonal cycle of pCO₂ in the Southern Ocean to explain the mechanistic basis for the seasonal biases in CMIP5 models. We find that despite significant differences in the spatial characteristics of the mean annual fluxes, the intra-model homogeneity in the seasonal cycle of FCO₂ is greater than observational products. FCO₂ biases in CMIP5 models can be grouped into two main categories i.e. group-SST and group-DIC. Group-SST models show an exaggeration of the seasonal rates of change of sea surface temperature (SST) in autumn and spring during the cooling and warming peaks. These higher-than-observed rates of change of SST tip the control of the seasonal cycle of pCO₂ and FCO₂ towards SST and result in a divergence between the observed and modelled seasonal cycles, particularly in the Sub-Antarctic Zone. While almost all analyzed models (9 out of 10) show these SST-driven biases, 3 out of 10 (namely NorESM1-ME, HadGEM-ES and MPI-ESM, collectively the group-DIC models) compensate the solubility bias because of their overly exaggerated primary production, such that biologically-driven DIC changes mainly regulate the seasonal cycle of FCO₂.

Style Definition ... [2]

V2 Changes 2018/4/17 11:06 AM
Formatted ... [3]

V2 Changes 2018/4/17 11:06 AM
Formatted ... [4]

V2 Changes 2018/4/17 11:06 AM
Deleted: Systems

V2 Changes 2018/4/17 11:06 AM
Formatted ... [5]

V2 Changes 2018/4/17 11:06 AM
Formatted ... [6]

V2 Changes 2018/4/17 11:06 AM
Deleted: global carbon cycle

V2 Changes 2018/4/17 11:06 AM
Formatted ... [7]

V2 Changes 2018/4/17 11:06 AM
Deleted: poorly

V2 Changes 2018/4/17 11:06 AM
Formatted ... [8]

V2 Changes 2018/4/17 11:06 AM
Deleted: observations estimates in

V2 Changes 2018/4/17 11:06 AM
Formatted ... [9]

V2 Changes 2018/4/17 11:06 AM
Deleted: proper

V2 Changes 2018/4/17 11:06 AM
Formatted ... [10]

V2 Changes 2018/4/17 11:06 AM
Deleted: necessary to model long-te ... [11]

V2 Changes 2018/4/17 11:06 AM
Formatted ... [12]

V2 Changes 2018/4/17 11:06 AM
Deleted: related climate impacts

V2 Changes 2018/4/17 11:06 AM
Formatted ... [13]

V2 Changes 2018/4/17 11:06 AM
Deleted: , comparing them with ... [14]

V2 Changes 2018/4/17 11:06 AM
Formatted ... [15]

V2 Changes 2018/4/17 11:06 AM
Deleted: models show greater zonal

V2 Changes 2018/4/17 11:06 AM
Formatted ... [16]

V2 Changes 2018/4/17 11:06 AM
Deleted: The

V2 Changes 2018/4/17 11:06 AM
Formatted ... [17]

V2 Changes 2018/4/17 11:06 AM
Deleted: one or the other of

V2 Changes 2018/4/17 11:06 AM
Formatted ... [18]

V2 Changes 2018/4/17 11:06 AM
Deleted: (

V2 Changes 2018/4/17 11:06 AM
Formatted ... [19]

V2 Changes 2018/4/17 11:06 AM
Deleted:) while observational prod ... [20]

V2 Changes 2018/4/17 11:06 AM
Formatted ... [21]

V2 Changes 2018/4/17 11:06 AM
Deleted: The

V2 Changes 2018/4/17 11:06 AM
Formatted ... [22]

V2 Changes 2018/4/17 11:06 AM

V2 Changes 2018/4/17 11:06 AM
Formatted ... [23]

V2 Changes 2018/4/17 11:06 AM

V2 Changes 2018/4/17 11:06 AM
Formatted ... [24]

V2 Changes 2018/4/17 11:06 AM

V2 Changes 2018/4/17 11:06 AM
Formatted ... [25]

V2 Changes 2018/4/17 11:06 AM
Formatted ... [26]

1. Introduction

The Southern Ocean (south of 30°S) takes up about a third of the total oceanic CO₂ uptake, slowing down the accumulation of CO₂ in the atmosphere (Fung et al., 2005; Le Quere et al., 2016; Takahashi et al., 2012). The combination of upwelling deep ocean circumpolar waters (which are rich in carbon and nutrients) and the subduction of fresh, colder mid-latitude waters makes it a key region in the role of sea-air gas exchange and heat uptake (Barbero et al., 2011; Gruber et al., 2009; Sallée et al., 2013). The Southern Ocean supplies about a third of the total nutrients responsible for biological production north of 30°S (Sarmiento et al., 2004), and accounts for about 75% of total ocean heat uptake (Frölicher et al., 2015). Recent studies suggest that the Southern Ocean CO₂ sink is expected to change as a result of anthropogenic warming, however, the sign and magnitude of the change is still disputed (Leung et al., 2015; Roy et al., 2011; Sarmiento et al., 1998; Segsneider and Bendtsen, 2013). While some studies suggest that the Southern Ocean CO₂ sink is weakening and will continue to do so (e.g. Le Quéré et al., 2007; Son et al., 2010; Thompson et al., 2011), other recent studies infer an increasing CO₂ sink (Landschutzer et al., 2015; Takahashi et al., 2012; Zickfeld et al., 2008).

Although the Southern Ocean plays a crucial role as a CO₂ reservoir and regulator of nutrients and heat, it remains under-sampled, especially during the winter season (JJA) (seasonal cycle in the Southern Hemisphere) (Bakker et al., 2014; Monteiro et al., 2010). Consequently, we largely rely on Earth System Models (ESM), inversions and ocean models for both process understanding and future simulation of CO₂ processes in the Southern Ocean. The Coupled Model Intercomparison Project (CMIP) provides an example of such a globally organized platform (Taylor et al., 2012). Although recent studies based on CMIP5 ESMs, forward and inversions models show that CMIP5 models agree on the CO₂ annual mean sink, they disagree with available observations on the phasing of the seasonal cycle of sea-air CO₂ flux (FCO₂) in the Southern Ocean (e.g. Anav et al., 2013; Lenton et al., 2013).

The seasonal cycle is a major mode of variability for chlorophyll (Thomalla et al., 2011) and CO₂ in the Southern Ocean (Monteiro et al., 2010; Lenton et al., 2013). The large-scale seasonal states of sea-air CO₂ fluxes (FCO₂) in the Southern Ocean comprise of extremes of strong summer in-gassing with a weaker in-gassing or even out-gassing in winter (Metzl et al., 2006). These extremes are linked by the autumn and spring transitions. In autumn CO₂ in-gassing weakens linked to the increasing entrainment of sub-surface waters, which are rich in dissolved inorganic carbon (DIC), (Lenton et al., 2013; Metzl et al., 2006; Sarmiento and Gruber, 2006). During spring, the increase of primary production consumes DIC at the surface and increases the ocean's capacity to take up atmospheric CO₂ (Gruber et al., 2009; Le Quéré and Saltzman, 2013; Pasquer et al., 2015; Gregor et al., 2017). The increase of sea surface temperature (SST) in summer reduces surface CO₂ solubility, which counteracts

V2 Changes 2018/4/17 11:06 AM

Formatted: Font:+Theme Body

V2 Changes 2018/4/17 11:06 AM

Deleted: -

V2 Changes 2018/4/17 11:06 AM

Formatted

... [29]

V2 Changes 2018/4/17 11:06 AM

Deleted: suggests

V2 Changes 2018/4/17 11:06 AM

Formatted

... [30]

V2 Changes 2018/4/17 11:06 AM

Deleted: and Gerber

V2 Changes 2018/4/17 11:06 AM

Formatted: Font:+Theme Body

V2 Changes 2018/4/17 11:06 AM

Deleted: Australian annual

V2 Changes 2018/4/17 11:06 AM

Formatted

... [31]

V2 Changes 2018/4/17 11:06 AM

Deleted: Recent

V2 Changes 2018/4/17 11:06 AM

Formatted: Font:+Theme Body

V2 Changes 2018/4/17 11:06 AM

Deleted:

V2 Changes 2018/4/17 11:06 AM

Formatted: Font:+Theme Body

V2 Changes 2018/4/17 11:06 AM

Deleted: ingassing

V2 Changes 2018/4/17 11:06 AM

Formatted: Font:+Theme Body

V2 Changes 2018/4/17 11:06 AM

Deleted: ingassing

V2 Changes 2018/4/17 11:06 AM

Formatted: Font:+Theme Body

V2 Changes 2018/4/17 11:06 AM

Deleted: outgassing

V2 Changes 2018/4/17 11:06 AM

Formatted: Font:+Theme Body

V2 Changes 2018/4/17 11:06 AM

Deleted: ingassing

V2 Changes 2018/4/17 11:06 AM

Formatted: Font:+Theme Body

V2 Changes 2018/4/17 11:06 AM

Deleted: ocean

V2 Changes 2018/4/17 11:06 AM

Formatted: Font:+Theme Body

V2 Changes 2018/4/17 11:06 AM

Deleted: ,

V2 Changes 2018/4/17 11:06 AM

Formatted: Normal1

146 the biological uptake and reduces the CO₂ flux from the atmosphere (Takahashi et al., 2002; Lenton et
147 al., 2013).

148
149 FCO₂ is also spatially variable in the Southern Ocean at the seasonal scale. North of 50°S is generally
150 the main CO₂ uptake zone (Hauck et al., 2015; Sabine et al., 2004). This region forms a major part of
151 the sub-Antarctic Zone and is characterized by the confluence of upwelled, colder and nutrient-rich
152 deep circumpolar water and mid-latitudes warm water (McNeil et al., 2007; Sallée et al., 2006). It is
153 characterized by enhanced biological uptake during spring and solubility-driven CO₂ uptake due to
154 cool surface waters (Marinov et al., 2006; Metzl, 2009; Takahashi et al., 2012). South of 60°S towards
155 the marginal ice Zone, CO₂ fluxes are largely dominated by out-gassing, driven by the upwelling of
156 circumpolar waters, which are rich in DIC (Matear and Lenton, 2008; McNeil et al., 2007).

157
158 The inability of CMIP5 ESM to simulate a comparable FCO₂ seasonal cycle with available observations
159 estimates in the Southern Ocean has been the subject of recent literature (e.g. Anav et al., 2013;
160 Kessler and Tjiputra, 2016) and the mechanisms associated with these biases are still not well
161 understood. This model-observations disagreement highlights that the current ESMs might not
162 adequately capture the dominant seasonal processes driving the FCO₂ in the Southern Ocean. It also
163 questions the sensitivity of models to adequately simulate the Southern Ocean century-scale CO₂ sink
164 and its sensitivity to climate change feedbacks (Lenton et al., 2013). Efforts to improve simulations of
165 CO₂ properties with respect to observations in the Southern Ocean are ongoing using forced ocean
166 models (e.g. Pasquer et al., 2015; Rodgers et al., 2014; Visinelli et al., 2016; Rosso et al., 2017).
167 However, it remains a challenge for fully coupled simulations. In a previous study, we developed a
168 diagnostic framework to evaluate the seasonal characteristics of the drivers of FCO₂ in ocean
169 biogeochemical models (Mongwe et al., 2016). We here apply this approach to 10 CMIP5 models
170 against observation product estimates in the Southern Ocean. The subsequent analysis is divided as
171 follows; the methods section (section 2) explains our methodological approach, followed by results
172 (section 3), which comprise four subsections. Section 3.1 explores the spatial variability of the annual
173 mean representation of FCO₂ in the 10 CMIP5 models against observation product estimates; section
174 3.2 quantifies the biases in the FCO₂ seasonal cycles in the 10 models. Section 3.3 investigates surface
175 ocean drivers of FCO₂ changes (temperature driven solubility and primary production), and finally,
176 section 3.4 examines the source terms in the DIC surface budget (primary production, entrainment
177 rates and vertical gradients) and their role in surface pCO₂ changes. The discussion (section 4) is an
178 examination of the mechanisms behind the pCO₂ and FCO₂ biases in the models. We conclude with a
179 synthesis of the main findings and their implications.

180
181

- V2 Changes 2018/4/17 11:06 AM
Deleted: zone
- V2 Changes 2018/4/17 11:06 AM
Formatted: Font:+Theme Body
- V2 Changes 2018/4/17 11:06 AM
Deleted:) .
- V2 Changes 2018/4/17 11:06 AM
Formatted: Font:+Theme Body
- V2 Changes 2018/4/17 11:06 AM
Deleted:
- V2 Changes 2018/4/17 11:06 AM
Formatted: Font:+Theme Body
- V2 Changes 2018/4/17 11:06 AM
Deleted: zone
- V2 Changes 2018/4/17 11:06 AM
Formatted: Font:+Theme Body
- V2 Changes 2018/4/17 11:06 AM
Deleted: outgassing
- V2 Changes 2018/4/17 11:06 AM
Formatted: Font:+Theme Body
- V2 Changes 2018/4/17 11:06 AM
Deleted: predict
- V2 Changes 2018/4/17 11:06 AM
Formatted: Font:+Theme Body
- V2 Changes 2018/4/17 11:06 AM
Deleted:
- V2 Changes 2018/4/17 11:06 AM
Formatted: Font:+Theme Body
- V2 Changes 2018/4/17 11:06 AM
Formatted: Font:+Theme Body
- V2 Changes 2018/4/17 11:06 AM
Deleted: quantitatively
- V2 Changes 2018/4/17 11:06 AM
Formatted: Font:+Theme Body
- V2 Changes 2018/4/17 11:06 AM
Formatted: Font:+Theme Body
- V2 Changes 2018/4/17 11:06 AM
Formatted: Font:+Theme Body
- V2 Changes 2018/4/17 11:06 AM
Formatted: Font:+Theme Body
- V2 Changes 2018/4/17 11:06 AM
Formatted: Normal1
- V2 Changes 2018/4/17 11:06 AM
Formatted: Font:+Theme Body, 14 pt, Bold
- V2 Changes 2018/4/17 11:06 AM
Deleted: ,
- V2 Changes 2018/4/17 11:06 AM
Formatted: Normal1

190 **2. Methods**

191

192 The Southern Ocean is here defined as the ocean south of the Sub-Tropical Front (STF, defined
193 according to Orsi et al., (1995), 11.3°C isotherm at 100m). It is divided into two main domains, the Sub-
194 Antarctic Zone; between the STF and the Polar Front (PF: 2°C isotherm at 200m) and the Antarctic
195 Zone, south of the PF. Within the Sub-Antarctic Zone and Antarctic Zone, we further partition the
196 domain into the three main basins of the Southern Ocean i.e. Pacific, Atlantic and the Indian zone.

197

198 **2.1 Observations datasets**

199

200 We used the Landschützer et al. (2014) data product (FCO₂ and partial pressure of CO₂ (pCO₂) as the
201 main suite of observations-based estimates against which to compare the models throughout the
202 analysis. Landschützer et al. (2014) dataset is synthesized from Surface Ocean CO₂ Atlas version 2
203 (SOCAT2) observations and high resolution winds using a Self-Organizing Map (SOM) through a Feed
204 Forward Neural Network (FNN) approach (Landschützer et al., 2013). While Landschützer et al.
205 (2014) dataset is based on more *in situ* observations (SOCAT2, 15 million source measurements)
206 (Bakker et al., 2014) in comparison to Takahashi et al., (2009) (3 million surface measurements), used
207 in Mongwe et al., (2016). We are nevertheless mindful that due to paucity of observations in the
208 Southern Ocean, this data product is still subject to significant uncertainties, as discussed in Ritter et
209 al. (2018). To evaluate the uncertainty between data products we compare the Landschützer et al.
210 (2014) data with Gregor et al. (2017) data product, which is based on two independent empirical
211 models: Support Vector Regression (SVR) and Random Forest Regression (RFR) as well as against
212 Takahashi et al. (2009) for pCO₂ in the Southern Ocean. We compare pCO₂ instead of FCO₂ firstly,
213 because Gregor et al., (2017) only provided fugacity and pCO₂, and being mindful that the choice of
214 wind product and transfer velocity constant in computing FCO₂ would increase the level of uncertainty
215 (Swart et al., 2014). Secondly, while the focus of the paper is on the examination biases in the air-sea
216 fluxes of CO₂, the major part of our analysis is based on pCO₂, which primarily determines the direction
217 and part of the magnitude of the fluxes. We find that the three data products agree on the seasonal
218 phasing of pCO₂ in the Sub-Antarctic Zone, but they show differences in the magnitudes (Fig. S1). In the
219 Antarctic Zone, all three datasets agree in both phasing and amplitude (Fig. S1). At this stage it is not
220 clear whether this agreement is due to all the methods converging even with the sparse data or the
221 reason for agreement is the lack of observations. Nevertheless, more independent in situ observations
222 will be helpful to resolve this issue. In this regard float observations from the SOCCOM program
223 (Johnson et al., 2017) and glider observations (Monteiro et al., 2015) for example, are likely to become

4

Formatted ... [33]
V2 Changes 2018/4/17 11:06 AM
Deleted: Ocean
V2 Changes 2018/4/17 11:06 AM
Formatted ... [34]
V2 Changes 2018/4/17 11:06 AM
Formatted ... [35]
V2 Changes 2018/4/17 11:06 AM
Deleted: to
V2 Changes 2018/4/17 11:06 AM
Formatted ... [36]
V2 Changes 2018/4/17 11:06 AM
Deleted:
V2 Changes 2018/4/17 11:06 AM
Formatted ... [37]
V2 Changes 2018/4/17 11:06 AM
Deleted:
V2 Changes 2018/4/17 11:06 AM
Formatted ... [38]
V2 Changes 2018/4/17 11:06 AM
Deleted:
V2 Changes 2018/4/17 11:06 AM
Formatted ... [39]
V2 Changes 2018/4/17 11:06 AM
Deleted: a
V2 Changes 2018/4/17 11:06 AM
Formatted ... [40]
V2 Changes 2018/4/17 11:06 AM
Deleted: ,
V2 Changes 2018/4/17 11:06 AM
Formatted ... [41]
V2 Changes 2018/4/17 11:06 AM
Deleted: flux
V2 Changes 2018/4/17 11:06 AM
Formatted ... [42]
V2 Changes 2018/4/17 11:06 AM
Deleted: diagnostic
V2 Changes 2018/4/17 11:06 AM
Formatted ... [43]
V2 Changes 2018/4/17 11:06 AM
Deleted: zone
V2 Changes 2018/4/17 11:06 AM
Formatted ... [44]
V2 Changes 2018/4/17 11:06 AM
Deleted: zone
V2 Changes 2018/4/17 11:06 AM
Formatted ... [45]
V2 Changes 2018/4/17 11:06 AM
Deleted: is reason for the agreement.
V2 Changes 2018/4/17 11:06 AM
Formatted ... [46]
V2 Changes 2018/4/17 11:06 AM
Deleted:)
V2 Changes 2018/4/17 11:06 AM
Formatted ... [47]
V2 Changes 2018/4/17 11:06 AM
Deleted: ,
V2 Changes 2018/4/17 11:06 AM
Formatted ... [32]

249 helpful in resolving these data uncertainties in addition to ongoing ship-based measurements.

250
251 We also used the Takahashi et al. (2009) in situ FCO₂ dataset as a complementary source for
252 comparison of spatial FCO₂ properties in the Southern Ocean. Takahashi et al. (2009) data estimates
253 are comprised of a compilation of about 3 million surface measurements globally, obtained from 1970
254 – 2000 and corrected for reference year 2000. This dataset is used, as provided, on a 4° (latitude) x 5°
255 (longitude) resolution. Using monthly mean sea surface temperature (SST) and salinity from the World
256 Ocean Atlas 2013 (WOA13) dataset (Locarnini et al., 2013), we reconstructed total alkalinity (TALK)
257 using the Lee et al. (2006) formulation. We also use this dataset as the main observations platform in
258 section 2.3. To calculate the uncertainty of the computed TALK, we compared the calculated total
259 alkalinity (TALK_{calc}) based on ship measurements of SST and surface salinity dataset with actual
260 observed TALK_{obs} of the same measurements for a set of winter (August) data collected in the Southern
261 Ocean. We found that TALK_{calc} compares well with TALK_{obs} (R² = 0.79) (Fig. S2, Supplementary). We
262 then used this computed monthly TALK and pCO₂ from Landschützer et al. (2014) to compute DIC
263 using CO2SYS (Pierrot et al., 2006, http://cdiac.ornl.gov/ftp/co2sys/CO2SYS_calc_XLS_v2.1), using K1,
264 K2 from Mehrbach et al. (1973), refitted by Dickson and Millero (1987). For interior ocean DIC, we
265 used the Global Ocean Data Analysis Project version 2 (GLODAP2) annual means dataset (Lauvset et
266 al., 2016). The Mixed Layer Depth (MLD) data was taken from de Boyer Montégut et al. (2004), on a 1°
267 x 1° grid, the data is provided as monthly means climatology and was used as provided. We also use
268 satellite chlorophyll dataset from Johnson et al. (2013).

269 270 2.2 CMIP5 Model data

271
272 We used 10 models from the Coupled Model Intercomparison Project version 5 (CMIP5) Earth System
273 Models (ESM) shown in Table 1. The selection criterion for the models was based on the availability of
274 essential variables for the analysis in the CMIP5 data portal (<http://pcmdi9.llnl.gov>) at the time of
275 writing: i.e. monthly FCO₂, pCO₂, chlorophyll, net primary production (NPP), surface oxygen, surface
276 Dissolved Inorganic Carbon (DIC), MLD, Sea Surface Temperature (SST), vertical temperature fields
277 and annual DIC for the historical scenario. The analysis is primarily based on the climatology over
278 1995 – 2005, which was selected to match a period closest to the available observational data product
279 (Landschützer et al. (2014), 1998 – 2011). However, we do examine the consistency of the seasonality
280 of FCO₂ over periods longer than 10 years by comparing the seasonal cycle of FCO₂ and temporal
281 standard deviation of 30 years (1975 – 2005) vs 10 years (1995 – 2005) for HadGEM2-ES and
282 CanESM2. We find that the seasonal cycle of FCO₂ remains consistent (R = 0.99) in both HadGEM2-ES

V2 Changes 2018/4/17 11:06 AM
Deleted:
V2 Changes 2018/4/17 11:06 AM
Formatted ... [49]
V2 Changes 2018/4/17 11:06 AM
Deleted: ,
V2 Changes 2018/4/17 11:06 AM
Formatted ... [50]
V2 Changes 2018/4/17 11:06 AM
Deleted: TALK_{obs}
V2 Changes 2018/4/17 11:06 AM
Formatted ... [51]
V2 Changes 2018/4/17 11:06 AM
Formatted ... [52]
V2 Changes 2018/4/17 11:06 AM
Formatted ... [53]
V2 Changes 2018/4/17 11:06 AM
Deleted: ,
V2 Changes 2018/4/17 11:06 AM
Formatted ... [54]
V2 Changes 2018/4/17 11:06 AM
Deleted: refitted
V2 Changes 2018/4/17 11:06 AM
Formatted ... [55]
V2 Changes 2018/4/17 11:06 AM
Deleted: ,
V2 Changes 2018/4/17 11:06 AM
Formatted ... [56]
V2 Changes 2018/4/17 11:06 AM
Deleted: ,
V2 Changes 2018/4/17 11:06 AM
Formatted ... [57]
V2 Changes 2018/4/17 11:06 AM
Deleted: ,
V2 Changes 2018/4/17 11:06 AM
Formatted ... [58]
V2 Changes 2018/4/17 11:06 AM
Deleted:
V2 Changes 2018/4/17 11:06 AM
Formatted ... [59]
V2 Changes 2018/4/17 11:06 AM
Formatted ... [60]
V2 Changes 2018/4/17 11:06 AM
Deleted:
V2 Changes 2018/4/17 11:06 AM
Formatted ... [61]
V2 Changes 2018/4/17 11:06 AM
Formatted ... [62]
V2 Changes 2018/4/17 11:06 AM
Formatted ... [63]
V2 Changes 2018/4/17 11:06 AM
Deleted: ,
V2 Changes 2018/4/17 11:06 AM
Formatted ... [48]

293 and CanESM2 over 30 years (Fig. S3). All CMIP5 model outputs were regridded into a common 1°x1°
 294 regular grid throughout the analysis, except for annual CO₂ mean fluxes, which were computed on the
 295 original grid for each model.

296 **Table 1:** A description of the 10 CMIP5 ESMs that were used in this analysis. It shows the ocean
 297 resolution, atmospheric resolution, and available nutrients for the biogeochemical component, sea-ice
 298 model, vertical levels and the marine biogeochemical component for each ESM.

Full name and Source	Model Name	Ocean Resolution	Atmospheric Resolution	Nutrients	Sea ice model	Vertical Coordinate & Levels	Ocean Biology	Reference
Canadian Centre for Climate Modelling and Analysis, Canada	CanESM2	CanOM4 0.9°x1.4°	2.8125° x 2.8125°	N (accounts for Fe limitation)	CanSIM1	z 40 levels	NPZD	Zahariev et al., 2008
Centro Euro-Mediterraneo sui Cambiamenti Climatici, Italy	CMCC-CESM	OPA8.2 0.5-2°x2°	3.8° x 3.7°	P, N, Fe, Si	CICE4	z 21 levels	PELAGOS	Vichi et al., 2007
Centre National de Recherches Météorologiques-Centre Européen de Recherche et de Formation Avancée en Calcul Scientifique, France	CNRM-CM5	NEMOv3.3 1°	1.4°	P, N, Fe, Si	GELATO5	z 42 levels	PISCES	Séférian et al., 2013
Institut Pierre-Simon Laplace, France	IPSL-CM5A-MR	NEMO2.3 0.5-2° x 2°	2.58° x 1.25°	P, N, Fe, Si	LIM2	z 31 levels	PISCES	Séférian et al., 2013
Max Planck Institute for Meteorology, Germany	MPI-ESM-MR	MPIOM 1.41°x0.89°	1.875° x 1.875°	P, N, Fe, Si	MPIOM	z 40 levels	HAMOCC	Ilyina et al., 2013

Deleted: year

V2 Changes 2018/4/17 11:06 AM
Formatted ... [65]

V2 Changes 2018/4/17 11:06 AM
Formatted Table ... [66]

V2 Changes 2018/4/17 11:06 AM
Formatted ... [67]

V2 Changes 2018/4/17 11:06 AM
Formatted ... [68]

V2 Changes 2018/4/17 11:06 AM
Formatted ... [69]

V2 Changes 2018/4/17 11:06 AM
Formatted ... [79]

V2 Changes 2018/4/17 11:06 AM
Formatted ... [70]

V2 Changes 2018/4/17 11:06 AM
Formatted ... [71]

V2 Changes 2018/4/17 11:06 AM
Formatted ... [76]

V2 Changes 2018/4/17 11:06 AM
Formatted ... [72]

V2 Changes 2018/4/17 11:06 AM
Formatted ... [73]

V2 Changes 2018/4/17 11:06 AM
Formatted ... [74]

V2 Changes 2018/4/17 11:06 AM
Formatted ... [75]

V2 Changes 2018/4/17 11:06 AM
Formatted ... [77]

V2 Changes 2018/4/17 11:06 AM
Formatted ... [78]

V2 Changes 2018/4/17 11:06 AM
Formatted ... [80]

V2 Changes 2018/4/17 11:06 AM
Formatted ... [81]

V2 Changes 2018/4/17 11:06 AM
Formatted ... [82]

V2 Changes 2018/4/17 11:06 AM
Formatted ... [83]

V2 Changes 2018/4/17 11:06 AM
Formatted ... [84]

V2 Changes 2018/4/17 11:06 AM
Formatted ... [85]

V2 Changes 2018/4/17 11:06 AM
Formatted ... [86]

V2 Changes 2018/4/17 11:06 AM
Formatted ... [87]

V2 Changes 2018/4/17 11:06 AM
Formatted ... [88]

V2 Changes 2018/4/17 11:06 AM
Formatted ... [89]

V2 Changes 2018/4/17 11:06 AM
Formatted ... [90]

V2 Changes 2018/4/17 11:06 AM
Formatted ... [91]

V2 Changes 2018/4/17 11:06 AM
Formatted ... [92]

V2 Changes 2018/4/17 11:06 AM
Formatted ... [93]

V2 Changes 2018/4/17 11:06 AM
Formatted ... [94]

V2 Changes 2018/4/17 11:06 AM
Formatted ... [95]

V2 Changes 2018/4/17 11:06 AM
Formatted ... [96]

V2 Changes 2018/4/17 11:06 AM
Formatted ... [97]

V2 Changes 2018/4/17 11:06 AM
Formatted ... [98]

V2 Changes 2018/4/17 11:06 AM
Formatted ... [99]

V2 Changes 2018/4/17 11:06 AM
Formatted ... [100]

V2 Changes 2018/4/17 11:06 AM
Formatted ... [101]

V2 Changes 2018/4/17 11:06 AM
Formatted ... [102]

V2 Changes 2018/4/17 11:06 AM
Formatted ... [103]

Community	CESM1-BGC	0.3° x 1°	0.9° x 1.25°	(P), N, Fe,	z	BEC	Moore et al.,
Earth System Model, USA				Si	60 levels		2004
Norwegian	NorESM1-ME	MICOM	2.5° x 1.9°	P, N, Fe, Si	CICE4.1	ρ	HAMOCC
Earth System Model, Norway		0.5° x 0.9°			53 levels		2013
Geophysical Fluid Dynamics Laboratory Earth System Model, USA	GFDL-ESM2M	0.3° x 1°	2.5° x 2.0°	N, P, SiO ₄ , Fe	SISp2	z	TOPAZ2
						50 levels	Dunne et al., 2013
Meteorological Research Institute-Earth System Model Version 1, Japan	MRI-ESM	0.5° x 1°		P, N	MRI.COM3	σ-z	NPZD
						51 levels	Adachi et al., 2013
Hadley Global Environment Model 2 - Earth System, UK	HadGEM-ES	0.3° x 1°	2.5° x 2.0°	N, Fe, S		40 levels	Diat-HadOCC
							Palmer and Totterdell, 2001

- Formatted ... [135]
- V2 Changes 2018/4/17 11:06 AM
- Formatted ... [136]
- V2 Changes 2018/4/17 11:06 AM
- Formatted ... [137]
- V2 Changes 2018/4/17 11:06 AM
- Formatted ... [138]
- V2 Changes 2018/4/17 11:06 AM
- Formatted ... [140]
- V2 Changes 2018/4/17 11:06 AM
- Formatted ... [141]
- V2 Changes 2018/4/17 11:06 AM
- Formatted ... [139]
- V2 Changes 2018/4/17 11:06 AM
- Formatted ... [142]
- V2 Changes 2018/4/17 11:06 AM
- Formatted ... [143]
- V2 Changes 2018/4/17 11:06 AM
- Formatted ... [144]
- V2 Changes 2018/4/17 11:06 AM
- Formatted ... [145]
- V2 Changes 2018/4/17 11:06 AM
- Formatted ... [146]
- V2 Changes 2018/4/17 11:06 AM
- Formatted ... [147]
- V2 Changes 2018/4/17 11:06 AM
- Formatted ... [148]
- V2 Changes 2018/4/17 11:06 AM
- Formatted ... [149]
- V2 Changes 2018/4/17 11:06 AM
- Formatted ... [150]
- V2 Changes 2018/4/17 11:06 AM
- Formatted ... [151]
- V2 Changes 2018/4/17 11:06 AM
- Formatted ... [152]
- V2 Changes 2018/4/17 11:06 AM
- Formatted ... [153]
- V2 Changes 2018/4/17 11:06 AM
- Formatted ... [154]
- V2 Changes 2018/4/17 11:06 AM
- Formatted ... [155]
- V2 Changes 2018/4/17 11:06 AM
- Formatted ... [156]
- V2 Changes 2018/4/17 11:06 AM
- Formatted ... [157]
- V2 Changes 2018/4/17 11:06 AM
- Formatted ... [158]
- V2 Changes 2018/4/17 11:06 AM
- Formatted ... [159]
- V2 Changes 2018/4/17 11:06 AM
- Moved (insertion) [1] ... [160]
- V2 Changes 2018/4/17 11:06 AM
- Formatted ... [161]
- V2 Changes 2018/4/17 11:06 AM
- Formatted ... [162]
- V2 Changes 2018/4/17 11:06 AM
- Formatted ... [163]
- V2 Changes 2018/4/17 11:06 AM
- Moved (insertion) [2] ... [164]
- V2 Changes 2018/4/17 11:06 AM
- Formatted ... [165]
- V2 Changes 2018/4/17 11:06 AM
- Moved (insertion) [4] ... [166]
- V2 Changes 2018/4/17 11:06 AM
- Formatted ... [167]
- V2 Changes 2018/4/17 11:06 AM
- Formatted ... [168]
- V2 Changes 2018/4/17 11:06 AM
- Formatted ... [169]
- V2 Changes 2018/4/17 11:06 AM
- Formatted ... [134]

303
304
305
306
307
308
309
310
311
312
313
314
315
316
317
318
319
320

2.3 Sea-Air CO₂ Flux Drivers: The Seasonal Cycle Diagnostic Framework

The seasonal cycle of the ocean-atmosphere pCO₂ gradient (ΔpCO₂) is the main driver of the variability of FCO₂ over comparable periods (Sarmiento and Gruber, 2006; Wanninkhof et al., 2009; Mongwe et al., 2016). Wind speed plays a dual role as a driver of FCO₂: it drives the seasonal evolution of buoyancy-mixing dynamics, which influences the biogeochemistry and upper water column physics (but these processes are incorporated into the variability of the DIC), as well as the rate of gas exchange across the air-sea interface (Wanninkhof et al., 2013). However, because winds in the Southern Ocean do not have large seasonal variation (Young, 1999), for this analysis, we neglect the role of wind as a secondary driver of the seasonal cycle of FCO₂. Consequently, the seasonal cycle of FCO₂ is directly linked to surface pCO₂ variability, influenced by changes in temperature, salinity, TALK and DIC and macronutrients (Sarmiento and Gruber, 2006; Wanninkhof et al., 2009). In this analysis we use this assumption as a basis to explore how the seasonal variability of temperature and DIC regulate the seasonal cycle of pCO₂ in CMIP5 models relative to observational product estimates.

The seasonal cycle diagnostic framework was developed as a way of scaling the relative contributions

7

321 from the rates of change of SST, and the total DIC-driven changes to the seasonal cycle of pCO₂ on to a
322 common DIC scale (Mongwe et al., 2016). We use the framework to explore how understanding
323 differences emerging from the temperature- and DIC-driven CO₂ variability could be helpful as a
324 diagnostic of the apparent observations – model seasonal cycle biases in the Southern Ocean.

325
326 The total rate of change of DIC in the surface layer consists of the contribution of air-sea exchanges,
327 biological, vertical and horizontal transport-driven changes (Eq. 1).

$$328 \left(\frac{\partial DIC}{\partial t}\right)_{Tot} = \left(\frac{\partial DIC}{\partial t}\right)_{air-sea} + \left(\frac{\partial DIC}{\partial t}\right)_{Bio} + \left(\frac{\partial DIC}{\partial t}\right)_{Vert} + \left(\frac{\partial DIC}{\partial t}\right)_{Hor} \quad (1)$$

330 Because we used zonal means from medium resolution models, we assume that the horizontal terms
331 are negligible, though mindful that there could be a seasonal cycle in the divergence of the horizontal
332 transport due to a latitudinal gradient in DIC perturbed by Ekman flow in some regions of the Sub-
333 Antarctic Zone (Rosso et al., 2017). This leaves air-sea exchange, vertical fluxes (advection and
334 diffusion) and biological processes as the dominant drivers of DIC.

335 Since temperature does not affect DIC changes directly, but only pCO₂ through solubility, it was
336 necessary to scale the influence of temperature into equivalent DIC units in order to compare the
337 influence of temperature vs DIC control of surface pCO₂ variability. Thus in order to constrain the
338 contribution of temperature on the seasonal variability of pCO₂ and FCO₂ we derived a new synthetic
339 temperature-linked term, “DIC equivalent” (DIC_T) defined as: the magnitude of DIC change that would
340 correspond to a change in pCO₂ driven by a particular temperature change. In this way the ΔpCO₂
341 driven solely by modelled or observed temperature change, is converted into equivalent DIC units,
342 which allows its contribution to be scaled against the observed or modelled total surface DIC change
343 (Eq.1). Shifts between temperature and DIC control of pCO₂ are in effect tipping points because they
344 reflect major shifts in the mechanisms that drive pCO₂ variability. We use this as the basis to
345 investigate the possible mechanisms behind model biases in the seasonal cycle of pCO₂.

346 This calculation of DIC_T is done in two steps: firstly, the temperature impact on pCO₂ is calculated
347 using the Takahashi et al. (1993) empirical expression that linearizes the temperature dependence of
348 the equilibrium constants.

$$349 \left(\frac{\partial pCO_2}{\partial t}\right)_{SST} = 0.0423 \times pCO_2 \times \left(\frac{\partial pCO_2}{\partial SST}\right) \quad (2)$$

350 Though this relationship between dSST and dpCO₂ is based on a linear assumption (Takahashi et al.,
351 1993), this formulation has been shown to hold and has been widely used in literature (e.g. Bakker et
352 al., 2014; Feely et al., 2004; Marinov and Gnanadesikan, 2011; Takahashi et al., 2002; Wanninkhof et

V2 Changes 2018/4/17 11:06 AM
Deleted:

V2 Changes 2018/4/17 11:06 AM
Formatted: Font:+Theme Body

V2 Changes 2018/4/17 11:06 AM
Formatted ... [170]

V2 Changes 2018/4/17 11:06 AM
Deleted:

V2 Changes 2018/4/17 11:06 AM
Deleted:

V2 Changes 2018/4/17 11:06 AM
Formatted: Font:+Theme Body

V2 Changes 2018/4/17 11:06 AM
Formatted ... [171]

V2 Changes 2018/4/17 11:06 AM
Deleted:

V2 Changes 2018/4/17 11:06 AM
Formatted: Font:+Theme Body

V2 Changes 2018/4/17 11:06 AM
Deleted: which

V2 Changes 2018/4/17 11:06 AM
Formatted: Font:+Theme Body

V2 Changes 2018/4/17 11:06 AM
Deleted: In

V2 Changes 2018/4/17 11:06 AM
Formatted: Normal1

V2 Changes 2018/4/17 11:06 AM
Formatted ... [172]

V2 Changes 2018/4/17 11:06 AM
Deleted: term

V2 Changes 2018/4/17 11:06 AM
Formatted ... [173]

V2 Changes 2018/4/17 11:06 AM
Deleted: ,

V2 Changes 2018/4/17 11:06 AM
Formatted ... [174]

V2 Changes 2018/4/17 11:06 AM
Deleted: ,

V2 Changes 2018/4/17 11:06 AM
Formatted: Font:+Theme Body

V2 Changes 2018/4/17 11:06 AM
Formatted ... [175]

V2 Changes 2018/4/17 11:06 AM
Deleted: ,

V2 Changes 2018/4/17 11:06 AM
Formatted: Normal1

371 al., 2009; Landschützer et al., 2018). We show in the supplementary material that the extension of this
372 expression into polar temperature ranges (SST < 2°C) only introduces a minor additional uncertainty
373 of 4 -5% (SM Fig. S4).

374 Secondly, the temperature-driven change in pCO₂ is converted to an equivalent DIC_T using the Revelle
375 factor.

$$376 \left(\frac{\partial \text{DIC}_T}{\partial t}\right)_{\text{SST}} = \frac{\text{DIC}}{\gamma_{\text{DIC}} \times \text{pCO}_2} \left(\frac{\partial \text{pCO}_2}{\partial t}\right)_{\text{SST}} \quad (3)$$

377 Here we also used a fixed value for the Revelle Factor ($\gamma_{\text{DIC}}=14$), typical of polar waters in the Southern
378 Ocean in order to assess the error linked to this assumption. We recomputed the Revelle factor in the
379 Sub-Antarctic and Antarctic Zones using annual mean climatologies of TALK, salinity, sea surface
380 temperature and nutrients. Firstly, we examined DIC changes for the nominal range of pCO₂ change
381 (340 – 399 μatm :1 μatm intervals) and then used this dataset to derive the Revelle factor. The range of
382 calculated Revelle factors in the Southern Ocean was between $\gamma_{\text{DIC}} \sim 12 - 15.5$ with an average of $\gamma_{\text{DIC}} =$
383 13.9 ± 1.3 . This justifies our use of $\gamma_{\text{DIC}} = 14$ for the conversion of the solubility-driven pCO₂ change to
384 an equivalent DIC (DICT) throughout the analysis. We have provided the uncertainty that this
385 conversion makes into the temperature constraint DIC_T, by using the upper and lower limits of the
386 Revelle factor ($\gamma_{\text{DIC}} = 12 - 15.5$) in the model framework. In the Supplementary Material (Fig. S5) we
387 show examples for observations in the Sub-Antarctic and Antarctic Zones, which indicate that the
388 extremes of the Revelle factor values ($\gamma_{\text{DIC}} = 12 - 15.5$) do not alter the phasing or magnitude of the
389 relative controls of temperature or DIC on the seasonal cycle of pCO₂.

390 The rate of change of DIC was discretized on a monthly mean as follows:

$$392 \left(\frac{\partial \text{DIC}_T}{\partial t}\right)_{\text{SST}} \approx \left(\frac{\Delta \text{DIC}}{\Delta t}\right)_{n,l} = \frac{\text{DIC}_{n+1,l} - \text{DIC}_{n,l}}{1 \text{ month}} \quad (4)$$

394 Where n is time in month, l is vertical level (in this case the surface, l=1). We here take the forward
395 derivative such that November rate is the difference between 15 November and 15 December, thus
396 being centered at the interval between the months.

397 Finally, to characterize periods of temperature or DIC dominance as main drivers of the instantaneous
398 (monthly) pCO₂ change we subtract Eq. 1 from Eq. 4, which yields a residual indicator M_{T-DIC} Eq. 5. M_T.

Deleted: 2010
V2 Changes 2018/4/17 11:06 AM
Formatted ... [177]
V2 Changes 2018/4/17 11:06 AM
Deleted: manor
V2 Changes 2018/4/17 11:06 AM
Formatted ... [178]
V2 Changes 2018/4/17 11:06 AM
Deleted:)
V2 Changes 2018/4/17 11:06 AM
Formatted ... [179]
V2 Changes 2018/4/17 11:06 AM
Deleted:
V2 Changes 2018/4/17 11:06 AM
Formatted ... [180]
V2 Changes 2018/4/17 11:06 AM
Formatted ... [181]
V2 Changes 2018/4/17 11:06 AM
Formatted ... [182]
V2 Changes 2018/4/17 11:06 AM
Deleted: but
V2 Changes 2018/4/17 11:06 AM
Formatted ... [183]
V2 Changes 2018/4/17 11:06 AM
Deleted: zones
V2 Changes 2018/4/17 11:06 AM
Formatted ... [184]
V2 Changes 2018/4/17 11:06 AM
Deleted: surface
V2 Changes 2018/4/17 11:06 AM
Formatted ... [185]
V2 Changes 2018/4/17 11:06 AM
Deleted:
V2 Changes 2018/4/17 11:06 AM
Formatted ... [186]
V2 Changes 2018/4/17 11:06 AM
Deleted: an
V2 Changes 2018/4/17 11:06 AM
Formatted ... [187]
V2 Changes 2018/4/17 11:06 AM
Deleted: zones
V2 Changes 2018/4/17 11:06 AM
Formatted ... [188]
V2 Changes 2018/4/17 11:06 AM
Deleted: show
V2 Changes 2018/4/17 11:06 AM
Formatted ... [189]
V2 Changes 2018/4/17 11:06 AM
Formatted ... [190]
V2 Changes 2018/4/17 11:06 AM
Deleted: December the 15th and
V2 Changes 2018/4/17 11:06 AM
Formatted ... [191]
V2 Changes 2018/4/17 11:06 AM
Deleted: the 15th
V2 Changes 2018/4/17 11:06 AM
Formatted ... [192]
V2 Changes 2018/4/17 11:06 AM
Deleted: 4
V2 Changes 2018/4/17 11:06 AM
Formatted ... [193]
V2 Changes 2018/4/17 11:06 AM
Formatted ... [194]
V2 Changes 2018/4/17 11:06 AM
Formatted ... [176]

429 DIC is then used as indicator of the dominant driver of instantaneous pCO₂ changes in this scale monthly
 430 time scale.

$$432 M_{T-DIC} = \left| \left(\frac{\partial DIC_T}{\partial t} \right)_{SST} \right| - \left| \left(\frac{\partial DIC}{\partial t} \right)_{Tot} \right| \quad (5)$$

434 $M_{T-DIC} > 0$ indicates that the pCO₂ variability is dominated by the temperature-driven solubility and
 435 when $M_{T-DIC} < 0$, it indicates that pCO₂ changes are mainly modulated by DIC processes (i.e. Biological
 436 CO₂ changes and vertical scale physical DIC mechanisms). We also examine the following DIC
 437 processes; i.) Biological DIC changes using chlorophyll, NPP, export carbon, surface oxygen, and ii.)
 438 Physical DIC mechanisms using estimated entrainment rates at the base of the mixed layer. Details of
 439 this calculation are in section 2.4.

440 In the Southern Ocean, salinity and TALK are considered lower-order drivers of the seasonal cycle of
 441 pCO₂ (Takahashi et al., 1993). In the supplementary material (Fig. S6), we show that salinity and TALK
 442 do not play a major role as drivers of the local seasonal cycle of pCO₂. We do so by computing the
 443 equivalent rate of change of DIC resulting from seasonal variability of salinity and TALK as done for
 444 temperature (Eq. 2), i.e. still assuming empirical linear relationships from Takahashi et al. (1993):

445 $\left(\frac{\ln(pCO_2)}{\ln(Talk)} \approx -9.4 \right)$ and $\left(\frac{\ln(pCO_2)}{\ln(Sal)} = 0.94 \right)$. By applying these relationships to the model data, we

446 confirmed that indeed salinity and TALK are secondary drivers of pCO₂ changes i.e. $\left[\left(\frac{\partial DIC}{\partial t} \right)_{Tot} \right]_{average} \approx$

447 $5 \mu\text{mol kg}^{-1} \text{ month}^{-1}$, while $\left[\left(\frac{\partial DIC}{\partial t} \right)_{Tot} \right]_{average} \approx 0.6 \mu\text{mol kg}^{-1} \text{ month}^{-1}$ and $\left[\left(\frac{\partial DIC}{\partial t} \right)_{TALK} \right]_{maximum} \approx 0.4$

448 $\mu\text{mol kg}^{-1} \text{ month}^{-1}$.

450 2.4 Entrainment mixing

451 CO₂ uptake by the Southern Ocean has been shown to weaken during winter linked to the entrainment
 452 of sub-surface DIC as the MLD deepens (e.g. Lenton et al., 2013; Metzl et al., 2006; Takahashi et al.,
 453 2009). Here we estimate this rate of entrainment (RE) using Eq. 6, which estimates the advection of
 454 preformed DIC at the base of the mixed layer:

$$457 RE = U_e \left(\frac{\partial DIC}{\partial z} \right)_{MLD} \quad (6)$$

$$458 RE_n = \left(\frac{\Delta MLD_n}{\Delta t} \right) \left(\frac{\Delta DIC}{\Delta z} \right)_{n,MLD} \quad (7)$$

$$459 \left(\frac{\Delta DIC}{\Delta z} \right)_{n,MLD} = \frac{DIC_{n,MLD_{n+1}} - DIC_{n,MLD_n}}{\Delta z} \quad (8)$$

460

10

Deleted: ,
 V2 Changes 2018/4/17 11:06 AM
 Formatted ... [196]
 V2 Changes 2018/4/17 11:06 AM
 Formatted ... [197]
 V2 Changes 2018/4/17 11:06 AM
 Deleted:
 V2 Changes 2018/4/17 11:06 AM
 Deleted:
 V2 Changes 2018/4/17 11:06 AM
 Formatted ... [198]
 V2 Changes 2018/4/17 11:06 AM
 Formatted ... [199]
 V2 Changes 2018/4/17 11:06 AM
 Deleted:) .
 V2 Changes 2018/4/17 11:06 AM
 Formatted ... [200]
 V2 Changes 2018/4/17 11:06 AM
 Deleted: : details
 V2 Changes 2018/4/17 11:06 AM
 Formatted ... [201]
 V2 Changes 2018/4/17 11:06 AM
 Deleted:
 V2 Changes 2018/4/17 11:06 AM
 Formatted ... [203]
 V2 Changes 2018/4/17 11:06 AM
 Deleted:
 V2 Changes 2018/4/17 11:06 AM
 Formatted ... [204]
 V2 Changes 2018/4/17 11:06 AM
 Formatted ... [202]
 V2 Changes 2018/4/17 11:06 AM
 Formatted ... [205]
 V2 Changes 2018/4/17 11:06 AM
 Formatted ... [206]
 V2 Changes 2018/4/17 11:06 AM
 Deleted:
 V2 Changes 2018/4/17 11:06 AM
 Formatted ... [207]
 V2 Changes 2018/4/17 11:06 AM
 Formatted ... [208]
 V2 Changes 2018/4/17 11:06 AM
 Formatted ... [209]
 V2 Changes 2018/4/17 11:06 AM
 Formatted ... [210]
 V2 Changes 2018/4/17 11:06 AM
 Moved up [2]: The seasonal cycl... [211]
 V2 Changes 2018/4/17 11:06 AM
 Formatted ... [212]
 V2 Changes 2018/4/17 11:06 AM
 Deleted: but these processes are ... [213]
 V2 Changes 2018/4/17 11:06 AM
 Moved up [1]: 2013
 V2 Changes 2018/4/17 11:06 AM
 Deleted:) however, because wind... [214]
 V2 Changes 2018/4/17 11:06 AM
 Moved up [3]: (Sarmiento and G... [215]
 V2 Changes 2018/4/17 11:06 AM
 Formatted ... [216]
 V2 Changes 2018/4/17 11:06 AM
 Moved up [4]: In this analysis w... [217]
 V2 Changes 2018/4/17 11:06 AM
 ... [218]
 V2 Changes 2018/4/17 11:06 AM
 Formatted ... [219]
 V2 Changes 2018/4/17 11:06 AM
 V2 Changes 2018/4/17 11:06 AM
 Formatted ... [220]
 V2 Changes 2018/4/17 11:06 AM
 V2 Changes 2018/4/17 11:06 AM
 Formatted ... [221]
 V2 Changes 2018/4/17 11:06 AM
 Formatted ... [222]
 V2 Changes 2018/4/17 11:06 AM

558 In which U_e is an equivalent entrainment velocity based on the rate of change of the MLD, and n is the
559 time in months. This approximation of vertical entrainment is necessary as it is not possible to
560 compute this term from the CMIP5 data because the vertical DIC distribution is only available as an
561 annual means. We use the entrainment rates to estimate the influence of subsurface/bottom DIC
562 changes on surface DIC changes, and subsequently pCO_2 and FCO_2 . Because we are mainly interested in
563 the period autumn-winter, where the MLD ≥ 60 m in the Sub-Antarctic Zone and ≥ 40 m in the
564 Antarctic Zone, at this depth seasonal variations in DIC are anticipated to be minimal, these estimates
565 can be used. The monthly and annual mean DIC from a NEMO PISCES $0.5 \times 0.5^\circ$ model output were,
566 used to estimate the uncertainty by comparing RE computed from both (Dufour et al., 2013). We found
567 the annual and monthly estimates to be indeed comparable with minimal differences (not shown). It is
568 noted as a caveat that this rate of entrainment is only a coarse estimate because we were using annual
569 means, and is intended only for the autumn-winter period when MLDs are deepened.

571 3. Results

573 3.1 Annual climatological sea-air CO_2 fluxes

574 The annual mean climatological distribution of FCO_2 in the Southern Ocean obtained from
575 observational products is spatially variable, but mainly characterized by two key features: (i) CO_2 in-
576 gassing north of 50° - 55° S (Polar Frontal Zone, PFZ) within and north of the Sub-Antarctic Zone, and
577 (ii), CO_2 out-gassing between the PF ($\sim 58^\circ$ S) and the Marginal Ice Zone (MIZ, $\sim 60^\circ$ - 68° S) (Fig. 1a-b).
578 Most CMIP5 models broadly capture these features, however, they also show significant differences in
579 space and magnitude between the basins of the Southern Ocean (Fig. 1). With the exception of CMCC-
580 CESM, which shows a northerly-extended CO_2 out-gassing band between about 40° S and 50° S, CMIP5
581 models generally show the CO_2 out-gassing zone between 50° S- 70° S in agreement with observational
582 estimates (Fig. 1).

583 The analyzed 10 CMIP5 models show a large spatial dispersion in the spatial representation of the
584 magnitudes of FCO_2 with respect to observations (Fig. 1, Table 2). They generally overestimate the
585 upwelling-driven CO_2 out-gassing (55° S - 70° S) in some basins relative to observations. IPSL-CM5A,
586 CanESM2, MPI-ESM, GFDL-ESM2M and MRI-ESM, for example, show CO_2 out-gassing fluxes reaching
587 up to $25 \text{ g m}^{-2} \text{ yr}^{-1}$, while observations only show a maximum of $8 \text{ g m}^{-2} \text{ yr}^{-1}$ (Fig. 1). Between 40° S-
588 56° S (Sub-Antarctic Zone), observations and CMIP5 models largely agree, showing a CO_2 in-gassing
589 feature, which is mainly attributable to biological processes (McNeil et al., 2007; Takahashi et al.,
590 2012). South of 65° S, in the MIZ, models generally show an excessive CO_2 in-gassing with respect to

Deleted: .

V2 Changes 2018/4/17 11:06 AM
Formatted ... [227]

V2 Changes 2018/4/17 11:06 AM
Deleted: estimates

V2 Changes 2018/4/17 11:06 AM
Formatted ... [228]

V2 Changes 2018/4/17 11:06 AM
Deleted: driven

V2 Changes 2018/4/17 11:06 AM
Formatted ... [229]

V2 Changes 2018/4/17 11:06 AM
Deleted: -

V2 Changes 2018/4/17 11:06 AM
Formatted ... [230]

V2 Changes 2018/4/17 11:06 AM
Deleted: zone

V2 Changes 2018/4/17 11:06 AM
Formatted ... [231]

V2 Changes 2018/4/17 11:06 AM
Deleted: zone,

V2 Changes 2018/4/17 11:06 AM
Formatted ... [232]

V2 Changes 2018/4/17 11:06 AM
Deleted: thus

V2 Changes 2018/4/17 11:06 AM
Formatted ... [233]

V2 Changes 2018/4/17 11:06 AM
Deleted: was

V2 Changes 2018/4/17 11:06 AM
Formatted ... [234]

V2 Changes 2018/4/17 11:06 AM
Deleted: that

V2 Changes 2018/4/17 11:06 AM
Formatted ... [235]

V2 Changes 2018/4/17 11:06 AM
Deleted: deepen

V2 Changes 2018/4/17 11:06 AM
Formatted ... [236]

V2 Changes 2018/4/17 11:06 AM
Formatted ... [237]

V2 Changes 2018/4/17 11:06 AM
Deleted: zone

V2 Changes 2018/4/17 11:06 AM
Formatted ... [238]

V2 Changes 2018/4/17 11:06 AM
Deleted:

V2 Changes 2018/4/17 11:06 AM
Formatted ... [239]

V2 Changes 2018/4/17 11:06 AM
Deleted: outgassing

V2 Changes 2018/4/17 11:06 AM
Formatted ... [240]

V2 Changes 2018/4/17 11:06 AM
Deleted: outgassing

V2 Changes 2018/4/17 11:06 AM
Deleted: -

V2 Changes 2018/4/17 11:06 AM
Formatted ... [241]

V2 Changes 2018/4/17 11:06 AM
Formatted ... [242]

V2 Changes 2018/4/17 11:06 AM

V2 Changes 2018/4/17 11:06 AM
Formatted ... [243]

V2 Changes 2018/4/17 11:06 AM

V2 Changes 2018/4/17 11:06 AM
Formatted ... [244]

V2 Changes 2018/4/17 11:06 AM

V2 Changes 2018/4/17 11:06 AM
Formatted ... [245]

V2 Changes 2018/4/17 11:06 AM

V2 Changes 2018/4/17 11:06 AM
Formatted ... [246]

V2 Changes 2018/4/17 11:06 AM

633 observations (with the exception of CanESM2, IPSL-CM5A-MR and CNRM-CM5). Note that as much as
634 this bias south of the MIZ might be a true divergence of CMIP5 models from the observed ocean, it is
635 also possibly due to the lack of observations in this region, especially during the winter season (Bakker
636 et al., 2014; Monteiro, 2010).

638 Table 2 shows the Pattern Correlation Coefficient (PCC) and the Root Mean Square Error (RMSE),
639 which are here used to quantify the model spatial and magnitude performances against Landschützer
640 et al. (2014) data product. Out of the 10 models, six show a moderate spatial correlation with
641 Landschützer et al. (2014) (PCC = 0.40 – 0.60), i.e. CNRM-CM5, GFDL-ESM2M, HadGEM2-ES, IPSL-
642 CM5A-MR, CESM1-BGC, NorESME-ME and CanESM2. While MPI-ESM-MR (PCC = 0.37), MRI-ESM (PCC
643 = 0.36) and CMCC-CESM (PCC = -0.09) show a weak to null spatial correlation with observations, the
644 latter is mainly due to the overestimated out-gassing region. Spatially, GFDL-ESM2M and NorESM1-ME
645 are the most comparable to Landschützer et al. (2014), (RMSE < 9), while CCMC-CESM, CanESM2, MRI-
646 ESM and CNRM-CM5 shows the most differences (RMSE > 15). The rest of the models show a modest
647 comparison (RMSE 9 – 11).

649 NorESM1-ME and CESM1-BGC are the only two of the 10 models showing a consistent spatial (RMSE
650 < 9) and magnitude (PCC ≈ 0.50) performance. From Table 2, it is evident that an appropriate
651 representation of the spatial properties of FCO₂ with respect to observations does not always
652 correspond to comparable magnitudes. CanESM2 for example, shows a good spatial comparison (PCC
653 = 0.54), yet a poor estimation of the magnitudes (RMSE = 19.5). In this case this is caused by an
654 overestimation of CO₂ uptake north of 55°S (≈ - 28 g m⁻² yr⁻¹) and CO₂ out-gassing (> 25 g m⁻² yr⁻¹) in
655 the Antarctic zone, resulting in a net total Southern Ocean annual weak sink (-0.05 Pg C m⁻² yr⁻¹).

657 3.2 Sea-Air CO₂ Flux Seasonal Cycle Variability and Biases

659 The seasonal cycle of FCO₂ is shown in Fig. 2. The seasonality of FCO₂ in the 10 CMIP5 models shows a
660 large dispersion in both phasing and amplitude, but mostly disagrees with observations in the phase of
661 the seasonal cycle as well as disagreeing with each other. More quantitatively, CMIP5 models show
662 weak to negative correlations with the Landschützer et al. (2014) data product in the Sub-Antarctic
663 Zone and have slightly higher correlations in the Antarctic Zone (see supplementary Fig. S7). This
664 discrepancy is consistent with the findings of Anav et al. (2013), who however used fixed latitude
665 criteria. Based on the phasing, the seasonality of FCO₂ in CMIP5 models can be a priori divided in two
666 main groups: group-DIC models, comprising of MPI-ESM, HadGEM-ES and NorESM1-ME, and group-
667 SST models, the remainder i.e. GFDL-ESM2M, CMCC-CESM, CNRM-CERFACS, IPSL-CM5A-MR, CESM1-
668 BGC, MRI-ESM and CanESM2. The naming convention is suggestive of the mechanism driving the

V2 Changes 2018/4/17 11:06 AM
Formatted: Font:+Theme Body

V2 Changes 2018/4/17 11:06 AM
Deleted: 6

V2 Changes 2018/4/17 11:06 AM
Formatted: ... [248]

V2 Changes 2018/4/17 11:06 AM
Deleted: outgassing

V2 Changes 2018/4/17 11:06 AM
Formatted: ... [249]

V2 Changes 2018/4/17 11:06 AM
Deleted: 2

V2 Changes 2018/4/17 11:06 AM
Formatted: Font:+Theme Body

V2 Changes 2018/4/17 11:06 AM
Deleted: 10

V2 Changes 2018/4/17 11:06 AM
Formatted: Font:+Theme Body

V2 Changes 2018/4/17 11:06 AM
Deleted: =

V2 Changes 2018/4/17 11:06 AM
Formatted: ... [250]

V2 Changes 2018/4/17 11:06 AM
Deleted:

V2 Changes 2018/4/17 11:06 AM
Formatted: ... [251]

V2 Changes 2018/4/17 11:06 AM
Deleted: outgassing

V2 Changes 2018/4/17 11:06 AM
Formatted: Font:+Theme Body

V2 Changes 2018/4/17 11:06 AM
Deleted: These inconsistencies in the spatial and magnitude performances highlights some of the limitations of using annual me ... [252]

V2 Changes 2018/4/17 11:06 AM
Formatted: Font:+Theme Body

V2 Changes 2018/4/17 11:06 AM
Deleted: disagree

V2 Changes 2018/4/17 11:06 AM
Formatted: ... [253]

V2 Changes 2018/4/17 11:06 AM
Deleted: ,

V2 Changes 2018/4/17 11:06 AM
Formatted: Font:+Theme Body

V2 Changes 2018/4/17 11:06 AM
Deleted:) findings,

V2 Changes 2018/4/17 11:06 AM
Formatted: Font:+Theme Body

V2 Changes 2018/4/17 11:06 AM
Deleted: ,

V2 Changes 2018/4/17 11:06 AM
Formatted: Normal1

708 seasonal cycle, as will be clarified further on. A similar grouping was also identified by Kessler and
709 Tjiputra (2016) using a different criterion. Fig. 3 shows the seasonal cycle of FCO₂ of an equally-
710 weighted ensemble of the two groups compared to observations, the shaded area shows the decadal
711 standard deviation for the models and the Landschützer et al. (2014) data product for 1998-2014
712 standard deviation, in the various regions.

713
714 In the Sub-Antarctic Zone, the observational products show a weakening of CO₂ uptake during winter
715 (less negative values in June-August) with values close to the zero at the onset of spring (September)
716 in all three basins. Similarly, during the spring season, all three basins are seen to maintain a steady
717 increase of CO₂ uptake until mid-summer (December), while they differ during autumn (March-May).
718 The Pacific basin shows an increase in CO₂ uptake during autumn that is not observed in the other
719 basins (only marginally in the Indian zone). In the Antarctic zone, the observed FCO₂ seasonal cycle is
720 mostly similar in all three basins (Fig. 3d-f). While this seasonal cycle consistency may suggest a
721 spatial uniformity of the mechanisms of FCO₂ at the Antarctic, we are also mindful that this may be due
722 to a result of the paucity of observations in this area. In the Antarctic Zone, all three basins show a
723 weakening of uptake or increasing of out-gassing from the onset of autumn (March) until mid-winter
724 (June-July). The winter CO₂ out-gassing is followed by a strengthening of the CO₂ uptake throughout
725 spring to summer, when it reaches a CO₂ in-gassing peak.

726
727 The differences in the seasonal cycle of FCO₂ across the three basins of the Sub-Antarctic Zone found in
728 the observational product (Fig. 2) are likely a consequence of spatial differences seen in Fig. 1. To
729 verify this, we calculated the correlation between the seasonal cycles from the Landschützer et al.
730 (2014) observational product in the three basins (Fig. 4). The FCO₂ seasonal cycle in the Sub-Antarctic
731 Atlantic and Indian basins are similar (R = 0.8), while the other basins are quite different to one
732 another (R = -0.1 for Pacific – Atlantic and R ~ 0.4 for Pacific – Indian). Contrary to the observational
733 product, CMIP5 models show the same seasonal cycle phasing across all three basins in the Sub-
734 Antarctic Zone (basin – basin correlation coefficients are always larger than 0.50 in Fig. 4 despite the
735 spatial differences in Fig. 2, with the exception of three models (i.e. CMCC-CESM, CESM-BGC1 and
736 GFDL-ESM2M)). Thus, contrary to Landschützer et al. (2014), CMIP5 models shows a zonal
737 homogeneity in the seasonal cycle of FCO₂, which may suggest that the drivers of CO₂ are less regional.
738 In the Antarctic Zone, CMIP5 models agree with observations in the spatial uniformity of the seasonal
739 cycle of FCO₂ across the three basins.

740
741 Group-DIC models are characterized by an exaggerated CO₂ uptake during spring-summer (Fig. 3) with
742 respect to observation estimates and CO₂ out-gassing during winter. These models generally agree
743 with observations in the phasing of CO₂ uptake during spring, but overestimate the magnitudes. It is

Deleted: it
V2 Changes 2018/4/17 11:06 AM
Formatted ... [255]
V2 Changes 2018/4/17 11:06 AM
Deleted: ,
V2 Changes 2018/4/17 11:06 AM
Formatted ... [256]
V2 Changes 2018/4/17 11:06 AM
Deleted:
V2 Changes 2018/4/17 11:06 AM
Formatted ... [257]
V2 Changes 2018/4/17 11:06 AM
Deleted: for
V2 Changes 2018/4/17 11:06 AM
Formatted ... [258]
V2 Changes 2018/4/17 11:06 AM
Deleted: zone
V2 Changes 2018/4/17 11:06 AM
Formatted ... [259]
V2 Changes 2018/4/17 11:06 AM
Deleted: Ocean
V2 Changes 2018/4/17 11:06 AM
Formatted ... [260]
V2 Changes 2018/4/17 11:06 AM
Deleted: Ocean
V2 Changes 2018/4/17 11:06 AM
Formatted ... [261]
V2 Changes 2018/4/17 11:06 AM
Deleted: zone
V2 Changes 2018/4/17 11:06 AM
Formatted ... [262]
V2 Changes 2018/4/17 11:06 AM
Deleted: CO₂
V2 Changes 2018/4/17 11:06 AM
Formatted ... [263]
V2 Changes 2018/4/17 11:06 AM
Deleted:) when it outgasses.
V2 Changes 2018/4/17 11:06 AM
Formatted ... [264]
V2 Changes 2018/4/17 11:06 AM
Deleted: outgassing
V2 Changes 2018/4/17 11:06 AM
Formatted ... [265]
V2 Changes 2018/4/17 11:06 AM
Deleted: ingassing
V2 Changes 2018/4/17 11:06 AM
Formatted ... [266]
V2 Changes 2018/4/17 11:06 AM
Deleted: zone
V2 Changes 2018/4/17 11:06 AM
Formatted ... [267]
V2 Changes 2018/4/17 11:06 AM
Deleted:),
V2 Changes 2018/4/17 11:06 AM
Formatted ... [268]
V2 Changes 2018/4/17 11:06 AM
Deleted: resemble the
V2 Changes 2018/4/17 11:06 AM
Formatted ... [269]
V2 Changes 2018/4/17 11:06 AM
Deleted: in the spatial behavior
V2 Changes 2018/4/17 11:06 AM
Formatted ... [270]
V2 Changes 2018/4/17 11:06 AM
Formatted ... [271]
V2 Changes 2018/4/17 11:06 AM
Formatted ... [272]
V2 Changes 2018/4/17 11:06 AM
Formatted ... [273]
V2 Changes 2018/4/17 11:06 AM

802 worth noting that the seasonal characteristics of group-DIC models are mostly in agreement with the
803 observations in the Atlantic and Indian basin in Sub-Antarctic Zone, ($R > 0.5$ in Fig. 4). The large
804 standard deviation ($\sim 0.01 \text{ g C m}^{-2} \text{ day}^{-1}$) during the winter and spring-summer seasons in the Atlantic
805 basin shows that though group-DIC models agree in the phase, magnitudes vary considerably (Fig. 3b).
806 For example MPI-ESM reaches up to $0.06 \text{ g C m}^{-2} \text{ day}^{-1}$ out-gassing during winter, while HadESM2-ES
807 and NorESM2 peak only at $\sim 0.03 \text{ g C m}^{-2} \text{ day}^{-1}$. Group-SST models on the other hand are characterized
808 by a CO_2 out-gassing peak in summer (Dec-Feb) and a CO_2 in-gassing peak at the end of autumn (May),
809 and their phase is opposite to the observational estimates in the Atlantic and Indian basins (Fig. 3b,c).
810 Group-SST models only show a strengthening of CO_2 uptake during spring in the Indian basin.
811 Interestingly, group-SST models compare relatively well with the observed FCO_2 seasonal cycle in the
812 Pacific basin, whereas group-DIC models disagree the most with the observed estimates (Fig. 3a). This
813 phasing difference within models and against observed estimates probably suggests that the
814 disagreement of CMIP5 models FCO_2 with observations is not a matter of a relative error/constant
815 magnitude offset, but most likely points to differences in the seasonal drivers of FCO_2 .

816
817 In the Antarctic Zone (Fig. 3d-f), both group-DIC and group-SST models perform better than in the
818 Sub-Antarctic, in respect of phasing and amplitude in as shown by the correlation analysis in Fig. S7.
819 Models reflect comparable pCO_2 seasonality in the different basins of the AZ to the observational
820 products (Fig. 4, with the exception of MRI-ESM and CanESM2 where $R < 0$ for all three basins). Here
821 FCO_2 magnitudes oscillate around zero with the largest disagreements occurring during mid-summer,
822 where observation estimates show a weak CO_2 sink ($\approx -0.03 \text{ g C m}^{-2} \text{ day}^{-1}$), and group-SST show a zero
823 net CO_2 flux and a strong uptake in group-DIC (e.g. $\approx -0.12 \text{ g C m}^{-2} \text{ day}^{-1}$ in the Pacific basin). The large
824 standard deviation ($\approx 0.01 \text{ g C m}^{-2} \text{ day}^{-1}$) here indicates considerable differences among models (Fig.
825 3d-f).

827 3.3 Seasonal Scale Drivers of Sea-Air CO_2 Flux

828
829 We now examine how changes in temperature and DIC regulate FCO_2 variability at the seasonal scale
830 following the method described in Sec. 2.3. Fig. 5 shows the monthly rates of change of SST (dSST/dt)
831 for the 10 models compared with WOA13 SST. CMIP5 generally shows agreement in the timing of the
832 switch from surface cooling ($\text{dSST}/\text{dt} < 0$) to warming ($\text{dSST}/\text{dt} > 0$) and vice versa; i.e. March
833 (summer to autumn), and September (winter to spring) respectively. In both the Sub-Antarctic and
834 Antarctic Zone, CMIP5 models agree with observations in this timing (Fig. 5). However, while they
835 agree in phasing, the amplitude of these warming and cooling rates are overestimated with respect to
836 the WOA13 dataset with the exception of NorESM1-ME. Subsequently these differences in the
837 magnitude of dSST/dt have important implications for the solubility of CO_2 in seawater; larger

Deleted: zone
V2 Changes 2018/4/17 11:06 AM
Formatted ... [285]
V2 Changes 2018/4/17 11:06 AM
Deleted: Ocean
V2 Changes 2018/4/17 11:06 AM
Formatted ... [286]
V2 Changes 2018/4/17 11:06 AM
Deleted: reach
V2 Changes 2018/4/17 11:06 AM
Formatted ... [287]
V2 Changes 2018/4/17 11:06 AM
Deleted: outgassing
V2 Changes 2018/4/17 11:06 AM
Formatted ... [288]
V2 Changes 2018/4/17 11:06 AM
Deleted: outgassing
V2 Changes 2018/4/17 11:06 AM
Formatted ... [289]
V2 Changes 2018/4/17 11:06 AM
Deleted:)
V2 Changes 2018/4/17 11:06 AM
Formatted ... [290]
V2 Changes 2018/4/17 11:06 AM
Deleted: Ocean
V2 Changes 2018/4/17 11:06 AM
Formatted ... [291]
V2 Changes 2018/4/17 11:06 AM
Deleted: Ocean
V2 Changes 2018/4/17 11:06 AM
Formatted ... [292]
V2 Changes 2018/4/17 11:06 AM
Deleted: differences
V2 Changes 2018/4/17 11:06 AM
Formatted ... [293]
V2 Changes 2018/4/17 11:06 AM
Deleted: point
V2 Changes 2018/4/17 11:06 AM
Formatted ... [294]
V2 Changes 2018/4/17 11:06 AM
Deleted: zone
V2 Changes 2018/4/17 11:06 AM
Formatted ... [295]
V2 Changes 2018/4/17 11:06 AM
Deleted: also in more quantitative terms
V2 Changes 2018/4/17 11:06 AM
Formatted ... [296]
V2 Changes 2018/4/17 11:06 AM
Deleted: However, the similarity in the
V2 Changes 2018/4/17 11:06 AM
Formatted ... [297]
V2 Changes 2018/4/17 11:06 AM
Deleted: of
V2 Changes 2018/4/17 11:06 AM
Formatted ... [298]
V2 Changes 2018/4/17 11:06 AM
Deleted: found in
V2 Changes 2018/4/17 11:06 AM
Formatted ... [299]
V2 Changes 2018/4/17 11:06 AM
Deleted: product is now properly s
V2 Changes 2018/4/17 11:06 AM
Formatted ... [300]
V2 Changes 2018/4/17 11:06 AM
Formatted ... [301]
V2 Changes 2018/4/17 11:06 AM
Formatted ... [302]
V2 Changes 2018/4/17 11:06 AM
Formatted ... [303]
V2 Changes 2018/4/17 11:06 AM
Formatted ... [304]
V2 Changes 2018/4/17 11:06 AM
Formatted ... [304]
V2 Changes 2018/4/17 11:06 AM
Formatted ... [304]

889 magnitudes of $|dSST/dt|$ are likely to enhance the response of the pCO_2 to temperature through CO_2
890 solubility changes. For example, because the observations in the Indian basin show a warming rate of
891 about $0.5^\circ C \text{ month}^{-1}$ lower compared to the other two basins, we expect a relatively weaker role of
892 surface temperature in this basin.

893
894 As described in sec. 2.3, the computed $dSst/dt$ magnitudes were used to estimate the equivalent rate
895 of change of DIC driven by CO_2 solubility using Eq. 2. The seasonal cycle of $|d(DIC_T/dt)_{SST}|$ vs
896 $|d(DIC/dt)_{Tot}|$, for the 10 models and observations is presented in the supplementary material (Fig.
897 S8) where we show the seasonal mean of M_{T-DIC} from (Eq. 3). As articulated in sec. 2.3, M_{T-DIC} (Fig. 6) is
898 the difference between the total surface DIC rate of change of DIC (Eq. 1) and the estimated equivalent
899 temperature-driven solubility DIC changes Eq. 3, such that when $|d(DIC_T/dt)_{SST}| > |d(DIC/dt)_{Tot}|$,
900 temperature is the dominant driver of the instantaneous pCO_2 changes, and conversely when
901 $|d(DIC_T/dt)_{SST}| < |d(DIC/dt)_{Tot}|$, DIC processes are the dominant mode in the instantaneous pCO_2
902 variability. The models showing the former feature are SST-driven and belong to group-SST, while the
903 models showing the latter are DIC-driven and belong to group-SST.

904
905 According to the M_{T-DIC} magnitudes in Fig. 6, the seasonal cycle of pCO_2 in the observational estimates
906 is predominantly DIC-driven most of the year in both the Sub-Antarctic and Antarctic Zone. Note that,
907 however, during periods of high $|dSST/dt|$, i.e. autumn and spring, observations show a moderate to
908 weak DIC control ($M_{T-DIC} \approx 0$). The Antarctic Zone is mostly characterized by a stronger DIC control
909 (mean Annual $M_{T-DIC} > 3$) except for during the spring season (Fig. 6). Consistent with the similarity
910 analysis presented in Fig. 4, the Antarctic Zone shows coherence in the sign of the temperature –DIC
911 indicator ($M_{T-DIC} > 0$) within the three basins.

914 3.4 Source terms in the DIC surface budget

915
916 To further constrain the surface DIC budget in Eq. 1, we examine the role of the biological source term
917 using chlorophyll and Net Primary Production (NPP) as proxies. Fig. 8 shows the seasonal cycle of
918 chlorophyll, NPP and the rate of surface DIC changes ($dDIC/dt$). The observed seasonal cycle of
919 chlorophyll (Johnson et al., 2013) shows a similar seasonal cycle within the three basins during the
920 spring-summer seasons (autumn-winter data are removed due to the satellite limitation) in both the
921 Sub-Antarctic and Antarctic Zone. Magnitudes are however different in the Sub-Antarctic Zone; the
922 Atlantic basin shows larger chlorophyll magnitudes (Chlorophyll reach up to 1.0 mg m^{-3}) compared to
923 the Pacific and Indian basins ($Chl < 1 \text{ mg m}^{-3}$).

Deleted: Ocean shows
V2 Changes 2018/4/17 11:06 AM
Formatted ... [311]
V2 Changes 2018/4/17 11:06 AM
Deleted:), here
V2 Changes 2018/4/17 11:06 AM
Formatted ... [312]
V2 Changes 2018/4/17 11:06 AM
Deleted: .
V2 Changes 2018/4/17 11:06 AM
Formatted ... [313]
V2 Changes 2018/4/17 11:06 AM
Deleted:
V2 Changes 2018/4/17 11:06 AM
Formatted ... [314]
V2 Changes 2018/4/17 11:06 AM
Deleted:
V2 Changes 2018/4/17 11:06 AM
Formatted ... [315]
V2 Changes 2018/4/17 11:06 AM
Deleted: is
V2 Changes 2018/4/17 11:06 AM
Formatted ... [316]
V2 Changes 2018/4/17 11:06 AM
Deleted: zone
V2 Changes 2018/4/17 11:06 AM
Formatted ... [317]
V2 Changes 2018/4/17 11:06 AM
Deleted:
V2 Changes 2018/4/17 11:06 AM
Formatted ... [318]
V2 Changes 2018/4/17 11:06 AM
Deleted: zone
V2 Changes 2018/4/17 11:06 AM
Formatted ... [319]
V2 Changes 2018/4/17 11:06 AM
Deleted: zone
V2 Changes 2018/4/17 11:06 AM
Formatted ... [320]
V2 Changes 2018/4/17 11:06 AM
Deleted:
V2 Changes 2018/4/17 11:06 AM
Formatted ... [321]
V2 Changes 2018/4/17 11:06 AM
Deleted: -
V2 Changes 2018/4/17 11:06 AM
Formatted ... [322]
V2 Changes 2018/4/17 11:06 AM
Deleted: zone
V2 Changes 2018/4/17 11:06 AM
Formatted ... [323]
V2 Changes 2018/4/17 11:06 AM
Deleted: zone
V2 Changes 2018/4/17 11:06 AM
Formatted ... [324]
V2 Changes 2018/4/17 11:06 AM
Deleted: ,
V2 Changes 2018/4/17 11:06 AM
Formatted ... [310]

953 CMIP5 models here show a clear partition between group-DIC and group-SST models. While they
954 mostly maintain the same phase, group-DIC shows larger amplitudes of chlorophyll relative to group-
955 SST and observed estimates in the Sub-Antarctic Zone. This difference is even clearer in NPP
956 magnitudes, where group-DIC models show a maximum of NPP $> 1 \text{ mmol m}^{-2} \text{ s}^{-1}$ in summer, while
957 group-SST magnitudes shows about half of it. Except for CESM1-BGC and CMCC-CESM (and NorESM1-
958 ME for NPP), each CMIP5 model generally maintains a similar chlorophyll seasonal cycle (phase and
959 magnitude) in all three basins of the Southern Ocean. This is contrary to the observations, which show
960 differences in the magnitude. Consistent with the observational product, CESM1-BGC simulates larger
961 amplitude in the Atlantic basin. While CMCC-CESM also has this feature, it also shows an
962 overestimated chlorophyll peak in the Indian basin. In the Antarctic Zone both observations and
963 CMIP5 models generally agree in both phase and magnitude (except for CanESM2) of the seasonal
964 cycle of chlorophyll in all three basins.

966 We now examine the influence of the vertical DIC rate in Eq. 1, using estimated entrainment rates (RE,
967 Eq. 5) based on MLD and vertical DIC gradients (see sec. 2.3). Fig. 7 shows the seasonal changes of
968 MLD compared with the rate from the observational product. CMIP5 models largely agree on the
969 timing of the onset of MLD deepening (February in the Pacific basin, and March for the Atlantic and
970 Indian basin) and shoaling (September) in the Sub-Antarctic Zone (with the exception of NorESM1-ME
971 and IPSL-CM5A in the Pacific basin). The Indian basin generally shows deeper winter MLD in both
972 observations and CMIP5 models in the Sub-Antarctic Zone. Note that while CMIP5 models generally
973 show the observed deeper MLDs in the Indian basin, they show a large variation; for example, the
974 winter maximum depth ranges from 100 m (CMCC-CESM, pacific basin) to 350 m (CanESM2, Indian
975 basin) in the Sub-Antarctic Zone. In the Antarctic Zone CMIP5 models are largely in agreement on the
976 timing of the onset of MLD deepening (February), but also variable in their winter maximum depth. It
977 is worth noting that the observed MLD seasonal cycle might be biased due to limited in situ
978 observations particularly in the Antarctic Zone, (de Boyer Montégut et al., 2004).

980 The estimated RE values in Fig. 10 show that almost all CMIP5 (with the exception of NorESM1-ME)
981 entrain subsurface DIC into the mixed layer during autumn–winter in agreement with the
982 observational estimates. In the Sub-Antarctic Zone, the estimates using the observational products
983 show the strongest entrainment in the Atlantic basin in May (RE reaches up to $10 \mu\text{mol kg}^{-1} \text{ month}^{-1}$),
984 while it is lower in the other basins. In the Antarctic Zone, observed RE conversely shows stronger
985 entrainment rates in the Pacific and Indian basin ($\text{RE} > 15 \mu\text{mol kg}^{-1} \text{ month}^{-1}$) in comparison to the
986 Atlantic basin ($\text{RE} = 11 \mu\text{mol kg}^{-1} \text{ month}^{-1}$). CMIP5 models entrainment rates are variable but not
987 showing any particular deficiency when compared with the observational estimates. Also, the group-
988 DIC and group-SST models show no clear distinction, the major striking features being the relatively

Deleted: zone
V2 Changes 2018/4/17 11:06 AM
Formatted ... [326]
V2 Changes 2018/4/17 11:06 AM
Deleted: modelsshow
V2 Changes 2018/4/17 11:06 AM
Deleted:
V2 Changes 2018/4/17 11:06 AM
Formatted ... [327]
V2 Changes 2018/4/17 11:06 AM
Formatted ... [328]
V2 Changes 2018/4/17 11:06 AM
Deleted: Consistently
V2 Changes 2018/4/17 11:06 AM
Formatted ... [329]
V2 Changes 2018/4/17 11:06 AM
Deleted: Ocean
V2 Changes 2018/4/17 11:06 AM
Formatted ... [330]
V2 Changes 2018/4/17 11:06 AM
Deleted: zone
V2 Changes 2018/4/17 11:06 AM
Formatted ... [331]
V2 Changes 2018/4/17 11:06 AM
Deleted: Ocean
V2 Changes 2018/4/17 11:06 AM
Formatted ... [332]
V2 Changes 2018/4/17 11:06 AM
Deleted: Ocean
V2 Changes 2018/4/17 11:06 AM
Formatted ... [333]
V2 Changes 2018/4/17 11:06 AM
Deleted: zone
V2 Changes 2018/4/17 11:06 AM
Formatted ... [334]
V2 Changes 2018/4/17 11:06 AM
Deleted: Ocean
V2 Changes 2018/4/17 11:06 AM
Formatted ... [335]
V2 Changes 2018/4/17 11:06 AM
Deleted: Ocean
V2 Changes 2018/4/17 11:06 AM
Formatted ... [336]
V2 Changes 2018/4/17 11:06 AM
Deleted: zone
V2 Changes 2018/4/17 11:06 AM
Formatted ... [337]
V2 Changes 2018/4/17 11:06 AM
Deleted: Ocean
V2 Changes 2018/4/17 11:06 AM
Formatted ... [338]
V2 Changes 2018/4/17 11:06 AM
Deleted: range
V2 Changes 2018/4/17 11:06 AM
Formatted ... [339]
V2 Changes 2018/4/17 11:06 AM
Deleted: Ocean
V2 Changes 2018/4/17 11:06 AM
Formatted ... [340]
V2 Changes 2018/4/17 11:06 AM
Deleted: Ocean
V2 Changes 2018/4/17 11:06 AM
Formatted ... [341]
V2 Changes 2018/4/17 11:06 AM
Formatted ... [342]
V2 Changes 2018/4/17 11:06 AM
Formatted ... [343]
V2 Changes 2018/4/17 11:06 AM
Formatted ... [344]
V2 Changes 2018/4/17 11:06 AM

L035 stronger entrainment in MPI-ESM and CanESM2 across the three basins in the Sub-Antarctic Zone, in
L036 mid to late winter ($RE = 15 \mu\text{mol kg}^{-1} \text{month}^{-1}$), and the large winter entrainment in IPSL-CM5A-MR in
L037 the Antarctic Pacific basin. The supply of DIC to the surface due to vertical entrainment is therefore
L038 generally comparable between model simulations and the available estimate.

L039
L040 However, our RE estimates are estimated at the base of the mixed layer, which is not necessarily a
L041 complete measure of the vertical flux of DIC at the surface. We therefore investigate the annual mean
L042 vertical DIC gradients in Fig. 10 as an indicator of where the surface uptake processes occur. The
L043 simulated CMIP5 profiles are similar to GLODAP2, but some differences arise. In the Sub-Antarctic
L044 Zone, GLODAP2 shows a shallower surface maximum in the Atlantic basin consistent with higher
L045 biomass in this basin ($(dDIC/dz)_{\text{max}} = 0.55 \mu\text{mol kg}^{-1} \text{m}^{-1}$, at 50 m) compared to the Pacific
L046 ($(dDIC/dz)_{\text{max}} = 0.60 \mu\text{mol kg}^{-1} \text{m}^{-1}$, at 80 m) and Indian basin ($(dDIC/dz)_{\text{max}} = 0.40 \mu\text{mol kg}^{-1} \text{m}^{-1}$, at
L047 80 m). CMIP5 models generally do not show this feature in the Sub-Antarctic Zone, except for CESM1-
L048 BGC1 ($(dDIC/dz)_{\text{max}} = 0.50 \mu\text{mol kg}^{-1} \text{m}^{-1}$, at 50 m). Instead, they show the surface maxima at the same
L049 depth in all three basins. In the Antarctic Zone both CMIP5 models and observations show larger
L050 $(dDIC/dz)_{\text{max}}$ magnitudes and nearer surface maxima (with the exception of CanESM2 and CESM1-
L051 BGC). This difference in the position and magnitude of the DIC maxima between the Sub-Antarctic and
L052 Antarctic Zone has important implications for surface DIC changes and subsequently $p\text{CO}_2$ seasonal
L053 variability. Because of the nearer surface DIC maxima in the Antarctic Zone, surface DIC changes are
L054 mostly influenced by these strong near-surface vertical gradients than MLD changes. This implies that
L055 even if the entrainment rates at the base of the MLD are comparable between the Sub-Antarctic and
L056 the Antarctic, the surface supply of DIC may be larger in the Antarctic Zone.

L059 4. Discussion

L060
L061 Recent studies have highlighted that important differences exist between the seasonal cycle of $p\text{CO}_2$ in
L062 models and observations in the Southern Ocean (Lenton et al., 2013; Anav et al., 2015; Mongwe, 2016).
L063 Paradoxically, although the models may be in relative agreement for the mean annual flux, they
L064 diverge in the phasing and magnitude of the seasonal cycle (Lenton et al., 2013; Anav et al., 2015;
L065 Mongwe, 2016). These differences in the seasonal cycle raise questions about the climate sensitivity of
L066 the carbon cycle in these models because they may reflect differences in the process sensitivities to
L067 drivers that are themselves climate sensitive.

- V2 Changes 2018/4/17 11:06 AM
Deleted: zone
- V2 Changes 2018/4/17 11:06 AM
Formatted: Font:+Theme Body
- V2 Changes 2018/4/17 11:06 AM
Deleted:)
- V2 Changes 2018/4/17 11:06 AM
Formatted: Font:+Theme Body
- V2 Changes 2018/4/17 11:06 AM
Deleted: Ocean
- V2 Changes 2018/4/17 11:06 AM
Formatted: Font:+Theme Body
- V2 Changes 2018/4/17 11:06 AM
Deleted: zone
- V2 Changes 2018/4/17 11:06 AM
Formatted: Font:+Theme Body
- V2 Changes 2018/4/17 11:06 AM
Deleted: zone
- V2 Changes 2018/4/17 11:06 AM
Formatted: Font:+Theme Body
- V2 Changes 2018/4/17 11:06 AM
Deleted: zone
- V2 Changes 2018/4/17 11:06 AM
Formatted: Font:+Theme Body
- V2 Changes 2018/4/17 11:06 AM
Deleted: shows
- V2 Changes 2018/4/17 11:06 AM
Formatted: Font:+Theme Body
- V2 Changes 2018/4/17 11:06 AM
Deleted: zone
- V2 Changes 2018/4/17 11:06 AM
Formatted: Font:+Theme Body
- V2 Changes 2018/4/17 11:06 AM
Deleted: zone
- V2 Changes 2018/4/17 11:06 AM
Formatted: Font:+Theme Body
- V2 Changes 2018/4/17 11:06 AM
Deleted: zone
- V2 Changes 2018/4/17 11:06 AM
Formatted: Font:+Theme Body
- V2 Changes 2018/4/17 11:06 AM
Formatted: Font:+Theme Body, 8 pt
- V2 Changes 2018/4/17 11:06 AM
Formatted: Font:+Theme Body
- V2 Changes 2018/4/17 11:06 AM
Deleted: ,
- V2 Changes 2018/4/17 11:06 AM
Formatted: Normal1

L080 In this study we expand on the framework proposed by Mongwe et al. (2016), which examined the
L081 competing roles of temperature and DIC as drivers of pCO₂ variability and the seasonal cycle of pCO₂ in
L082 the Southern Ocean, to explain the mechanistic basis for seasonal biases of pCO₂ and FCO₂ between
L083 observational products and CMIP5 models. This analysis of 10 CMIP5 models and one observational
L084 product (Landschutzer et al., 2014) highlighted that although the models showed different seasonal
L085 cycles (Fig. 2), they could be grouped into two categories (SST- and DIC-driven) according to their
L086 mean seasonal bias of temperature or DIC control (Fig. 3 & 6).

L087
L088 A few general insights emerge from this analysis. Firstly, despite significant differences in the spatial
L089 characteristics of the mean annual fluxes (Fig. 1), models show unexpectedly greater inter-basin
L090 coherence in the phasing seasonal cycle of FCO₂ and SST-DIC control than observational products (Fig.
L091 3 & 6). Clear inter-basin differences have been highlighted in studies on the climatology and
L092 interannual variability that examined pCO₂ and CO₂ fluxes based on data products (Landschutzer et al.,
L093 2015; Gregor et al., 2017), as well as phytoplankton chlorophyll based on remote sensing (Thomalla et
L094 al., 2011; Carranza et al., 2016). Briefly, the Atlantic basin shows the highest mean primary
L095 production in contrast to the Pacific basin, which has the lowest (Thomalla et al., 2011). Similarly,
L096 strong inter-basin differences for pCO₂ and FCO₂ have been highlighted and ascribed to SST control
L097 (Landschützer et al., 2016) and wind stress - mixed layer depth (Gregor et al., 2017). The combined
L098 effect of these regional differences in forcing of pCO₂ and FCO₂ would be expected to be reflected in the
L099 CMIP5 models as well. A quantitative analysis of the correlation of the phasing of the seasonal cycle of
L100 FCO₂ between basins for different models shows that all the models except three (CMCC-CESM, GFDL-
L101 ESM2M CESM1-CESM) are characterized by strong inter-basin correlation in both the SAZ and the AZ
L102 (Fig. 4). This suggests that the carbon cycle in these CMIP5 models is not sensitive to inter-basin
L103 differences in the drivers as is the case for observations. This most likely implies that CMIP5 models
L104 are not sensitive to regional FCO₂ variability at the basin scale, so FCO₂ seasonal biases are zonally
L105 uniform.

L106
L107 Secondly, an important part of this analysis is based on the assumption that the observational
L108 products that are used to constrain the spatial and temporal variability of pCO₂ and FCO₂ reflect the
L109 correct seasonal cycles of the Southern Ocean. This assumption requires significant caution not only
L110 due to the limitations in the sparseness of the *in situ* observations but also due to limitations of the
L111 empirical techniques in overcoming these data gaps (Landschutzer et al., 2014; Rödenbeck et al., 2015;
L112 Gregor et al., 2017a, b; Ritter et al., 2018). The uncertainty analysis from these studies suggests that,
L113 while the seasonal bias in observations may be less in the SAZ and PFZ, it is the highest in the AZ
L114 where access is limited mostly to summer, and winter ice cover results in uncertainties that may limit
L115 the significance of the data model comparisons. It is important to note that though the observation

- V2 Changes 2018/4/17 11:06 AM
Deleted: modes
- V2 Changes 2018/4/17 11:06 AM
Formatted: Font:+Theme Body
- V2 Changes 2018/4/17 11:06 AM
Deleted:
- V2 Changes 2018/4/17 11:06 AM
Formatted: Font:+Theme Body
- V2 Changes 2018/4/17 11:06 AM
Deleted:)
- V2 Changes 2018/4/17 11:06 AM
Formatted: Font:+Theme Body
- V2 Changes 2018/4/17 11:06 AM
Deleted:
- V2 Changes 2018/4/17 11:06 AM
Formatted: Font:+Theme Body
- V2 Changes 2018/4/17 11:06 AM
Deleted: Ocean
- V2 Changes 2018/4/17 11:06 AM
Formatted: Font:+Theme Body
- V2 Changes 2018/4/17 11:06 AM
Deleted: Ocean
- V2 Changes 2018/4/17 11:06 AM
Formatted: Font:+Theme Body
- V2 Changes 2018/4/17 11:06 AM
Deleted: hows
- V2 Changes 2018/4/17 11:06 AM
Formatted: Font:+Theme Body
- V2 Changes 2018/4/17 11:06 AM
Deleted: 3
- V2 Changes 2018/4/17 11:06 AM
Formatted: Font:+Theme Body
- V2 Changes 2018/4/17 11:06 AM
Formatted: Font:+Theme Body
- V2 Changes 2018/4/17 11:06 AM
Deleted: modes
- V2 Changes 2018/4/17 11:06 AM
Formatted: Font:+Theme Body
- V2 Changes 2018/4/17 11:06 AM
Deleted: result
- V2 Changes 2018/4/17 11:06 AM
Formatted: Font:+Theme Body
- V2 Changes 2018/4/17 11:06 AM
Deleted: -
- V2 Changes 2018/4/17 11:06 AM
Formatted: Font:+Theme Body
- V2 Changes 2018/4/17 11:06 AM
Deleted: ,
- V2 Changes 2018/4/17 11:06 AM
Formatted: Normal1

L127 product that we use here (Landschützer et al., (2014) is based on more surface measurement (10
L128 millions, SOCAT v3) compared to previous datasets (e.g. Takahashi et al., 2009, 3 millions), the data
L129 are still sparse in time and space in the Southern Ocean. Thus, in using this data product as our main
L130 observational estimates for this analysis we are mindful of the limitations in the discussion below.

L131
L132 Thirdly, the seasonal cycle of $\Delta p\text{CO}_2$ is the dominant mode of variability in FCO_2 (Mongwe et al., 2016;
L133 Wanninkhof et al., 2009). Though winds provide the kinematic forcing for air-sea fluxes of CO_2 and
L134 indirectly affect FCO_2 through mixed layer dynamics and associated biogeochemical responses
L135 (Mahadevan et al., 2012; du Plessis et al., 2017), $\Delta p\text{CO}_2$ sets the direction of the flux. Surface $p\text{CO}_2$
L136 changes are mainly driven by DIC and SST (Hauck et al., 2015; Takahashi et al., 1993). Subsequently
L137 the sensitivity of CMIP5 models to how changes in DIC and SST regulate the seasonal cycle of FCO_2 is
L138 fundamental to the model's ability to resolve the observed FCO_2 seasonal cycle. Thus, here we
L139 examined the influence of DIC and SST on FCO_2 at seasonal scale for 10 CMIP5 models with respect to
L140 observed estimates. Because temperature does not directly affect DIC changes, we first scaled up the
L141 impact of SST changes on $p\text{CO}_2$ through surface CO_2 solubility to equivalent DIC units using the Revelle
L142 factor (section 2.3). In this way, we can distinguish the influence of surface solubility and DIC changes
L143 (i.e. biological and physical) on $p\text{CO}_2$ and hence on FCO_2 .

L144
L145 Fourthly, using this analysis framework (sec 2.3, summarized in Fig. 6) we found that CMIP5 models
L146 FCO_2 biases cluster in two groups, namely group-DIC ($M_{T\text{-DIC}} < 0$) and group-SST ($M_{T\text{-DIC}} > 0$). Group-DIC
L147 models are characterized by an overestimation of the influence of DIC on $p\text{CO}_2$ with respect to
L148 observations estimates, which instead indicate that physical and biogeochemical changes in the DIC
L149 concentration mostly regulate the seasonal cycle of FCO_2 (in short, DIC control). Group-SST models
L150 show an excessive temperature influence on $p\text{CO}_2$; here surface CO_2 solubility biases are mainly
L151 responsible for the departure of modelled FCO_2 from the observational products. While CMIP5 models
L152 mostly show a singular dominant influence of these extremes, observations show a modest influence
L153 of both, with a dominance of DIC changes as the main driver of seasonal FCO_2 variability. Below we
L154 discuss the seasonal cycle characteristics and possible mechanisms for these two groups of CMIP5
L155 models in the Sub-Antarctic and Antarctic Zones of the Southern Ocean.

L157 4.1 Sub-Antarctic Zone (SAZ)

L158
L159 Our diagnostic analysis indicates that the seasonal cycle of $p\text{CO}_2$ in the observational product
L160 (Landschützer et al., 2014) is mostly DIC controlled across all three basins of the SAZ ($M_{T\text{-DIC}} < 0$ in Fig.
L161 6). The Atlantic basin shows a stronger DIC control (Annual mean $M_{T\text{-DIC}} \geq 2$) compared to the Pacific
L162 and Indian basin (Annual mean $M_{T\text{-DIC}} \approx 1$). This stronger influence of DIC on $p\text{CO}_2$ in the Atlantic basin,

V2 Changes 2018/4/17 11:06 AM

Formatted: Font:+Theme Body

V2 Changes 2018/4/17 11:06 AM

Formatted: Font:+Theme Body

V2 Changes 2018/4/17 11:06 AM

Deleted: its

V2 Changes 2018/4/17 11:06 AM

Formatted: Font:+Theme Body

V2 Changes 2018/4/17 11:06 AM

Deleted: regulates

V2 Changes 2018/4/17 11:06 AM

Formatted: Font:+Theme Body

V2 Changes 2018/4/17 11:06 AM

Formatted: Font:+Theme Body

V2 Changes 2018/4/17 11:06 AM

Formatted: Font:+Theme Body

V2 Changes 2018/4/17 11:06 AM

Deleted: But because

V2 Changes 2018/4/17 11:06 AM

Formatted: Font:+Theme Body

V2 Changes 2018/4/17 11:06 AM

Deleted: affects

V2 Changes 2018/4/17 11:06 AM

Formatted: Font:+Theme Body

V2 Changes 2018/4/17 11:06 AM

Formatted: Font:+Theme Body

V2 Changes 2018/4/17 11:06 AM

Deleted: then

V2 Changes 2018/4/17 11:06 AM

Formatted: Font:+Theme Body

V2 Changes 2018/4/17 11:06 AM

Deleted: modeled

V2 Changes 2018/4/17 11:06 AM

Formatted: Font:+Theme Body

V2 Changes 2018/4/17 11:06 AM

Deleted: Ocean

V2 Changes 2018/4/17 11:06 AM

Formatted: Font:+Theme Body

V2 Changes 2018/4/17 11:06 AM

Deleted: Ocean

V2 Changes 2018/4/17 11:06 AM

Formatted: Font:+Theme Body

V2 Changes 2018/4/17 11:06 AM

Deleted: Ocean

V2 Changes 2018/4/17 11:06 AM

Formatted: Font:+Theme Body

V2 Changes 2018/4/17 11:06 AM

Deleted: .

V2 Changes 2018/4/17 11:06 AM

Formatted: Normal1

L172 is consistent with higher primary production in this basin (Graham et al., 2015; Thomalla et al., 2011),
L173 here shown by the larger mean seasonal chlorophyll from remote sensing in the Atlantic basin with
L174 respect to the Pacific and Indian basin (Fig. 8). This significant basin difference is most likely linked to
L175 the fact that the Atlantic basin has longer periods of shallow MLD compared to the Pacific and Indian
L176 basins (Fig. 7a-c, Nov – Mar & Nov - Feb respectively) and has been shown to have higher supplies of
L177 continental shelves and land-based iron (Boyd and Ellwood, 2010; Tagliabue et al., 2012; 2014). These
L178 conditions are more likely to enhance primary production that translates into a higher rate of change
L179 of surface DIC (Fig. 8), which becomes the major driver of FCO₂ variability. In contrast, shorter periods
L180 of shallow MLD and lower iron inputs in the Pacific basin (Tagliabue et al., 2012), likely account for a
L181 lower chlorophyll biomass and hence the weaker DIC control evidenced in our analysis ($M_{T-DIC} \approx 0$ in
L182 Fig. 6). In the Indian basin, the winter mixed layer is deeper than in the Atlantic and deepens earlier in
L183 the season (Fig. 7c). These conditions limit chlorophyll concentration (Fig. 8) and possibly contribute
L184 to the lower rates of surface temperature change because of the enhanced mixing (cf Fig. 5a-c). As a
L185 consequence, the resulting net driver in the Indian and Pacific basins is a weaker DIC control, because
L186 both biological DIC and solubility changes are relatively weaker and they oppose each other. Because
L187 of this, when the magnitudes of the rate of change of SST are larger during cooling and warming
L188 seasonal peaks (autumn and spring respectively), DIC control is weaker ($M_{T-DIC} \approx 0$) during these
L189 seasons.

L191 CMIP5 models do not capture these basin-specific features as demonstrated with the correlation
L192 analysis in Fig. 4, with the exception of three group-SST models (i.e. CESM1-BGC, GFDL-ESM2M and
L193 CMCC-CESM). These, in contrast, mostly show comparable FCO₂ phasing in the three basins. The
L194 seasonal cycle of CO₂ flux in the Southern Ocean (3,4) is both zonally and meridionally uniform for
L195 most CMIP5 models, in contrast to observational data product (Fig. 3). This suggests that CMIP5
L196 models show equal sensitivity to basin scale FCO₂ drivers, suggesting that pCO₂ and FCO₂ driving
L197 mechanisms are less local than for observations. Thus the understanding of fine-scale (mesoscale and
L198 sub-mesoscale) processes responsible for basin-scale FCO₂ variability will be an important
L199 contribution to the next generation of ESM. Studies based on new available data from higher
L200 resolution autonomous platforms like Monteiro et al., (2015), Williams et al., (2017). Briggs et al.,
L201 (2018) and Rosso et al., (2017) may be useful constraints to these dynamics in ESMs.

L203 The major feature of group-SST models in the SAZ is the out-gassing during summer and in-gassing
L204 mid-autumn to winter (Fig. 3a-c, Apr-Aug), which our diagnostics in Fig. 6 attribute to temperature
L205 (solubility) control. The summer period coincides with the highest warming rates (dSST/dt, Fig 5a-c),
L206 and associated reduction in solubility of CO₂. Similarly, exaggerated cooling rates at the onset of
L207 autumn (Fig. 5a-c) enhance CO₂ solubility causing a change in the direction of FCO₂ into strengthening

Deleted:
V2 Changes 2018/4/17 11:06 AM
Formatted ... [350]
V2 Changes 2018/4/17 11:06 AM
Deleted: a number of factors:
V2 Changes 2018/4/17 11:06 AM
Formatted ... [351]
V2 Changes 2018/4/17 11:06 AM
Deleted:
V2 Changes 2018/4/17 11:06 AM
Formatted ... [352]
V2 Changes 2018/4/17 11:06 AM
Deleted: Ocean
V2 Changes 2018/4/17 11:06 AM
Formatted ... [353]
V2 Changes 2018/4/17 11:06 AM
Deleted: Ocean
V2 Changes 2018/4/17 11:06 AM
Formatted ... [354]
V2 Changes 2018/4/17 11:06 AM
Deleted: This spatial uniformity
V2 Changes 2018/4/17 11:06 AM
Formatted ... [355]
V2 Changes 2018/4/17 11:06 AM
Deleted: CMIP5 models is both zor ... [356]
V2 Changes 2018/4/17 11:06 AM
Formatted ... [357]
V2 Changes 2018/4/17 11:06 AM
Deleted: Fig.
V2 Changes 2018/4/17 11:06 AM
Formatted ... [358]
V2 Changes 2018/4/17 11:06 AM
Deleted:
V2 Changes 2018/4/17 11:06 AM
Formatted ... [359]
V2 Changes 2018/4/17 11:06 AM
Deleted:), which is
V2 Changes 2018/4/17 11:06 AM
Formatted ... [360]
V2 Changes 2018/4/17 11:06 AM
Deleted: observation products
V2 Changes 2018/4/17 11:06 AM
Formatted ... [361]
V2 Changes 2018/4/17 11:06 AM
Deleted: outgassing
V2 Changes 2018/4/17 11:06 AM
Formatted ... [362]
V2 Changes 2018/4/17 11:06 AM
Deleted: ingassing
V2 Changes 2018/4/17 11:06 AM
Formatted ... [363]
V2 Changes 2018/4/17 11:06 AM
Deleted: Dec-Feb
V2 Changes 2018/4/17 11:06 AM
Formatted ... [364]
V2 Changes 2018/4/17 11:06 AM
Deleted: ,
V2 Changes 2018/4/17 11:06 AM
Formatted ... [349]

L239 CO₂ in-gassing (Fig 3a-c). Thus, while group-SST models have a seasonal amplitude of FCO₂
L240 comparable to observations, they are out of phase (Fig. 3) as was the case in a previous analysis of a
L241 forced ocean model (Mongwe et al., 2016).

L242
L243 In addition to increasing CO₂ solubility, the rapid cooling at the onset of autumn also deepens the MLD
L244 (March-June, Fig. 7), which induces entrainment of DIC, increasing surface CO₂ concentration and
L245 weakening the ocean-atmosphere gradient, and, in some instances, reversing the air-sea flux to out-
L246 gassing (Lenton et al., 2013a; Mahadevan et al., 2011; Metzl et al., 2006). While these processes
L247 (cooling and DIC entrainment) are likely to co-occur in the Southern Ocean, in CMIP5 models they are
L248 characterized by their extremes: temperature impact of solubility exceeds the rate of entrainment
L249 (Fig. 6 & 10). Because of the dominance of the solubility effect in group-SST models, the impact of DIC
L250 entrainment on surface pCO₂ changes, the weakening of CO₂ in-gassing / out-gassing only happens in
L251 mid-late winter (June-July -August) when entrainment fluxes peak (Fig. 10) and the SST rate
L252 approaches zero (Fig. 5).

L253
L254 In the spring-summer transition, primary production is expected to enhance the net CO₂ uptake
L255 (Thomalla et al., 2011; Le Quéré and Saltzman, 2013). However, the elevated surface warming rates
L256 during spring reduces CO₂ solubility in group-SST models and overwhelms the role of primary
L257 production in the seasonal cycle of pCO₂ and FCO₂ (atmospheric CO₂ uptake). As a consequence, these
L258 group-SST models mostly show a constant or weakening net CO₂ uptake flux during spring in the
L259 Pacific and Atlantic basin, even though primary production is occurring and is relatively elevated (Fig.
L260 3 & 8). Though some models show chlorophyll concentrations comparable to observations (e.g. GFDL-
L261 ESM2M, CNRM-CM5, CanESM2), and sometimes greater (e.g. MRI-ESM), the impact of temperature-
L262 driven solubility still dominates due to the phasing of the rates of the two drivers (Fig. 2a-c). The
L263 Indian basin however shows the only exception to this phenomenon. Here, the amplitude of the
L264 seasonal surface warming is relatively smaller (~ 0.5 °C⁻¹ month⁻¹ lower than the Pacific and Atlantic
L265 basins), and the biologically-driven CO₂ uptake becomes notable and shows a net strengthening of the
L266 sink of CO₂ during spring (Fig. 3c).

L267
L268 Though almost all analyzed CMIP5 models (with the exception of NorESM1-ME) exaggerate the
L269 warming and cooling rates in autumn and spring, group-DIC models do not manifest the expected
L270 temperature-driven solubility impact on pCO₂ and FCO₂ (Fig. 2). Instead, the seasonal cycle of pCO₂ and
L271 FCO₂ are controlled by DIC changes, which are driven by an overestimated seasonal primary
L272 production and the associated export carbon (Fig. 8). It is striking how in these models the seasonal
L273 cycle of chlorophyll and FCO₂ are in phase (Fig 3a-c, 8a-c, with linear correlation coefficients always

Deleted: ingassing
V2 Changes 2018/4/17 11:06 AM
Formatted ... [366]
V2 Changes 2018/4/17 11:06 AM
Formatted ... [367]
V2 Changes 2018/4/17 11:06 AM
Deleted: outgassing
V2 Changes 2018/4/17 11:06 AM
Formatted ... [368]
V2 Changes 2018/4/17 11:06 AM
Deleted: ingassing / outgassing
V2 Changes 2018/4/17 11:06 AM
Formatted ... [369]
V2 Changes 2018/4/17 11:06 AM
Deleted: -
V2 Changes 2018/4/17 11:06 AM
Formatted ... [370]
V2 Changes 2018/4/17 11:06 AM
Deleted: anticipated
V2 Changes 2018/4/17 11:06 AM
Formatted ... [371]
V2 Changes 2018/4/17 11:06 AM
Deleted: Ocean
V2 Changes 2018/4/17 11:06 AM
Formatted ... [372]
V2 Changes 2018/4/17 11:06 AM
Deleted:
V2 Changes 2018/4/17 11:06 AM
Formatted ... [373]
V2 Changes 2018/4/17 11:06 AM
Deleted: Ocean
V2 Changes 2018/4/17 11:06 AM
Formatted ... [374]
V2 Changes 2018/4/17 11:06 AM
Deleted:
V2 Changes 2018/4/17 11:06 AM
Formatted ... [375]
V2 Changes 2018/4/17 11:06 AM
Deleted: show
V2 Changes 2018/4/17 11:06 AM
Formatted ... [376]
V2 Changes 2018/4/17 11:06 AM
Deleted: analysed
V2 Changes 2018/4/17 11:06 AM
Formatted ... [377]
V2 Changes 2018/4/17 11:06 AM
Deleted:)
V2 Changes 2018/4/17 11:06 AM
Formatted ... [378]
V2 Changes 2018/4/17 11:06 AM
Deleted: . However, this is
V2 Changes 2018/4/17 11:06 AM
Formatted ... [379]
V2 Changes 2018/4/17 11:06 AM
Deleted: export fluxes
V2 Changes 2018/4/17 11:06 AM
Formatted ... [380]
V2 Changes 2018/4/17 11:06 AM
Deleted: ,
V2 Changes 2018/4/17 11:06 AM
Formatted ... [365]

larger than 0.9, not shown) but, as we discuss below, this is not because the temperature rates of change are correctly scaled but because the biogeochemical process rates are exaggerated (Fig. 8). Because of the particularly enhanced production in group-DIC models, the CO₂ sink is stronger (Fig. 8) with respect to observation estimates during spring. This is visible in the reduction of surface DIC (negative dDIC/dt in Fig. 8a, g-i), which can only be explained by drawdown due to the formation and export of organic matter (Le Quéré and Saltzman, 2013). However, note that in the same way, after the December production peak, both CMIP5 models and observations show an increase of surface DIC concentrations (positive dDIC/dt) until March (Fig. 8, g-i). These DIC growth rates are particularly enhanced in group-DIC models compared to some group-SST and observations (Fig. S9). The onset of these DIC increases also coincides with the depletion of surface oxygen (Fig. S9), which we speculate is due to the remineralization of organic matter to DIC through respiration. Unfortunately, only a few models have stored the respiration rates, therefore the full reason for this DIC rebound remains to be examined at a later stage. We would however tend to exclude other processes, because the onset of CO₂ out-gassing seen in March in group-DIC models occurs prior to significant MLD deepening (Fig. 7) and entrainment fluxes, therefore remineralization is likely be a key process here (Fig. 8).

4.2 Antarctic Zone (AZ)

The seasonal cycle framework summarized in Fig. 6 shows that the variability of FCO₂ and pCO₂ in the Landschützer et al. (2014) product is characterized by a stronger DIC control (annual mean M_{T-DIC} < -2) relative to the Sub-Antarctic (M_{T-DIC} ≈ -1), except in the spring season (M_{T-DIC} > -1). This DIC control is spatially uniform in the Antarctic Zone across all three basins (Fig. 4). The available datasets indicate that the combination of weaker SST rates due to lower solar heating fluxes (Fig. 5), and stronger shallower vertical DIC maxima (Fig. 10) favour a stronger DIC control through larger surface DIC rates. The spatial uniformity in the seasonality of FCO₂ is also evident in the satellite chlorophyll and calculated dDIC/dt from GLODAP2 in Fig. 9. Contrary to the Sub-Antarctic this might be suggesting that FCO₂ mechanisms here are less local. It could be hypothesized that the seasonal extent of sea-ice, deeper mixing and heat balance differences affect this region more uniformly compared to the Sub-Antarctic Zone, and hence the mechanisms of FCO₂ are spatially homogeneous. However, we cannot forget that sparseness of observations in this region is a key limitation to data products (Bakker et al., 2014; Gregor et al., 2017; Monteiro et al., 2010; Rödenbeck et al., 2013) that might hamper the emergence of basin-specific features. Consequently, this highlights the importance and need to prioritize independent observations in the Southern Ocean south of the polar front and in the Marginal Ice Zone. Increased observational efforts should also include a variety of platforms such as

V2 Changes 2018/4/17 11:06 AM

Deleted: ,

V2 Changes 2018/4/17 11:06 AM

Formatted: Font:+Theme Body

V2 Changes 2018/4/17 11:06 AM

Deleted: makes us

V2 Changes 2018/4/17 11:06 AM

Deleted: that this

V2 Changes 2018/4/17 11:06 AM

Formatted: Font:+Theme Body

V2 Changes 2018/4/17 11:06 AM

Formatted: Font:+Theme Body

V2 Changes 2018/4/17 11:06 AM

Deleted: remineralisation

V2 Changes 2018/4/17 11:06 AM

Formatted: Font:+Theme Body

V2 Changes 2018/4/17 11:06 AM

Deleted: ultimate

V2 Changes 2018/4/17 11:06 AM

Formatted: Font:+Theme Body

V2 Changes 2018/4/17 11:06 AM

Deleted: outgassing

V2 Changes 2018/4/17 11:06 AM

Formatted: Font:+Theme Body

V2 Changes 2018/4/17 11:06 AM

Deleted: zone

V2 Changes 2018/4/17 11:06 AM

Formatted: Font:+Theme Body

V2 Changes 2018/4/17 11:06 AM

Deleted:

V2 Changes 2018/4/17 11:06 AM

Formatted: Font:+Theme Body

V2 Changes 2018/4/17 11:06 AM

Deleted: are

V2 Changes 2018/4/17 11:06 AM

Formatted

... [381]

V2 Changes 2018/4/17 11:06 AM

Deleted: zone

V2 Changes 2018/4/17 11:06 AM

Formatted: Font:+Theme Body

V2 Changes 2018/4/17 11:06 AM

Deleted: known

V2 Changes 2018/4/17 11:06 AM

Formatted: Font:+Theme Body

V2 Changes 2018/4/17 11:06 AM

Deleted:

V2 Changes 2018/4/17 11:06 AM

Formatted: Font:+Theme Body

V2 Changes 2018/4/17 11:06 AM

Deleted: ,

V2 Changes 2018/4/17 11:06 AM

Formatted: Normal1

L361 autonomous vehicles like gliders (Monteiro et al., 2015) and biogeochemical floats (Johnson et al.,
L362 2017) in addition to ongoing ship-based measurements.

L363
L364 In general terms, CMIP5 models are mostly in agreement (with an exception of MRI-ESM) with the
L365 observational product on the dominant role of DIC to regulating the seasonal cycle of FCO₂ (Fig. 6d-f),
L366 though not all models agree in the phase of the seasonal cycle of FCO₂ (e.g. CanESM2, Fig. 2). Though
L367 CMIP5 models still mostly show the SST rates biases in autumn and spring with respect to observed
L368 estimates, the stronger and near-surface vertical DIC maxima (Fig. 10), likely favor DIC as a dominant
L369 driver of FCO₂ changes. Differences between group-SST and group-DIC models are only evident in mid-
L370 summer when SST rates heighten and primary production peaks (Fig. 3 & 9). Probably because of sea
L371 ice presence, the onset of SST warming is a month later (November) here in comparison to the Sub-
L372 Antarctic (October). This subsequently allows the onset of primary production before the surface
L373 warming, which then permits the biological CO₂ uptake to be notable in group-SST models. Thus the
L374 two model groups here agree in the FCO₂ in-gassing during spring with group-SST models being the
L375 closest to the observational product. The MRI-ESM is the only model showing anomalous solubility
L376 dominance during autumn and spring as in the Sub-Antarctic Zone.

L377
L378 This coherence of CMIP5 models and observations in the Antarctic Zone may suggest that CMIP5
L379 models compare better to observations in this region (Fig. 4). However, because CMIP5 models also
L380 show this spatial homogeneity in the Sub-Antarctic Zone (contrary to observational estimates), it is
L381 not clear whether this indicates an improved skill in CMIP5 model to the mechanisms of FCO₂ in this
L382 region, or both CMIP5 models and observational product lacks spatial sensitivity to the drivers of
L383 FCO₂. The sparseness of observations in the AZ points to the latter.

L384
L385 The cause of differences in the seasonal rates of SST change in group-SST models remains a subject of
L386 ongoing research. The Southern Ocean is a part of the global ocean (upwelling) where earth systems
L387 models show a persistent warming SST bias (Hirahara et al., 2014). Several studies point to highlight
L388 potential explanations but the main reasons remains uncertain. For example, CMIP5 models
L389 differences in the magnitude and meridional location of the peak of wind speeds in the Southern Ocean
L390 (Bracegirdle et al., 2013) and MLD differences (Meijers, 2014; Sallée et al., 2013) may be such that the
L391 net effect of change on surface turbulence and mixing leads to these amplified surface temperature
L392 rates. Other known CMIP5 models' biases that which may contribute includes; heat fluxes and storage
L393 (Frölicher et al., 2015) as well as sea-ice dynamics (Turner et al., 2013). Notwithstanding these,
L394 investigation of the reasons for sources of these dSST/dt biases is out of the scope of this study. Our
L395 aim here is to show that understanding biases in the drivers of pCO₂ (DIC and SST) at the seasonal
L396 scale is necessary to understand differences in the seasonal cycle of FCO₂ between models and

V2 Changes 2018/4/17 11:06 AM

Deleted:

V2 Changes 2018/4/17 11:06 AM

Formatted: Font:+Theme Body

V2 Changes 2018/4/17 11:06 AM

Deleted: ,

V2 Changes 2018/4/17 11:06 AM

Formatted: Font:+Theme Body

V2 Changes 2018/4/17 11:06 AM

Deleted: We notice here that the reason why CMIP5 models develop a winter bloom in the AZ requires further investigation (Hague and Vichi, submitted).

V2 Changes 2018/4/17 11:06 AM

Formatted: Font:+Theme Body

V2 Changes 2018/4/17 11:06 AM

Deleted: ingassing

V2 Changes 2018/4/17 11:06 AM

Formatted: Font:+Theme Body

V2 Changes 2018/4/17 11:06 AM

Deleted: zone

V2 Changes 2018/4/17 11:06 AM

Formatted: Font:+Theme Body

V2 Changes 2018/4/17 11:06 AM

Deleted: zone,

V2 Changes 2018/4/17 11:06 AM

Formatted: Font:+Theme Body

V2 Changes 2018/4/17 11:06 AM

Formatted: Font:+Theme Body

V2 Changes 2018/4/17 11:06 AM

Formatted: Normal1, No widow/orphan control

V2 Changes 2018/4/17 11:06 AM

Deleted: ,

V2 Changes 2018/4/17 11:06 AM

Formatted: Normal1

L406 observational products. However we recommend that the mechanistic basis for the differences the
L407 seasonal rates of warming and cooling be a matter of urgent investigated further

L408 .

L409

L410

L411

L412

L413 5. Synthesis

L414

L415 We used a seasonal cycle framework to highlight and examine two major biases in respect of pCO₂ and
L416 FCO₂ in 10 CMIP5 models in the Southern Ocean.

L417

L418 Firstly, we examined the general exaggeration of the seasonal rates of change of SST in autumn and
L419 spring seasons during peak cooling and warming respectively with respect to available observations.
L420 These elevated rates of SST change tip the control of the seasonal cycle of pCO₂ and FCO₂ towards SST
L421 from DIC and result in a divergence between the observed and modelled seasonal cycles, particularly
L422 in the Sub-Antarctic Zone. While almost all analyzed models (9 of 10) show these SST-driven biases, 3
L423 of the 10 (namely NorESM1-ME, HadGEM-ES and MPI-ESM) don't show these solubility biases because
L424 of their overly exaggerated primary production (and remineralization) rates such that biologically-
L425 driven DIC changes mainly regulate the seasonal cycle of FCO₂. These models reproduce the observed
L426 phasing of FCO₂ as a result of an incorrect scaling of the biogeochemical fluxes. In the Antarctic Zone,
L427 CMIP5 models compare better with observations relative to the Sub-Antarctic Zone. This is mostly
L428 because both CMIP5 models and observational product estimates show a spatial and temporal
L429 uniformity in the characteristics of FCO₂ in the Antarctic Zone. However, it is not certain if this is
L430 because model process dynamics perform better in this high latitude zone or that the observational
L431 products variability is itself limited by the lack of *in situ* data. This remains an open question that
L432 needs to be explored further and highlights the need for increased scale-sensitive and independent
L433 observations south of the Polar Front and into the sea-ice zone.

L434

L435 The second major bias is that contrary to observational products estimates, CMIP5 models generally
L436 show an equal sensitivity to basin scale FCO₂ drivers (except for CMCC-ESM, GFDL-ESM2M and
L437 CESM1-BGC) and hence the seasonal cycle of FCO₂ has similar phasing in all three basins of the Sub-
L438 Antarctic Zone. This is in contrast to observational and remote sensing products that highlight strong
L439 seasonal and interannually varying basin contrasts in both pCO₂ and phytoplankton biomass. It is not
L440 clear if this is due to inadequate carbon process parameterization or improper representation of the

V2 Changes 2018/4/17 11:06 AM

Formatted: Font:+Theme Body

V2 Changes 2018/4/17 11:06 AM

Formatted: Normal1

V2 Changes 2018/4/17 11:06 AM

Formatted: Font:+Theme Body, Font color: Black, English (US)

V2 Changes 2018/4/17 11:06 AM

Formatted: Font:+Theme Body

V2 Changes 2018/4/17 11:06 AM

Formatted: Font:+Theme Body

V2 Changes 2018/4/17 11:06 AM

Deleted: analysed

V2 Changes 2018/4/17 11:06 AM

Formatted: Font:+Theme Body

V2 Changes 2018/4/17 11:06 AM

Deleted:

V2 Changes 2018/4/17 11:06 AM

Formatted: Font:+Theme Body

V2 Changes 2018/4/17 11:06 AM

Deleted: zone

V2 Changes 2018/4/17 11:06 AM

Formatted: Font:+Theme Body

V2 Changes 2018/4/17 11:06 AM

Deleted: zone

V2 Changes 2018/4/17 11:06 AM

Formatted: Font:+Theme Body

V2 Changes 2018/4/17 11:06 AM

Deleted:

V2 Changes 2018/4/17 11:06 AM

Formatted: Font:+Theme Body

V2 Changes 2018/4/17 11:06 AM

Deleted:

V2 Changes 2018/4/17 11:06 AM

Formatted: Font:+Theme Body

V2 Changes 2018/4/17 11:06 AM

Deleted: zone

V2 Changes 2018/4/17 11:06 AM

Formatted: Font:+Theme Body

V2 Changes 2018/4/17 11:06 AM

Deleted: gaps in

V2 Changes 2018/4/17 11:06 AM

Formatted: Font:+Theme Body

V2 Changes 2018/4/17 11:06 AM

Deleted: ,

V2 Changes 2018/4/17 11:06 AM

Formatted: Normal1

L449 dynamics of the physics. This should be investigated further with CMIP6 models and our analysis
L450 framework is proposed as a useful tool to diagnose the dominant drivers. Contrary to observed
L451 estimates, CMIP5 models simulate FCO₂ seasonal dynamics that are zonally homogeneous and we
L452 suggest that any investigation of local (basin-scale) mechanisms, dynamics and long term trends of
L453 FCO₂ using CMIP5 models must remain tentative and should be treated with caution. This highlights a
L454 key area of development for the next generation of models such those planned to be used for CMIP6.
L455

V2 Changes 2018/4/17 11:06 AM
Deleted: for this reason it is suggested

V2 Changes 2018/4/17 11:06 AM
Formatted: Font:+Theme Body

V2 Changes 2018/4/17 11:06 AM
Deleted:

V2 Changes 2018/4/17 11:06 AM
Formatted: Font:+Theme Body

V2 Changes 2018/4/17 11:06 AM
Deleted: cautious.

V2 Changes 2018/4/17 11:06 AM
Formatted: Font:+Theme Body

V2 Changes 2018/4/17 11:06 AM
Formatted: Font:+Theme Body

V2 Changes 2018/4/17 11:06 AM
Formatted: Font:+Theme Body

V2 Changes 2018/4/17 11:06 AM
Formatted: Font:+Theme Body

V2 Changes 2018/4/17 11:06 AM
Formatted: Normal1

V2 Changes 2018/4/17 11:06 AM
Deleted:

V2 Changes 2018/4/17 11:06 AM
Formatted: Font:+Theme Body

V2 Changes 2018/4/17 11:06 AM
Deleted:

V2 Changes 2018/4/17 11:06 AM
Formatted: Font:+Theme Body

V2 Changes 2018/4/17 11:06 AM
Deleted: - ... [382]

V2 Changes 2018/4/17 11:06 AM
Formatted: Font:+Theme Body, 18 pt

V2 Changes 2018/4/17 11:06 AM
Formatted: Font:+Theme Body

V2 Changes 2018/4/17 11:06 AM
Formatted: Font:+Theme Body

V2 Changes 2018/4/17 11:06 AM
Deleted: ,

V2 Changes 2018/4/17 11:06 AM
Formatted: Normal1

L457 **Acknowledgements**

L459 This work was undertaken with financial support from the following South African institutions: CSIR
L460 Parliamentary Grant, National Research Foundation (NRF SANAP programme), Department of Science
L461 and Technology South Africa (DST), and the Applied Centre for Climate and Earth Systems Science
L462 (ACCESS). We thank the CSIR Centre for High Performance Computing (CHPC) for providing the
L463 resources for doing this analysis. We also want to thank Peter Landschützer, Taro Takahashi and Luke
L464 Gregor for making their data products available as well as the three reviewers for their productive
L465 comments that we think have strengthened the paper
L466

L467 **References**

L469 Anav, A., Friedlingstein, P., Kidston, M., Bopp, L., Ciais, P., Cox, P., Jones, C., Jung, M., Myneni, R. and Zhu,
L470 Z.: Evaluating the land and ocean components of the global carbon cycle in the CMIP5 earth system
L471 models, *J. Clim.*, 26(18), 6801–6843, doi:10.1175/JCLI-D-12-00417.1, 2013.
L472

L473 Bakker, D. C. E., Pfeil, B., Smith, K., Hankin, S., Olsen, A., Alin, S. R., Cosca, C., Harasawa, S., Kozyr, A.,
L474 Nojiri, Y., O'Brien, K. M., Schuster, U., Telszewski, M., Tilbrook, B., Wada, C., Akl, J., Barbero, L., Bates, N.
L475 R., Boutin, J., Bozec, Y., Cai, W.-J., Castle, R. D., Chavez, F. P., Chen, L., Chierici, M., Currie, K., De Baar, H. J.
L476 W., Evans, W., Feely, R. A., Fransson, A., Gao, Z., Hales, B., Hardman-Mountford, N. J., Hoppema, M.,
L477 Huang, W.-J., Hunt, C. W., Huss, B., Ichikawa, T., Johannessen, T., Jones, E. M., Jones, S. D., Jutterström, S.,
L478 Kitidis, V., Körtzinger, A., Landschützer, P., Lauvset, S. K., Lefèvre, N., Manke, A. B., Mathis, J. T., Merlivat,
L479 L., Metzl, N., Murata, A., Newberger, T., Omar, A. M., Ono, T., Park, G.-H., Paterson, K., Pierrot, D., Ríos, A.
L480 F., Sabine, C. L., Saito, S., Salisbury, J., Sarma, V. V. S. S., Schlitzer, R., Sieger, R., Skjelvan, I., Steinhoff, T.,
L481

L489 Sullivan, K. F., Sun, H., Sutton, A. J., Suzuki, T., Sweeney, C., Takahashi, T., Tjiputra, J. F., Tsurushima, N.,
L490 Van Heuven, S. M. A. C., Vandemark, D., Vlahos, P., Wallace, D. W. R., Wanninkhof, R. H. and Watson, A.
L491 J.: An update to the surface ocean CO₂ atlas (SOCAT version 2), Earth Syst. Sci. Data, 6(1), 69–90,
L492 doi:10.5194/essd-6-69-2014, 2014.

L493
L494 Barbero, L., Boutin, J., Merlivat, L., Martin, N., Takahashi, T., Sutherland, S. C. and Wanninkhof, R.:
L495 Importance of water mass formation regions for the air-sea CO₂ flux estimate in the southern ocean,
L496 Global Biogeochem. Cycles, 25(1), 1–16, doi:10.1029/2010GB003818, 2011.

L497
L498 Boyd, P. W. and Ellwood, M. J.: The biogeochemical cycle of iron in the ocean, Nat. Geosci., 3(10), 675–
L499 682, doi:10.1038/ngeo964, 2010.

L500
L501 [Bracegirdle, T. J., Shuckburgh, E., Sallee, J. B., Wang, Z., Meijers, A. J. S., Bruneau, N., Phillips, T.](#)
L502 [and Wilcox, L. J.: Assessment of surface winds over the atlantic, indian, and pacific ocean](#)
L503 [sectors of the southern ocean in cmip5 models: Historical bias, forcing response, and state](#)
L504 [dependence, J. Geophys. Res. Atmos., 118\(2\), 547–562, doi:10.1002/jgrd.50153, 2013.](#)

L505
L506 de Boyer Montégut, C., Madec, G., Fischer, A. S., Lazar, A. and Iudicone, D.: Mixed layer depth over the
L507 global ocean: An examination of profile data and a profile-based climatology, J. Geophys. Res. C Ocean.,
L508 109(12), 1–20, doi:10.1029/2004JC002378, 2004.

L509
L510 Dickson, A. G. and Millero, F. J.: A comparison of the equilibrium constants for the dissociation of
L511 carbonic acid in seawater media, Deep Sea Res. Part A, Oceanogr. Res. Pap., 34(10), 1733–1743,
L512 doi:10.1016/0198-0149(87)90021-5, 1987.

L513
L514 Dufour, C. O., Sommer, J. Le, Gehlen, M., Orr, J. C., Molines, J. M., Simeon, J. and Barnier, B.: Eddy
L515 compensation and controls of the enhanced sea-to-air CO₂ flux during positive phases of the Southern
L516 Annular Mode, Global Biogeochem. Cycles, 27(3), 950–961, doi:10.1002/gbc.20090, 2013.

L517
L518 Feely, R. A., Wanninkhof, R., McGillis, W., Carr M. E and Cosca, C.: Effects of wind speed and gas
L519 exchange parameterizations on the air-sea CO₂ fluxes in the equatorial Pacific Ocean, J. Geophys. Res.,
L520 109(C8), C08S03, doi:10.1029/2003JC001896, 2004.

L521
L522 Frölicher, T. L., Sarmiento, J. L., Paynter, D. J., Dunne, J. P., Krasting, J. P. and Winton, M.: Dominance of
L523 the Southern Ocean in anthropogenic carbon and heat uptake in CMIP5 models, J. Clim., 28(2), 862–
L524 886, doi:10.1175/JCLI-D-14-00117.1, 2015.

V2 Changes 2018/4/17 11:06 AM

Moved (insertion) [5]

V2 Changes 2018/4/17 11:06 AM

Formatted: Font:+Theme Body, 12 pt

V2 Changes 2018/4/17 11:06 AM

Formatted: Font:+Theme Body

V2 Changes 2018/4/17 11:06 AM

Formatted: Normal1

l525
l526 Fung, I. Y., Doney, S. C., Lindsay, K. and John, J.: Evolution of carbon sinks in a changing climate, Proc.
l527 Natl. Acad. Sci., 102(32), 11201–11206, doi:10.1073/pnas.0504949102, 2005.
l528
l529 Graham, R. M., De Boer, A. M., van Sebille, E., Kohfeld, K. E. and Schlosser, C.: Inferring source regions
l530 and supply mechanisms of iron in the Southern Ocean from satellite chlorophyll data, Deep. Res. Part I
l531 Oceanogr. Res. Pap., 104, 9–25, doi:10.1016/j.dsr.2015.05.007, 2015.
l532
l533 Gregor, L., Kok, S. and Monteiro, P. M. S.: Empirical methods for the estimation of Southern Ocean CO₂:
l534 support vector and random forest regression, Biogeosciences, 14(23), 5551–5569, doi:10.5194/bg-14-
l535 5551-2017, 2017a.
l536
l537 Gregor, L., Kok, S. and Monteiro, P. M. S.: Interannual drivers of the seasonal cycle of CO₂ fluxes in the
l538 Southern Ocean, Biogeosciences Discuss., (September), 1–28, doi:10.5194/bg-2017-363, 2017b.
l539
l540 Gruber, N., Gloor, M., Mikaloff Fletcher, S. E., Doney, S. C., Dutkiewicz, S., Follows, M. J., Gerber, M.,
l541 Jacobson, A. R., Joos, F., Lindsay, K., Menemenlis, D., Mouchet, A., Müller, S. A., Sarmiento, J. L. and
l542 Takahashi, T.: Oceanic sources, sinks, and transport of atmospheric CO₂, Global Biogeochem. Cycles,
l543 23(1), 1–21, doi:10.1029/2008GB003349, 2009.
l544
l545 Hauck, J. and Völker, C.: A multi-model study on the Southern Ocean CO₂ uptake and the role of the
l546 biological carbon pump in the 21st century, EGU Gen. Assem., 17, 12225,
l547 doi:10.1002/2015GB005140.Received, 2015.
l548
l549 Hauck, J., Völker, C., Wolf-Gladrow, D. a., Laufkötter, C., Vogt, M., Aumont, O., Bopp, L., Buitenhuis, E. T.,
l550 Doney, S. C., Dunne, J., Gruber, N., John, J., Le Quéré, C., Lima, I. D., Nakano, H. and Totterdell, I.: On the
l551 Southern Ocean CO₂ uptake and the role of the biological carbon pump in the 21st century, Global
l552 Biogeochem. Cycles, 29, 1451–1470, doi:10.1002/2015GB005140, 2015.
l553
l554 [Hirahara, S., Ishii, M. and Fukuda, Y.: Centennial-scale sea surface temperature analysis and its](#)
l555 [uncertainty, J. Clim., 27\(1\), 57–75, doi:10.1175/JCLI-D-12-00837.1, 2014.](#)
l556
l557 Ilyina, T., Six, K. D., Segsneider, J., Maier-Reimer, E., Li, H. and Núñez-Riboni, I.: Global ocean
l558 biogeochemistry model HAMOCC: Model architecture and performance as component of the MPI-Earth
l559 system model in different CMIP5 experimental realizations, J. Adv. Model. Earth Syst., 5(2), 287–315,
l560 doi:10.1029/2012MS000178, 2013.

V2 Changes 2018/4/17 11:06 AM

Formatted: Font:+Theme Body

V2 Changes 2018/4/17 11:06 AM

Formatted: Normal1

V2 Changes 2018/4/17 11:06 AM

Deleted: doi:

V2 Changes 2018/4/17 11:06 AM

Formatted: Font:+Theme Body

V2 Changes 2018/4/17 11:06 AM

Formatted: Font:+Theme Body

V2 Changes 2018/4/17 11:06 AM

Formatted: Normal1

V2 Changes 2018/4/17 11:06 AM

Deleted: ,

V2 Changes 2018/4/17 11:06 AM

Formatted: Normal1

L562
L563 Johnson, K. S., Plant, J. N., Coletti, L. J., Jannasch, H. W., Sakamoto, C. M., Riser, S. C., Swift, D. D., Williams,
L564 N. L., Boss, E., Haëntjens, N., Talley, L. D. and Sarmiento, J. L.: Biogeochemical sensor performance in
L565 the SOCCOM profiling float array, *J. Geophys. Res. Ocean.*, (September), doi:10.1002/2017JC012838,
L566 2017.

L567
L568 Johnson, R., Strutton, P. G., Wright, S. W., McMinn, A. and Meiners, K. M.: Three improved satellite
L569 chlorophyll algorithms for the Southern Ocean, *J. Geophys. Res. Ocean.*, 118(7), 3694–3703,
L570 doi:10.1002/jgrc.20270, 2013.

L571
L572 Kessler, A. and Tjiputra, J.: The Southern Ocean as a constraint to reduce uncertainty in future ocean
L573 carbon sinks, *Earth Syst. Dyn.*, 7(2), 295–312, doi:10.5194/esd-7-295-2016, 2016.

L574
L575 Landschützer, P., Gruber, N. and Bakker, D. C. E. Stemmler, I. and Six, K. D.: Strengthening seasonal
L576 marine CO₂ variations due to increasing atmospheric CO₂. *Nature Climate Change*, 8, 146-150, Doi:
L577 10.1038/s41558-017-0057-x, 2018.

L578
L579 Landschützer, P., Gruber, N. and Bakker, D. C. E.: Decadal variations and trends of the global ocean
L580 carbon sink, *Global Biogeochem. Cycles*, 30(10), 1396–1417, doi:10.1002/2015GB005359, 2016.

L581
L582 Landschützer, P., Gruber, N., Haumann, F. A., Rodenbeck, C., Bakker, D. C. E., van Heuven, S., Hoppema,
L583 M., Metzl, N., Sweeney, C., Takahashi, T., Tilbrook, B. and Wanninkhof, R.: The reinvigoration of the
L584 Southern Ocean carbon sink, *Science* (80-.), 349(6253), 1221–1224, doi:10.1126/science.aab2620,
L585 2015.

L586
L587 Landschützer, P., Gruber, N., Bakker, D. C. E. and Schuster, U.: Recent variability of the global ocean
L588 carbon sink, *Glob. Planet. Change*, 927–949, doi:10.1002/2014GB004853.Received, 2014.

L589
L590 Landschützer, P., Gruber, N., Bakker, D. C. E., Schuster, U., Nakaoka, S., Payne, M. R., Sasse, T. P. and
L591 Zeng, J.: A neural network-based estimate of the seasonal to inter-annual variability of the Atlantic
L592 Ocean carbon sink, *Biogeosciences*, 10(11), 7793–7815, doi:10.5194/bg-10-7793-2013, 2013.

L593
L594 Lauvset, S. K., Key, R. M., Olsen, A., Van Heuven, S., Velo, A., Lin, X., Schirnack, C., Kozyr, A., Tanhua, T.,
L595 Hoppema, M., Jutterström, S., Steinfeldt, R., Jeansson, E., Ishii, M., Perez, F. F., Suzuki, T. and Watelet, S.:
L596 A new global interior ocean mapped climatology: The 1° × 1° GLODAP version 2, *Earth Syst. Sci. Data*,
L597 8(2), 325–340, doi:10.5194/essd-8-325-2016, 2016.

V2 Changes 2018/4/17 11:06 AM

Deleted:

V2 Changes 2018/4/17 11:06 AM

Formatted: Font:+Theme Body

V2 Changes 2018/4/17 11:06 AM

Deleted: Landschutzer

V2 Changes 2018/4/17 11:06 AM

Formatted: Font:+Theme Body

V2 Changes 2018/4/17 11:06 AM

Moved (insertion) [6]

V2 Changes 2018/4/17 11:06 AM

Formatted: Font:+Theme Body

V2 Changes 2018/4/17 11:06 AM

Formatted: Font:+Theme Body

V2 Changes 2018/4/17 11:06 AM

Formatted: Normal1

V2 Changes 2018/4/17 11:06 AM

Deleted: ,

V2 Changes 2018/4/17 11:06 AM

Formatted: Normal1

l600
l601 Lee, K., Tong, L. T., Millero, F. J., Sabine, C. L., Dickson, A. G., Goyet, C., Park, G. H., Wanninkhof, R., Feely,
l602 R. A. and Key, R. M.: Global relationships of total alkalinity with salinity and temperature in surface
l603 waters of the world's oceans, *Geophys. Res. Lett.*, 33(19), 1–5, doi:10.1029/2006GL027207, 2006.
l604
l605 Lenton, A., Metzl, N., Takahashi, T., Kuchinke, M., Matear, R. J., Roy, T., Sutherland, S. C., Sweeney, C. and
l606 Tilbrook, B.: The observed evolution of oceanic pCO₂ and its drivers over the last two decades, *Global*
l607 *Biogeochem. Cycles*, 26(2), 1–14, doi:10.1029/2011GB004095, 2012.
l608
l609 Lenton, A., Tilbrook, B., Law, R., Bakker, D., Doney, S. C., Gruber, N., Hoppema, M., Ishii, M., Lovenduski,
l610 N. S., Matear, R. J., McNeil, B. I., Metzl, N., Mikaloff Fletcher, S. E., Monteiro, P., Rödenbeck, C., Sweeney,
l611 C. and Takahashi, T.: Sea-air CO₂ fluxes in the Southern Ocean for the period
l612 1990–2009, *Biogeosciences Discuss.*, 10(1), 285–333, doi:10.5194/bgd-10-285-2013,
l613 2013.
l614
l615 Leung, S., Cabre, A. and Marinov, I.: A latitudinally banded phytoplankton response to 21st century
l616 climate change in the Southern Ocean across the CMIP5 model suite, *Biogeosciences*, 12(19), 5715–
l617 5734, doi:10.5194/bg-12-5715-2015, 2015.
l618
l619 Locarnini, R. A., Mishonov, A. V., Antonov, J. I., Boyer, T. P., Garcia, H. E., Baranova, O. K., Zweng, M. M.,
l620 Paver, C. R., Reagan, J. R., Johnson, D. R., Hamilton, M. and Seidov, D.: *World Ocean Atlas 2013. Vol. 1:*
l621 *Temperature.*, 2013.
l622
l623 Mahadevan, A., Tagliabue, A., Bopp, L., Lenton, A., Memery, L. and Levy, M.: Impact of episodic vertical
l624 fluxes on sea surface pCO₂, *Philos. Trans. R. Soc. A Math. Phys. Eng. Sci.*, 369(1943), 2009–2025,
l625 doi:10.1098/rsta.2010.0340, 2011.
l626
l627 Mahadevan, A., D'Asaro, E., Lee, C. and Perry, M. J.: Eddy-driven stratification initiates North Atlantic
l628 spring phytoplankton blooms, *Science* (80-.), 336(6090), 54–58, doi:10.1126/science.1218740, 2012.
l629 Marinov, I. and Gnanadesikan, A.: Changes in ocean circulation and carbon storage are decoupled from
l630 air-sea CO₂ fluxes, *Biogeosciences*, 8(2), 505–513, doi:10.5194/bg-8-505-2011, 2011.
l631
l632 Marinov, I., Gnanadesikan, A., Toggweiler, J. R. and Sarmiento, J. L.: The Southern Ocean
l633 biogeochemical divide, *Nature*, 441(7096), 964–967, doi:10.1038/nature04883, 2006.
l634
l635 Matear, R. J. and Lenton, A.: Impact of Historical Climate Change on the Southern Ocean Carbon Cycle, J.

l636 Clim., 21(22), 5820–5834, doi:10.1175/2008JCLI2194.1, 2008.

l637

l638 McNeil, B. I., Metzl, N., Key, R. M., Matear, R. J. and Corbiere, A.: An empirical estimate of the Southern

l639 Ocean air-sea CO₂ flux, *Global Biogeochem. Cycles*, 21(3), 1–16, doi:10.1029/2007GB002991, 2007.

l640

l641 Mehrbach, C., Culberson, C. H., Hawley, J. E. and Pytkowicz, R. M.: Measurement of the Apparent

l642 Dissociation Constants of Carbonic Acid in Seawater At Atmospheric Pressure, *Limnol. Oceanogr.*,

l643 18(6), 897–907, doi:10.4319/lo.1973.18.6.0897, 1973.

l644

l645 Metzl, N.: Decadal increase of oceanic carbon dioxide in Southern Indian Ocean surface waters (1991-

l646 2007), *Deep. Res. Part II Top. Stud. Oceanogr.*, 56(8–10), 607–619, doi:10.1016/j.dsr2.2008.12.007,

l647 2009.

l648 Metzl, N., Brunet, C., Jabaud-Jan, A., Poisson, A. and Schauer, B.: Summer and winter air-sea CO₂ fluxes

l649 in the Southern Ocean, *Deep. Res. Part I Oceanogr. Res. Pap.*, 53(9), 1548–1563,

l650 doi:10.1016/j.dsr.2006.07.006, 2006.

l651

l652 Mongwe, N. P., Chang, N. and Monteiro, P. M. S.: The seasonal cycle as a mode to diagnose biases in

l653 modelled CO₂ fluxes in the Southern Ocean, *Ocean Model.*, 106, 90–103,

l654 doi:10.1016/j.ocemod.2016.09.006, 2016.

l655

l656 Monteiro, P. M. S., [et al. \(2010\), A global sea surface carbon observing system: Assessment of changing](#)

l657 [sea surface CO₂ and air-sea CO₂ fluxes, in Proceedings of the “OceanObs’09: Sustained Ocean](#)

l658 [Observations and Information for Society” Conference, edited by J. Hall, D. E. Harrison,](#)

l659 [and D. Stammer, ESA Publ. WPP-306, Venice, Italy, doi:10.5270/OceanObs09.cwp.64, 21–25 Sept.](#)

l660

l661 Monteiro, P. M. S., Gregor, L., Lévy, M., Maenner, S., Sabine, C. L. and Swart, S.: Intra-seasonal variability

l662 linked to sampling alias in air – sea CO₂ fluxes in the Southern Ocean, *Geophys. Res. Lett.*, 1–8,

l663 doi:10.1002/2015GL066009, 2015.

l664

l665 Moore, J. K., Doney, S. C. and Lindsay, K.: Upper ocean ecosystem dynamics and iron cycling in a global

l666 three-dimensional model, *Global Biogeochem. Cycles*, 18(4), 1–21, doi:10.1029/2004GB002220, 2004.

l667

l668 Orsi, A. H., Whitworth, T. and Nowlin, W. D.: On the meridional extent and fronts of the Antarctic

l669 Circumpolar Current, *Deep. Res. Part I*, 42(5), 641–673, doi:10.1016/0967-0637(95)00021-W, 1995.

l670

l671 Pasquer, B., Metzl, N., Goosse, H. and Lancelot, C.: What drives the seasonality of air-sea CO₂ fluxes in

V2 Changes 2018/4/17 11:06 AM
Deleted: Monteiro, P. M. S., Monteiro, P. M.

V2 Changes 2018/4/17 11:06 AM
Formatted: Normal1, Border:Top: (No border), Bottom: (No border), Left: (No border), Right: (No border), Between : (No border)

V2 Changes 2018/4/17 11:06 AM
Moved up [5]: S.,

V2 Changes 2018/4/17 11:06 AM
Moved up [6]: P.

V2 Changes 2018/4/17 11:06 AM
Formatted: Font:+Theme Body

V2 Changes 2018/4/17 11:06 AM
Deleted: M. S., Monteiro, P. M. S., Monteiro, P. M. S., Monteiro, P. M. S., Monteiro, P. M.

V2 Changes 2018/4/17 11:06 AM
Moved down [7]: . S.,

V2 Changes 2018/4/17 11:06 AM
Deleted: Monteiro, P. M. S., Monteiro,

V2 Changes 2018/4/17 11:06 AM
Formatted: Font:+Theme Body, 12 pt

V2 Changes 2018/4/17 11:06 AM
Formatted: Font:+Theme Body

V2 Changes 2018/4/17 11:06 AM
Deleted: Monteiro, P. M. S., Monteiro, P. M. S., Monteiro, P. M. S. and Monteiro, P. M. S.: A Global Sea Surface Carbon Observing System: Assessment of Changing Sea Surface CO₂ and Air-Sea CO₂ Fluxes, *Proc. Ocean. Sustain. Ocean Obs. Inf. Soc.*, (1), 702–714, doi:10.5270/OceanObs09.cwp.64, 2010.

V2 Changes 2018/4/17 11:06 AM
Formatted: Font:+Theme Body

V2 Changes 2018/4/17 11:06 AM
Formatted: Font:+Theme Body

V2 Changes 2018/4/17 11:06 AM
Formatted: Normal1

V2 Changes 2018/4/17 11:06 AM
Deleted: ,

V2 Changes 2018/4/17 11:06 AM
Formatted: Normal1

l687 the ice-free zone of the Southern Ocean: A 1D coupled physical-biogeochemical model approach, Mar.
l688 Chem., 177, 554–565, doi:10.1016/j.marchem.2015.08.008, 2015.

l689

l690 Pierrot, D. E. Lewis, and D. W. R. Wallace. 2006. MS Excel Program Developed for CO₂ System
l691 Calculations. ORNL/CDIAC-105a. Carbon Dioxide Information Analysis Center, Oak Ridge National
l692 Laboratory, U.S. Department of Energy, Oak Ridge, Tennessee. doi:
l693 10.3334/CDIAC/otg.CO2SYS_XLS_CDIAC105a

l694

l695 du Plessis, M., Swart, S., Anson, I. J. and Mahadevan, A.: Submesoscale processes promote seasonal
l696 restratification in the Subantarctic Ocean, J. Geophys. Res. Ocean., 122(4), 2960–2975,
l697 doi:10.1002/2016JC012494, 2017.

l698

l699 Le Quéré, C. and Saltzman, E. S.: Surface Ocean-Lower Atmosphere Processes., 2013.

l700 Le Quéré, C., Rödenbeck, C., Buitenhuis, E. T., Conway, T. J., Langenfelds, R., Gomez, A., Labuschagne, C.,
l701 Ramonet, M., Nakazawa, T., Metzl, N., Gillett, N. and Heimann, M.: Saturation of the southern ocean CO₂
l702 sink due to recent climate change, Science (80-.), 316(5832), 1735–1738,
l703 doi:10.1126/science.1136188, 2007.

l704

l705 Le Quéré, C., Andrew, R. M., Canadell, J. G., Sitch, S., Ivar Korsbakken, J., Peters, G. P., Manning, A. C.,
l706 Boden, T. A., Tans, P. P., Houghton, R. A., Keeling, R. F., Alin, S., Andrews, O. D., Anthoni, P., Barbero, L.,
l707 Bopp, L., Chevallier, F., Chini, L. P., Ciais, P., Currie, K., Delire, C., Doney, S. C., Friedlingstein, P.,
l708 Gkritzalis, T., Harris, I., Hauck, J., Haverd, V., Hoppema, M., Klein Goldewijk, K., Jain, A. K., Kato, E.,
l709 Körtzinger, A., Landschützer, P., Lefèvre, N., Lenton, A., Lienert, S., Lombardozzi, D., Melton, J. R., Metzl,
l710 N., Millero, F., Monteiro, P. M. S., Munro, D. R., Nabel, J. E. M. S., Nakaoka, S. I., O'Brien, K., Olsen, A.,
l711 Omar, A. M., Ono, T., Pierrot, D., Poulter, B., Rödenbeck, C., Salisbury, J., Schuster, U., Schwinger, J.,
l712 Séférian, R., Skjelvan, I., Stocker, B. D., Sutton, A. J., Takahashi, T., Tian, H., Tilbrook, B., Van Der Laan-
l713 Luijkx, I. T., Van Der Werf, G. R., Viovy, N., Walker, A. P., Wiltshire, A. J. and Zaehle, S.: Global Carbon
l714 Budget 2016, Earth Syst. Sci. Data, 8(2), 605–649, doi:10.5194/essd-8-605-2016, 2016.

l715

l716 Ritter, R., Landschützer, P., Gruber, N., Fay, A. R., Iida, Y., Jones, S., Nakaoka, S., Park, G. H., Peylin, P.,
l717 Rödenbeck, C., Rodgers, K. B., Shutler, J. D. and Zeng, J.: Observation-Based Trends of the Southern
l718 Ocean Carbon Sink, Geophys. Res. Lett., doi:10.1002/2017GL074837, 2017.

l719

l720 Rödenbeck, C., Keeling, R. F., Bakker, D. C. E., Metzl, N., Olsen, A., Sabine, C. and Heimann, M.: Global
l721 surface-ocean pCO₂ and sea-air CO₂ flux variability from an observation-driven ocean mixed-layer
l722 scheme, Ocean Sci., 9(2), 193–216, doi:10.5194/os-9-193-2013, 2013.

V2 Changes 2018/4/17 11:06 AM

Deleted: Air

V2 Changes 2018/4/17 11:06 AM

Formatted: Font:+Theme Body

V2 Changes 2018/4/17 11:06 AM

Deleted: ,

V2 Changes 2018/4/17 11:06 AM

Formatted: Normal1

L724
 L725 Rodgers, K. B., Aumont, O., Mikaloff Fletcher, S. E., Plancherel, Y., Bopp, L., De Boyer Montégut, C.,
 L726 Iudicone, D., Keeling, R. F., Madec, G. and Wanninkhof, R.: Strong sensitivity of Southern Ocean carbon
 L727 uptake and nutrient cycling to wind stirring, *Biogeosciences*, 11(15), 4077–4098, doi:10.5194/bg-11-
 L728 4077-2014, 2014.
 L729
 L730 Rosso, I., Mazloff, M. R., Verdy, A. and Talley, L. D.: Space and time variability of the Southern Ocean
 L731 carbon budget, *J. Geophys. Res. Ocean.*, 122(9), 7407–7432, doi:10.1002/2016JC012646, 2017.
 L732
 L733 Roy, T., Bopp, L., Gehlen, M., Schneider, B., Cadule, P., Frölicher, T. L., Segschneider, J., Tjiputra, J.,
 L734 Heinze, C. and Joos, F.: Regional impacts of climate change and atmospheric CO₂ on future ocean
 L735 carbon uptake: A multimodel linear feedback analysis, *J. Clim.*, 24(9), 2300–2318,
 L736 doi:10.1175/2010JCLI3787.1, 2011.
 L737
 L738 Sabine, C. L., Feely, R. A., Gruber, N., Key, R. M., Lee, K., Bullister, J. L., Wanninkhof, R., Wong, C. S.,
 L739 Wallace, D. W. R., Tilbrook, B., Millero, F. J., Peng, T. H., Kozyr, A., Ono, T. and Rios, A. F.: The oceanic
 L740 sink for anthropogenic CO₂, *Science* (80-.), 305(5682), 367–371, doi:10.1126/science.1097403, 2004.
 L741
 L742 Sallée, J. B., Wienders, N., Speer, K. and Morrow, R.: Formation of subantarctic mode water in the
 L743 southeastern Indian Ocean, *Ocean Dyn.*, 56(5–6), 525–542, doi:10.1007/s10236-005-0054-x, 2006.
 L744
 L745 Sallée, J. B., Shuckburgh, E., Bruneau, N., Meijers, A. J. S., Bracegirdle, T. J., Wang, Z. and Roy, T.:
 L746 Assessment of Southern Ocean water mass circulation and characteristics in CMIP5 models: Historical
 L747 bias and forcing response, *J. Geophys. Res. Ocean.*, 118(4), 1830–1844, doi:10.1002/jgrc.20135, 2013.
 L748
 L749 Sarmiento, J. L. and Gruber, N.: *Ocean Biogeochemical Dynamics*, Carbon N. Y., 67,
 L750 doi:10.1063/1.2754608, 2006.
 L751
 L752 Sarmiento, J. L., Gruber, N., Brzezinski, M. A. and Dunne, J. P.: High-latitude controls of thermocline
 L753 nutrients and low latitude biological productivity, *Nature*, 427(6969), 56–60,
 L754 doi:10.1038/nature02127, 2004.
 L755
 L756 Sarmiento, J. L., Hughes, T. M. C., Stouffer, R. J. and Manabe, S.: Simulated response of the ocean carbon
 L757 cycle to anthropogenic climate warming, *Nature*, 393(6682), 245–249, doi:10.1038/30455, 1998.
 L758
 L759 Sférian, R., Bopp, L., Gehlen, M., Orr, J. C., Ethé, C., Cadule, P., Aumont, O., Salas y Méria, D., Voldoire, A.

V2 Changes 2018/4/17 11:06 AM

Formatted: Font:+Theme Body

V2 Changes 2018/4/17 11:06 AM

Formatted: Normal1

V2 Changes 2018/4/17 11:06 AM

Formatted: Font:+Theme Body

V2 Changes 2018/4/17 11:06 AM

Formatted: Font:+Theme Body

V2 Changes 2018/4/17 11:06 AM

Formatted: Normal1

V2 Changes 2018/4/17 11:06 AM

Deleted: ,

V2 Changes 2018/4/17 11:06 AM

Formatted: Normal1

and Madec, G.: Skill assessment of three earth system models with common marine biogeochemistry, *Clim. Dyn.*, 40(9–10), 2549–2573, doi:10.1007/s00382-012-1362-8, 2013.

Segschneider, J. and Bendtsen, J.: Temperature-dependent remineralization in a warming ocean increases surface pCO₂ through changes in marine ecosystem composition, *Global Biogeochem. Cycles*, 27(4), 1214–1225, doi:10.1002/2013GB004684, 2013.

Son, S. W., Gerber, E. P., Perlwitz, J., Polvani, L. M., Gillett, N. P., Seo, K. H., Eyring, V., Shepherd, T. G., Waugh, D., Akiyoshi, H., Austin, J., Baumgaertner, A., Bekki, S., Braesicke, P., Brühl, C., Butchart, N., Chipperfield, M. P., Cugnet, D., Dameris, M., Dhomse, S., Frith, S., Garny, H., Garcia, R., Hardiman, S. C., Jöckel, P., Lamarque, J. F., Mancini, E., Marchand, M., Michou, M., Nakamura, T., Morgenstern, O., Pitari, G., Plummer, D. A., Pyle, J., Rozanov, E., Scinocca, J. F., Shibata, K., Smale, D., Teyssdre, H., Tian, W. and Yamashita, Y.: Impact of stratospheric ozone on Southern Hemisphere circulation change: A multimodel assessment, *J. Geophys. Res. Atmos.*, 115(19), 1–18, doi:10.1029/2010JD014271, 2010.

Swart, N. C., Fyfe, J. C., Saenko, O. A. and Eby, M.: Wind-driven changes in the ocean carbon sink, *Biogeosciences*, 11(21), 6107–6117, doi:10.5194/bg-11-6107-2014, 2014.

Tagliabue, A., Mtshali, T., Aumont, O., Bowie, A. R., Klunder, M. B., Roychoudhury, A. N. and Swart, S.: A global compilation of dissolved iron measurements: Focus on distributions and processes in the Southern Ocean, *Biogeosciences*, 9(6), 2333–2349, doi:10.5194/bg-9-2333-2012, 2012.

Tagliabue, A., Williams, R. G., Rogan, N., Achterberg, E. P. and Boyd, P. W.: A ventilation-based framework to explain the regeneration-scavenging balance of iron in the ocean, *Geophys. Res. Lett.*, 41(20), 7227–7236, doi:10.1002/2014GL061066, 2014.

Takahashi, T., Olafsson, J., Goddard, J. G., Chipman, D. W. and Sutherland, S. C.: Seasonal variation of CO₂ and nutrients in the high-latitude surface oceans: A comparative study, *Global Biogeochem. Cycles*, 7(4), 843–878, doi:10.1029/93GB02263, 1993.

Takahashi, T., Sutherland, S. C., Sweeney, C., Poisson, A., Metz, N., Tilbrook, B., Bates, N., Wanninkhof, R., Feely, R. A., Sabine, C., Olafsson, J. and Nojiri, Y.: Global sea-air CO₂ flux based on climatological surface ocean pCO₂, and seasonal biological and temperature effects, *Deep. Res. Part II Top. Stud. Oceanogr.*, 49, 1601–1622, doi:10.1016/S0967-0645(02)00003-6, 2002.

Takahashi, T., Sutherland, S. C., Wanninkhof, R., Sweeney, C., Feely, R. A., Chipman, D. W., Hales, B.,

l796 Friederich, G., Chavez, F., Sabine, C., Watson, A., Bakker, D. C. E., Schuster, U., Metzl, N., Yoshikawa-
 l797 Inoue, H., Ishii, M., Midorikawa, T., Nojiri, Y., Körtzinger, A., Steinhoff, T., Hoppema, M., Olafsson, J.,
 l798 Arnarson, T. S., Tilbrook, B., Johannessen, T., Olsen, A., Bellerby, R., Wong, C. S., Delille, B., Bates, N. R.
 l799 and de Baar, H. J. W.: Climatological mean and decadal change in surface ocean pCO₂, and net sea-air
 l800 CO₂ flux over the global oceans, *Deep. Res. Part II Top. Stud. Oceanogr.*, 56(8–10), 554–577,
 l801 doi:10.1016/j.dsr2.2008.12.009, 2009.
 l802
 l803 Takahashi, T., Sweeney, C., Hales, B., Chipman, D., Newberger, T., Goddard, J., Iannuzzi, R. and
 l804 Sutherland, S.: The Changing Carbon Cycle in the Southern Ocean, *Oceanography*, 25(3), 26–37,
 l805 doi:10.5670/oceanog.2012.71, 2012.
 l806
 l807 Taylor, K. E., Stouffer, R. J. and Meehl, G. A.: An overview of CMIP5 and the experiment design, *Bull. Am.*
 l808 *Meteorol. Soc.*, 93(4), 485–498, doi:10.1175/BAMS-D-11-00094.1, 2012.
 l809
 l810 Thomalla, S. J., Fauchereau, N., Swart, S. and Monteiro, P. M. S.: Regional scale characteristics of the
 l811 seasonal cycle of chlorophyll in the Southern Ocean, *Biogeosciences*, 8(10), 2849–2866,
 l812 doi:10.5194/bg-8-2849-2011, 2011.
 l813
 l814 Thompson, D. W. J., Solomon, S., Kushner, P. J., England, M. H., Grise, K. M. and Karoly, D. J.: Signatures
 l815 of the Antarctic ozone hole in Southern Hemisphere surface climate change, *Nat. Geosci.*, 4(11), 741–
 l816 749, doi:10.1038/ngeo1296, 2011.
 l817
 l818 [Vichi, M., Pinardi, N. and Masina, S.: A generalized model of pelagic biogeochemistry for the global](#)
 l819 [ocean ecosystem. Part I: Theory, *J. Mar. Syst.*, 64\(1–4\), 89–109, doi:DOI](#)
 l820 [10.1016/j.jmarsys.2006.03.006, 2007.](#)
 l821
 l822 Visinelli, L., Masina, S., Vichi, M., Storto, A. and Lovato, T.: Impacts of data assimilation on the global
 l823 ocean carbonate system, *J. Mar. Syst.*, 158, 106–119, doi:10.1016/j.jmarsys.2016.02.011, 2016.
 l824
 l825 Wanninkhof, R., Asher, W. E., Ho, D. T., Sweeney, C. and McGillis, W. R.: Advances in Quantifying Air-Sea
 l826 Gas Exchange and Environmental Forcing, *Ann. Rev. Mar. Sci.*, 1(1), 213–244,
 l827 doi:10.1146/annurev.marine.010908.163742, 2009.
 l828
 l829 [Wanninkhof, R., Park, G. H., Takahashi, T., Sweeney, C., Feely, R., Nojiri, Y., Gruber, N., Doney, S. C.,](#)
 l830 [McKinley, G. A., Lenton, A., Le Quere, C., Heinze, C., Schwinger, J., Graven, H. and Khatiwala, S.: Global](#)
 l831 [ocean carbon uptake: Magnitude, variability and trends, *Biogeosciences*, 10\(3\), 1983–2000.](#)

V2 Changes 2018/4/17 11:06 AM
Formatted: Font+Theme Body

V2 Changes 2018/4/17 11:06 AM
Formatted: Normal1

V2 Changes 2018/4/17 11:06 AM
Deleted: ,

V2 Changes 2018/4/17 11:06 AM
Formatted: Normal1

L832 [doi:10.5194/bg-10-1983-2013](https://doi.org/10.5194/bg-10-1983-2013), 2013.

L833
L834 [Williams, N. L., Juraneck, L. W., Feely, R. A., Johnson, K. S., Sarmiento, J. L., Talley, L. D., Dickson, A. G.,](#)
L835 [Gray, A. R., Wanninkhof, R., Russell, J. L., Riser, S. C. and Takeshita, Y.: Calculating surface ocean pCO2](#)
L836 [from biogeochemical Argo floats equipped with pH: An uncertainty analysis, Global Biogeochem.](#)
L837 [Cycles, 31\(3\), 591–604, doi:10.1002/2016GB005541, 2017.](#)

L838 ▲
L839 Young, I. R.: Seasonal Variability of the Global Ocean Wind and Wave Climate, Int. J. Clim., 19(July
L840 2015), 931–950, doi:10.1002/(SICI)1097-0088(199907)19, 1999.

L841
L842 Zahariev, K., Christian, J. R. and Denman, K. L.: Preindustrial, historical, and fertilization simulations
L843 using a global ocean carbon model with new parameterizations of iron limitation, calcification, and
L844 N2fixation, Prog. Oceanogr., 77(1), 56–82, doi:10.1016/j.pocean.2008.01.007, 2008.

L845
L846 Zickfeld, K., Fyfe, J. C., Eby, M. and Weaver, A. J.: Comment on “Saturation of the southern ocean CO2
L847 sink due to recent climate change”, Science, 319(5863), 570; author reply 570,
L848 doi:10.1126/science.1146886, 2008.

L849 x
L850 ▲
L851 ▲
L852 ▲
L853
L854
L855
L856
L857
L858
L859
L860
L861 ▲
L862
L863
L864
L865
L866
L867

V2 Changes 2018/4/17 11:06 AM

Moved (insertion) [7]

V2 Changes 2018/4/17 11:06 AM

Deleted:

V2 Changes 2018/4/17 11:06 AM

Formatted: Font:+Theme Body

V2 Changes 2018/4/17 11:06 AM

Formatted: Font:+Theme Body

V2 Changes 2018/4/17 11:06 AM

Formatted: Normal1

V2 Changes 2018/4/17 11:06 AM

Deleted: "

V2 Changes 2018/4/17 11:06 AM

Formatted: Font:+Theme Body

V2 Changes 2018/4/17 11:06 AM

Deleted: ",,

V2 Changes 2018/4/17 11:06 AM

Formatted: Font:+Theme Body

V2 Changes 2018/4/17 11:06 AM

Deleted: .

... [383]

V2 Changes 2018/4/17 11:06 AM

Formatted: Font:+Theme Body, Not Bold

V2 Changes 2018/4/17 11:06 AM

Formatted: Font:+Theme Body, 11 pt, Not Bold

V2 Changes 2018/4/17 11:06 AM

Formatted: Font:+Theme Body

V2 Changes 2018/4/17 11:06 AM

Formatted: Font:+Theme Body, 11 pt

V2 Changes 2018/4/17 11:06 AM

Formatted: Normal1, No widow/orphan control

V2 Changes 2018/4/17 11:06 AM

Formatted: Font:+Theme Body, 11 pt, Not Bold

V2 Changes 2018/4/17 11:06 AM

Deleted: .

V2 Changes 2018/4/17 11:06 AM

Formatted: Normal1

L873
L874
L875
L876
L877
L878

L879
L880
L881
L882
L883
L884
L885
L886
L887
L888
L889
L890
L891
L892
L893
L894
L895

Figures

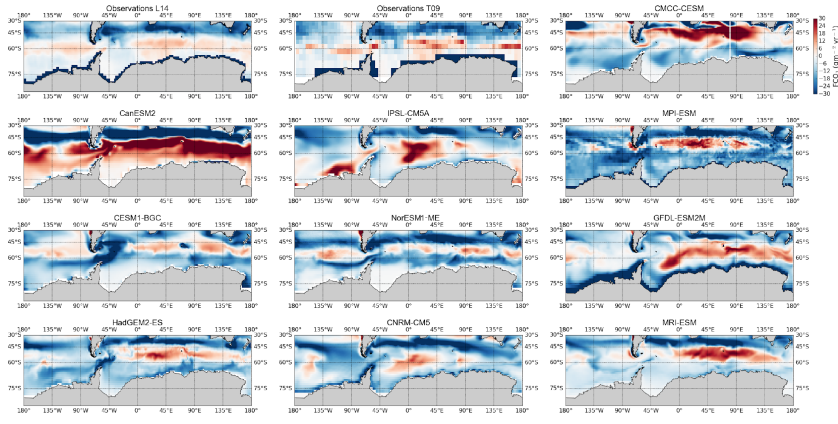
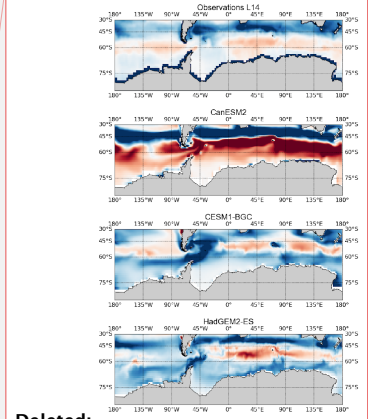


Fig. 1: The annual mean climatological distribution Sea-Air CO₂ Flux (FCO₂, in gC m⁻² yr⁻¹) for observations (L14: Landschützer et al., 2014 and T09: Takahashi et al., 2009) and 10 CMIP5 models over 1995 – 2005. CMIP5 models broadly capture the spatial distribution of FCO₂ with respect to L14 and T09, however, they also show significant differences in space and magnitude between the basins of the Southern Ocean with a few exceptions.

V2 Changes 2018/4/17 11:06 AM
Formatted: Font:Calibri

V2 Changes 2018/4/17 11:06 AM



Deleted:

V2 Changes 2018/4/17 11:06 AM
Formatted: Font:Calibri

V2 Changes 2018/4/17 11:06 AM

Deleted: Annual

V2 Changes 2018/4/17 11:06 AM

Formatted: Font:Calibri

V2 Changes 2018/4/17 11:06 AM

Formatted: Font:Calibri

V2 Changes 2018/4/17 11:06 AM

Formatted: Font:Calibri

V2 Changes 2018/4/17 11:06 AM

Formatted: Font:Calibri

V2 Changes 2018/4/17 11:06 AM

Deleted: ,

V2 Changes 2018/4/17 11:06 AM

Formatted: Normal1

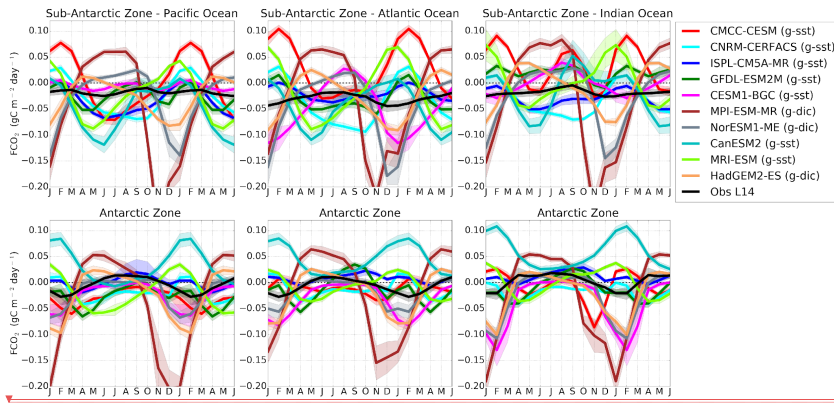


Fig. 2: Seasonal cycle of Sea-Air CO₂ Flux (FCO₂, in gC m⁻² yr⁻¹) in observations and 10 CMIP5 models in the Sub-Antarctic and Antarctic zones of the Pacific Ocean (first column), Atlantic Ocean (second column) and Indian Ocean (third column). The shaded area shows the temporal standard deviation over the considered period (1995 – 2005). *g-sst* and *g-dic* shows the clustering of CMIP5 models into group-SST and group-DIC as shown in Fig. 3 (section 3.2).

V2 Changes 2018/4/17 11:06 AM

Sub-Antarctic Zone - Pacific Ocean

Deleted:

V2 Changes 2018/4/17 11:06 AM

Formatted: Font:Calibri

V2 Changes 2018/4/17 11:06 AM

Deleted: .

V2 Changes 2018/4/17 11:06 AM

Formatted: Font:Calibri

V2 Changes 2018/4/17 11:06 AM

Deleted: .

V2 Changes 2018/4/17 11:06 AM

Formatted: Normal1

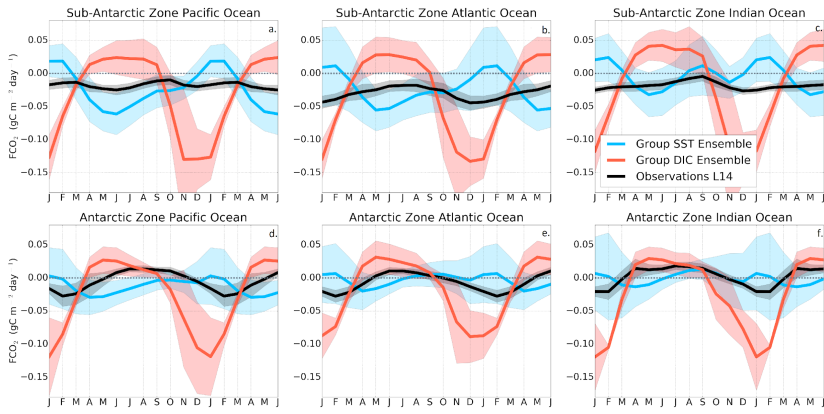


Fig. 3. Seasonal cycle of the equally-weighted ensemble means of FCO_2 ($\text{gC m}^{-2} \text{yr}^{-1}$) from Fig. 2 for group DIC models (MPI-ESM, HadGEM-ES and NorESM) and group SST models (GFDL-ESM2M, CMCC-CESM, CNRM-CERFACS, IPSL-CM5A-MR, CESM1-BGC, NorESM2, MRI-ESM and CanESM2). The shaded areas show the ensemble standard deviation. The black line is the Landschützer et al. (2014) observations.

V2 Changes 2018/4/17 11:06 AM

Deleted:

V2 Changes 2018/4/17 11:06 AM
Formatted: Font:Calibri

V2 Changes 2018/4/17 11:06 AM
Deleted:

V2 Changes 2018/4/17 11:06 AM
Formatted: Font:Calibri

V2 Changes 2018/4/17 11:06 AM
Deleted: ,

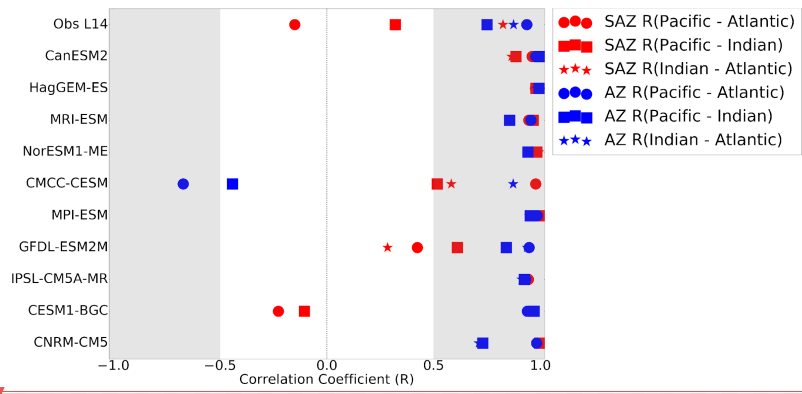
V2 Changes 2018/4/17 11:06 AM
Formatted: Font:Calibri

V2 Changes 2018/4/17 11:06 AM
Deleted: .,

V2 Changes 2018/4/17 11:06 AM
Formatted: Font:Calibri

V2 Changes 2018/4/17 11:06 AM
Deleted: .

V2 Changes 2018/4/17 11:06 AM
Formatted: Normal1



V2 Changes 2018/4/17 11:06 AM

Deleted:

V2 Changes 2018/4/17 11:06 AM

Formatted: Font:Calibri

L938
L939
L940
L941
L942
L943
L944
L945
L946
L947
L948
L949
L950
L951
L952
L953
L954
L955
L956
L957
L958
L959
L960
L961

Fig. 4: The correlation coefficients (R) of basin – basin seasonal cycles of FCO₂ for observations (Landschützer et al., 2014) and 10 CMIP5 models in the three basins of the Southern Ocean i.e. Pacific, Atlantic and Indian basin.

V2 Changes 2018/4/17 11:06 AM

Deleted: ,

V2 Changes 2018/4/17 11:06 AM

Formatted: Normal1

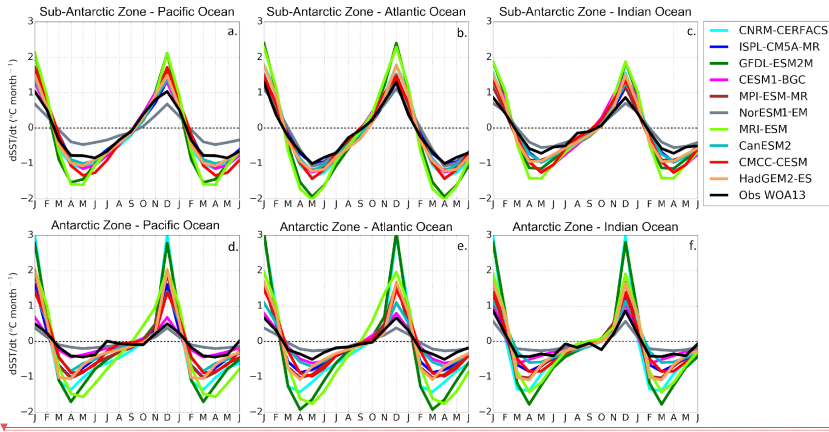


Fig. 5: Mean seasonal cycle of the estimated rate of change of sea-surface temperature ($dSST/dt$, $^{\circ}C$ month $^{-1}$) for the Sub-Antarctic and Antarctic zones of the Pacific Ocean (first column), Atlantic Ocean (second column) and Indian Ocean (third column).

V2 Changes 2018/4/17 11:06 AM

Deleted:

V2 Changes 2018/4/17 11:06 AM
Formatted: Font:Calibri

V2 Changes 2018/4/17 11:06 AM
Deleted:

V2 Changes 2018/4/17 11:06 AM
Formatted: Font:Calibri

V2 Changes 2018/4/17 11:06 AM
Deleted: ,

V2 Changes 2018/4/17 11:06 AM
Formatted: Normal1

L963
L964
L965
L966
L967
L968
L969
L970
L971
L972
L973
L974
L975
L976
L977
L978
L979
L980
L981

L984
L985
L986
L987
L988
L989
L990
L991
L992
L993
L994
L995
L996
L997
L998
L999

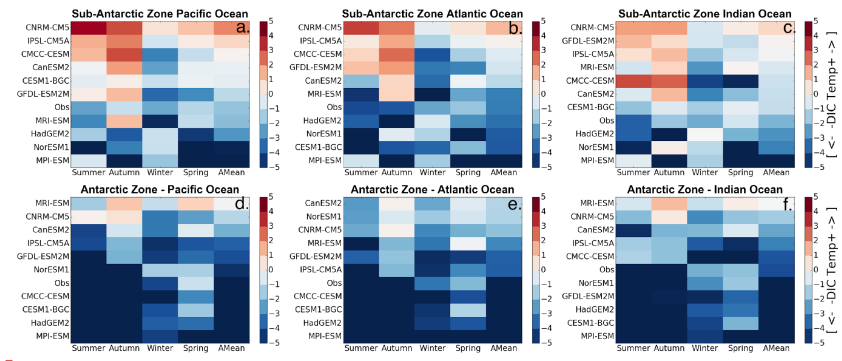
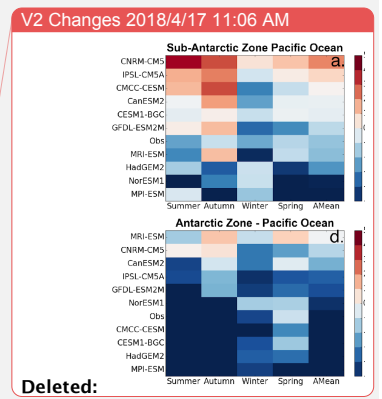


Fig. 6: Mean seasonal and annual values of the DIC–temperature control index (M_{T-DIC}). The increase in the red color intensity indicates increase in the strength of the temperature driver and the blue intensity shows the strength of the DIC driver. The models are sorted according to the annual mean value of the indicator presented in the last column (Amean).



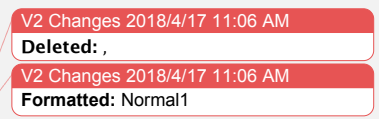
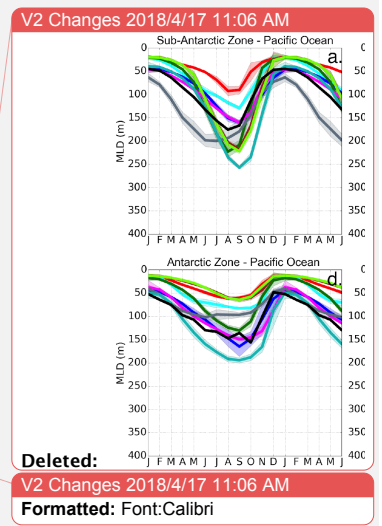
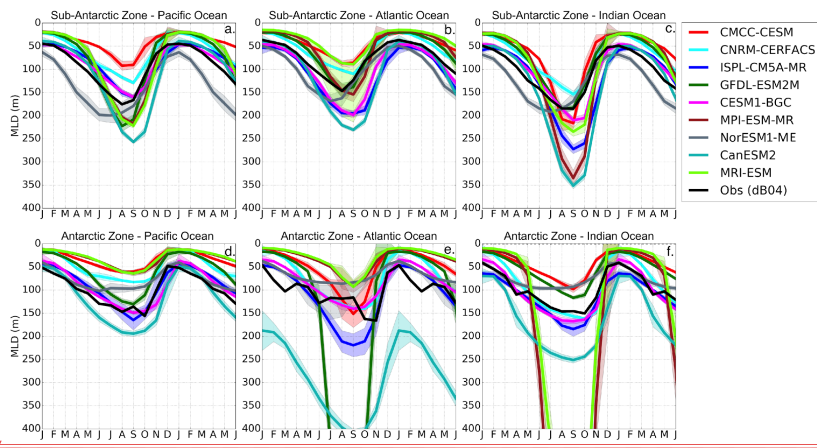
Deleted:
V2 Changes 2018/4/17 11:06 AM
Formatted: Font:Calibri

V2 Changes 2018/4/17 11:06 AM
Deleted:)

V2 Changes 2018/4/17 11:06 AM
Formatted: Font:Calibri

V2 Changes 2018/4/17 11:06 AM
Deleted: ,

V2 Changes 2018/4/17 11:06 AM
Formatted: Normal1



2002
2003
2004
2005
2006
2007
2008
2009
2010
2011
2012
2013
2014
2015
2016
2017

Fig. 7: Seasonal cycle of the Mixed Layer Depth (MLD) in the Sub-Antarctic and Antarctic zones of the Pacific Ocean (first column), Atlantic Ocean (second column) and Indian Ocean (third column).

2019
2020
2021
2022
2023
2024
2025
2026
2027
2028

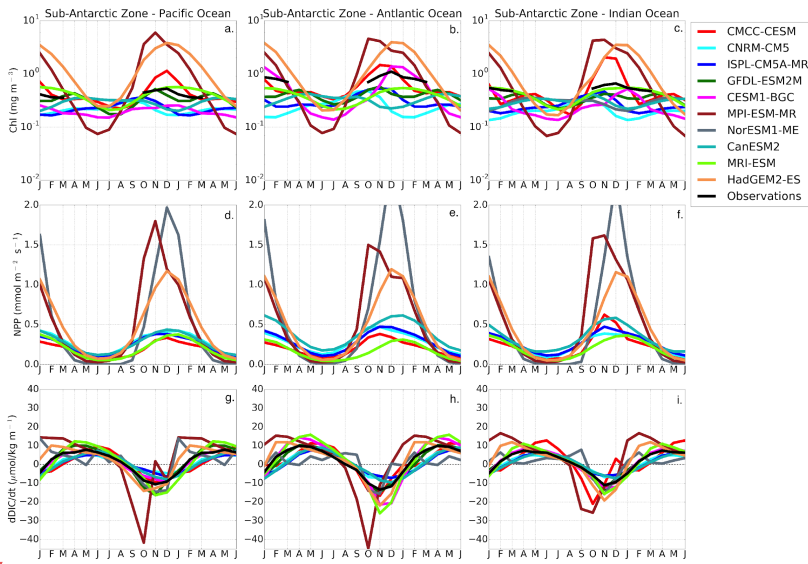
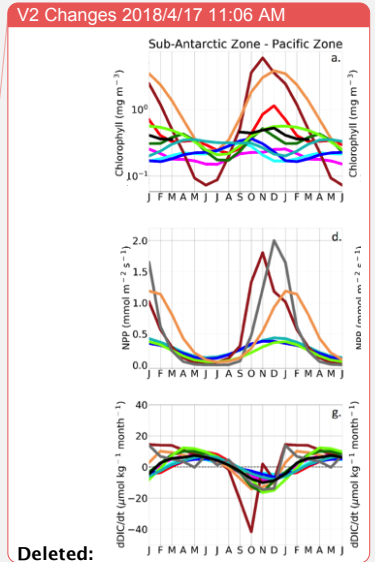


Fig. 8: The seasonal cycle of chlorophyll (mg m^{-3}), Net Primary Production ($\text{mmol m}^{-2} \text{s}^{-1}$) and the surface rate of change of DIC ($\mu\text{mol kg}^{-1} \text{month}^{-1}$) in the Sub-Antarctic zone of the Pacific Ocean (first column), Atlantic Ocean (second column) and Indian Ocean (third column).



V2 Changes 2018/4/17 11:06 AM
Deleted: .
V2 Changes 2018/4/17 11:06 AM
Formatted: Font:Calibri

V2 Changes 2018/4/17 11:06 AM
Deleted: .
V2 Changes 2018/4/17 11:06 AM
Formatted: Normal1

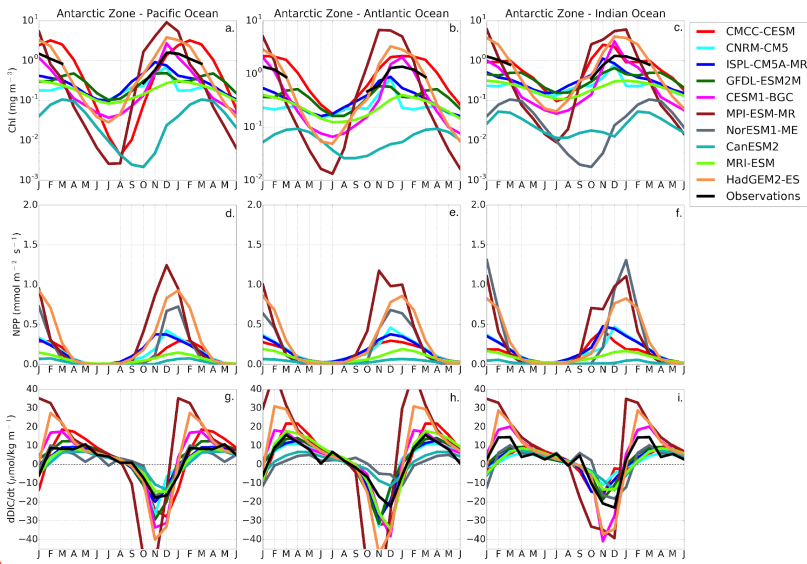


Fig. 9 Same as Fig. 8 for the Antarctic zone.

V2 Changes 2018/4/17 11:06 AM

Deleted:

V2 Changes 2018/4/17 11:06 AM

Formatted: Font:Calibri

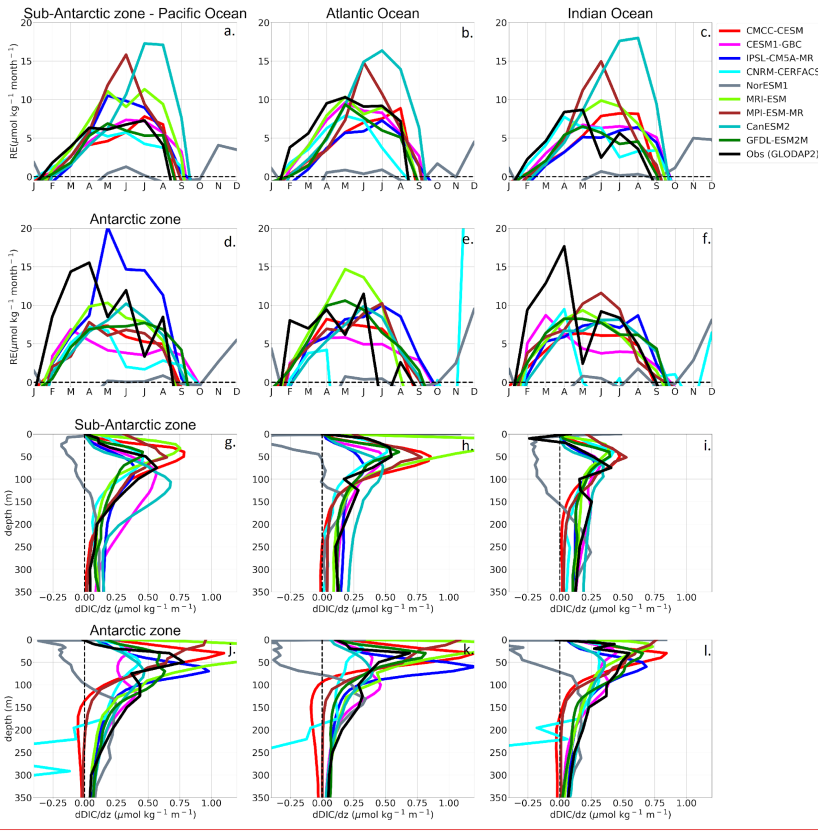
V2 Changes 2018/4/17 11:06 AM

Deleted: .

V2 Changes 2018/4/17 11:06 AM

Formatted: Normal1

2030
2031
2032
2033



V2 Changes 2018/4/17 11:06 AM

Deleted:

V2 Changes 2018/4/17 11:06 AM

Formatted: Font:Calibri

035
036
037
038
039
040
041
042
043
044
045
046

Fig. 10: (a-f) Estimated DIC entrainment fluxes ($\text{mol kg}^{-1} \text{ month}^{-1}$) at the base of the mixed layer and (g-i) vertical DIC gradients ($\mu\text{mol kg}^{-1} \text{ m}^{-1}$) in the Sub-Antarctic and Antarctic zone of the Pacific Ocean (first column), Atlantic Ocean (second column) and Indian Ocean (third column).

V2 Changes 2018/4/17 11:06 AM

Deleted: ,

V2 Changes 2018/4/17 11:06 AM

Formatted: Normal1

1048 **Table 2:** Sea-Air CO₂ fluxes (Pg C yr⁻¹) annual mean uptake in the Southern Ocean (first column), here
 1049 defined as south of the Sub-tropical front, Sub-Antarctic zone (second column) and Antarctic zone (third
 1050 column). The third and fourth column shows the Pattern Correlation Coefficient (PCC) and Root Mean
 1051 Square Error (RMSE) for the whole Southern Ocean for each model. [Observations here refer to](#)
 1052 [Landschützer et al., 2014](#).

Table 2: Sea-Air CO₂ Fluxes Mean Annual Uptake, PCC and RMSE

Model	Southern Ocean	Sub-Antarctic zone	Antarctic zone	PCC	RMSE
CNRM-CM5	-0.823 ± 0.003	-0.682 ± 0.002	-0.122 ± 0.001	0.44	17.9
GFDL-ESM2M	-0.161 ± 0.005	-0.074 ± 0.004	-0.077 ± 0.002	0.43	8.47
HadGEM2-ES	-0.489 ± 0.005	-0.284 ± 0.003	-0.197 ± 0.001	0.55	10.9
IPSL-CM5A-MR	-0.496 ± 0.003	-0.582 ± 0.006	0.101 ± 0.003	0.53	10.5
MPI-ESM-MR	-0.870 ± 0.006	-0.530 ± 0.002	-0.326 ± 0.002	0.37	9.87
MRI-ESM	-0.048 ± 0.002	0.022 ± 0.003	-0.070 ± 0.001	0.36	15.6
NorESM1	-0.699 ± 0.004	-0.412 ± 0.003	-0.270 ± 0.002	0.60	8.96
CESM1-BGC	-0.532 ± 0.006	-0.132 ± 0.003	-0.385 ± 0.004	0.47	9.15
CMCC-CESM	0.121 ± 0.006	0.367 ± 0.004	-0.225 ± 0.003	-0.09	17.9
CanESM2	-0.058 ± 0.008	-0.720 ± 0.006	0.661 ± 0.004	0.54	19.5
Observations	-0.253 ± 0.3	-0.296 ± 0.3	0.053 ± 0.3		

1053

Table 2: Sea-Air CO₂ Fluxes Mean Annual Uptake, PCC and RMSE

Formatted: normal
 V2 Changes 2018/4/17 11:06 AM
 Deleted: forth
 V2 Changes 2018/4/17 11:06 AM
 Formatted ... [384]
 V2 Changes 2018/4/17 11:06 AM
 Deleted:
 V2 Changes 2018/4/17 11:06 AM
 Deleted: ,
 V2 Changes 2018/4/17 11:06 AM
 Formatted: Normal1

46